FINAL REPORT
28 JULY 1972

JET PROPULSION LABORATORY
CALIFORNIA INSTITUTE OF TECHNOLOGY
PASADENA, CALIFORNIA

FINAL REPORT
28 JULY 1972

OUTER PLANETS MISSION TELEVISION
SUBSYSTEM OPTICS STUDY

This work was performed for the Jet Propulsion
Laboratory, California Institute of Technology
and sponsored by the National Aeronautics and
Space Administration under Contract NAS7-100.

JPL CONTRACT 953320
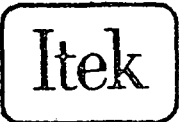
Itek

Optical Systems Division

ITEK CORPORATION ● 10 MAGUIRE ROAD ● LEXINGTON, MASSACHUSETTS 02173

TECHNICAL CONTENT STATEMENT

"This report contains information prepared by
Itek Corporation under JPL subcontract. Its
content is not necessarily endorsed by the Jet
Propulsion Laboratory, California Institute of
Technology, or the National Aeronautics and
Space Administration."
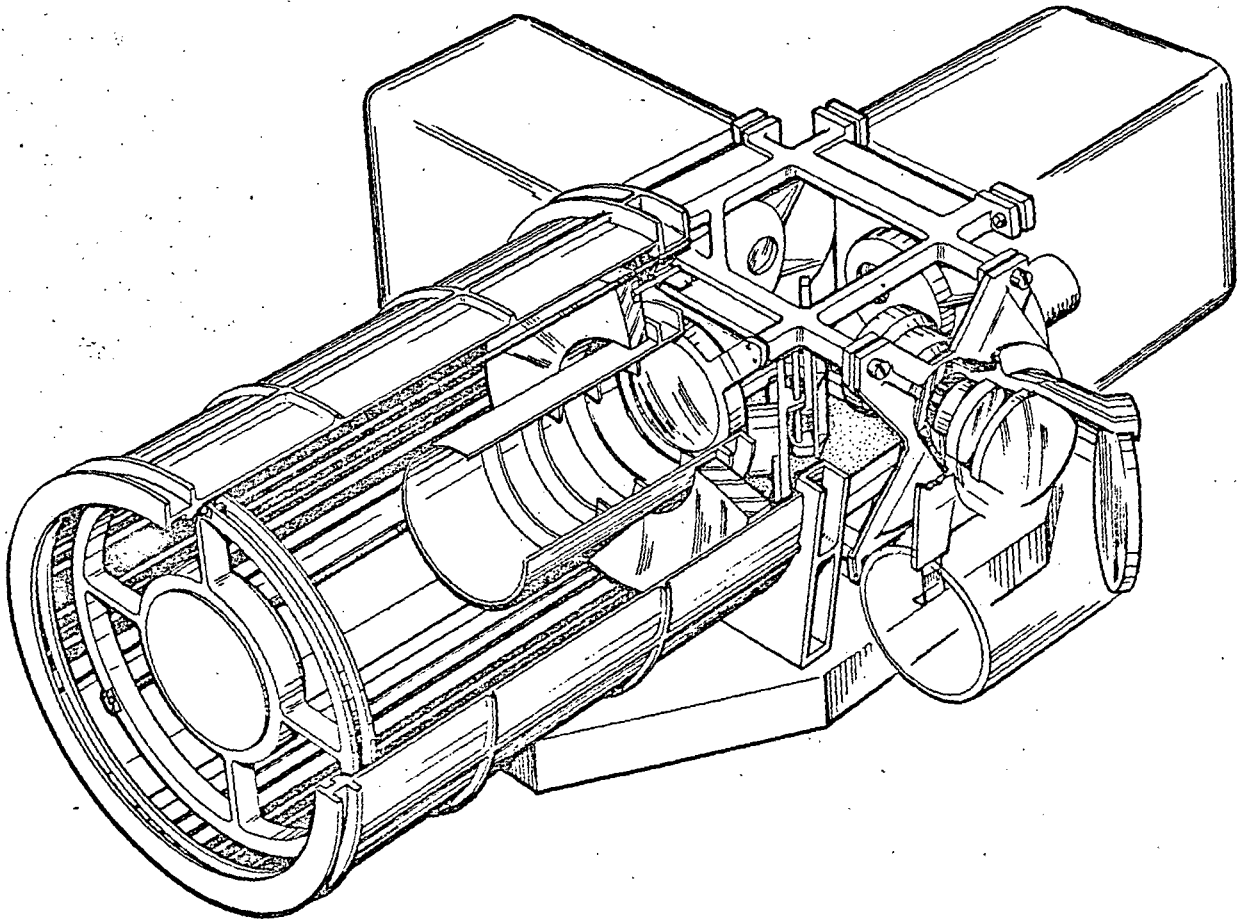
Candidate TV imaging optical system for Mariner Jupiter/Saturn 77 Mission

ABSTRACT

Under JPL contract 953320, Itek Corporation performed an optics study to establish a candidate optical system design for the proposed NASA Mariner Jupiter/Saturn 77 Mission. The study was performed over the 6-month period from January through June 1972.

The candidate optical system contains both a wide angle (A) and a narrow angle (B) lens with the following performance parameters:

- Wide Angle Lens (Refractor)

    - Focal length   200 millimeters
    - Relative aperture   f/2.64
    - MTF $\geq$65% at 35 lp/mm for 400 nm $\leq \lambda \leq$ 700 nm
    - Transmittance $\geq$40% for 400 nm $\leq \lambda \leq$ 700 nm

- Narrow Angle Lens (Cassegrain With Correctors)

    - Focal length   1,000 millimeters
    - Relative aperture   f/4.4
    - MTF $\geq$65% at 35 lp/mm for 350 nm $\leq \lambda \leq$ 700 nm
    - Transmittance $\geq$40% for 350 nm $\leq \lambda \leq$ 700 nm

An additional feature is a transfer mirror mechanism that allows image transfer from the B lens to the vidicon initially used for the A lens. This feature adds an operational redundancy to the optical system in allowing for narrow angle viewing if the narrow angle vidicon were to fail. In this failure mode, photography in the wide angle mode would be discontinued.

The structure of the candidate system consists mainly of aluminum with substructures of Invar for athermalization. The total optical system weighs (excluding vidicons) approximately 30 pounds and has overall dimensions of 26.6 by 19.5 by 12.3 inches.

CONTENTS

5

TABLES

ITEK DRAWINGS ASSOCIATED WITH STUDY

Drawing Number	Title
186075	Study Plan
186092	Config. 1 L/O—First-Order Design
186093	Config. 2 L/O—First-Order Design
186094	Config. 3 L/O—First-Order Design
186095	Config. 4 L/O—First-Order Design
186096	Opposed Camera, Double Mirror Design Switching Technique
186097	Config. 1 Mechanical L/O (Truss)
186098	Config. 3 Mechanical L/O (Truss)
186099	Config. 3 Mechanical L/O (Tubular)
186100	Config. 4 Mechanical L/O (Tubular)
915175-Rev A (2 sheets)	Candidate TV Imaging Optical System—Mariner Jupiter/Saturn 77 Mission

1. INTRODUCTION

1.1 BACKGROUND AND STUDY GOALS

· Under JPL contract 953320, Itek Corporation, Lexington, Massachusetts, performed an optics study to establish a candidate optical system design for the television imaging subsystem on outer planet missions. This system would be applicable for use on the proposed NASA Mariner Jupiter/Saturn 1977 Flyby Mission. The study was performed over the 6-month period from January through June 1972.

The basic task of the study was to establish the design of a single unit optical system that contains a wide angle (A) lens for use with an associated vidicon and a narrow angle (B) lens for use with another vidicon, with provision to transfer the image from the B lens to the vidicon used by the A lens. The image transfer feature adds an operational redundancy to the optical system in allowing for narrow angle viewing if the narrow angle vidicon were to fail. In this failure mode, photography in the wide angle mode would be discontinued. It is expected that the narrow (B) lens will be used for approximately 85 percent of the TV imaging time. The transfer mirror scheme provides a backup to ensure imaging from the B lens on outer planet missions in the order of 4 or more years duration.

The weight limit of the optical system is 30 pounds. The design study parameters for the optics are as follows:

- Wide Angle Lens

  - Focal length   200 millimeters
  - Relative aperture   f/2.64
  - MTF $\geq 65\%$ at 35 lp/mm for 400 nm $\leq \lambda \leq$ 700 nm
  - Transmittance $\geq 40\%$ for 400 nm $\leq \lambda \leq$ 700 nm

- Narrow Angle Lens

  - Focal length   1,000 millimeters
  - Relative aperture   f/4.4
  - MTF $\leq 65\%$ at 35 lp/mm for 350 nm $\leq \lambda \leq$ 700 nm
  - Transmittance $\leq 40\%$ for 350 nm $\leq \lambda \leq$ 700 nm

The detailed technical requirements of the study are given in Appendix A, Technical Requirements for Outer Planet Mission Television Subsystem Optics Study (dated 18 November 1971), and Appendixes B and C, JPL Technical Direction Memoranda no. 1 (dated 27 January 1972) and no. 2 (dated 23 March 1972).

1.2 STUDY APPROACH

As depicted in Fig. 1-1, a number of design factors were considered in establishing the proposed optical system. First-order optical analyses and subsequent lens design were performed to determine the optimum optical configuration for each lens. Thermo-optical analysis was used to aid in the selection of an optical configuration as well as to define the structural material and configuration requirements for supporting the optical elements in the proposed system design. Materials selection for optics and structure required consideration of the dynamic environmental conditions during launch and the environmental factors of relatively long duration spaceflight, i.e., radiation effects, long term stability in a vacuum, thermal characteristics, strength versus weight characteristics, etc. Mechanical design aspects involved designing a reliable transfer mirror mechanism and integrating Mariner-type shutter and filter wheel mechanisms into the system.

The activities leading up to the establishment of four preliminary configurations, including first-order analysis, preliminary lens design, thermo-optical analysis, mechanical layout, and weight estimates, are considered the preliminary phase of the study. These activities are presented as blocks 1 through 4 in Fig. 1-1 and are discussed in Section 2 and Appendixes D through G of this report. The activities relating to the study of a candidate, including configuration selection and detailed system analysis, are considered the system study phase. These activities are presented as blocks 5 and 6 in Fig. 1-1 and are discussed in Section 3 of this report.

Preliminary Studies

1	2	3	4
Evaluate requirements and determine applicable optics	Establish four first-order optical system configurations, utilizing combinations of two wide angle (A) lens possibilities and two narrow angle (B) lens possibilities	Preliminary lens design and thermo-optical analysis on selected lens configurations	Mechanism layout and preliminary weight estimates on selected optical system configurations

System Studies

5	6	7
Interim design conference at JPL Selection of optical configuration for system study	System study of candidate configuration: A lens—refractor B lens—Cassegrain Orthogonal vidicons with mirror for B lens imaging to either of two vidicons	Presentation of study final results at JPL Publication of final report

6A	6B	6C
Structural/ athermalization, analysis, and design	Final optical design	Mechanical design

Fig. 1-1 — Outer planet mission TV subsystem optics study approach

1-3

2. PRELIMINARY STUDY PHASE—OPTICAL CONFIGURATION EVALUATION

2.1 GENERAL CONSIDERATIONS

2.1.1 Radiation Considerations for Optical Materials Selection

Radiation is a significant consideration in optical materials selection. JPL data indicate that for a minimum perijove distance of 4.3 Jupiter radii,* a nominal Jovian proton fluence level of 10^8 protons/cm^2 (20 MeV equivalent, 7.5×10^{11} protons/cm^2 upper limit) and a nominal Jovian electron fluence level of 7.5×10^9 electrons/cm^2 (3 MeV equivalent, 5.7×10^{10} upper limit) exist. These values assume 100-mil aluminum shielding. For an unshielded package, the nominal proton dosage is 1.8×10^9 protons/cm^2, and the upper limit loading is 4.7×10^{12} protons/cm^2. Electron fluences vary little as a function of aluminum shielding. These values are more than comparable to those of the earth's Van Allen belts when integrated over similar mission times, as per the data of Vette.†

To these loads must be added the effects of the radioisotope thermoelectric generator gamma and neutron fluxes (approximately 350 photons/$cm^2 \cdot sec$ and 10^9 neutrons/cm^2, respectively), as well as the more typical mission loads of near earth and solar magnetic and electromagnetic radiation, near earth and interplanetary radiation, Van Allen belt protons and electrons, solar wind protons, galactic cosmic rays, and solar proton loadings.

Clearly then, although the dosage values for the configurations will be dependent on the duty cycle and the time that the optics are unshielded, as well as perijove distance, these radiation loadings must be considered in selecting mirror materials.

To our knowledge and based on discussions with vendors supplying the new generation mirror materials (ULE fused silica, Cer-Vit, Crystron-Zero, and Zerodur), only Cer-Vit has been exposed to equivalent (temporally compressed but no substrate heating) radiation dosages.‡ Although the referenced tests were for higher dosages of lower energy particles (3.5×10^{13} electrons/cm^2, 1 MeV), they produced significant surface deformation on Cer-Vit samples, whether used as aluminized substrates or replica diffraction gratings (3/4 fringe for the 3.5×10^{13} electrons/cm^2

---

*As dictated by a 10^8 protons/cm^2 fluence threshold with 100-mil aluminum S/C shielding and nominal loading; 3.5×10^4 hour; damage from nominal electron fluence would allow approach to 3.9 planet radii (assumes a 10^{10} electrons/cm^2 threshold).

† J. I. Vette, et al. NASA SP-3024-1996/7, Models of the Trapped Radiation Environment, Vol. I, Inner Zone Protons and Electrons; Vol. II, Inner and Outer Zone Electrons; Vol. III, Electrons at Synchronous Altitudes.

‡R. C. Gunter, Jr., Replica Coating Study, Interim Report—Phase V, College of the Holy Cross, Worcester, Mass., Jan 15, 1969. Limited testing has shown the transmission of ULE to be reduced 25 percent for 10^5 rads of 1-MeV α photons.

dosage and 10 fringes for the 2.1×10^{15} electrons/cm^2 dosage). This compares to a surface deformation of synthetic fused silica samples of 1/3 fringe for the 2.1×10^{15} electrons/cm^2, 1 MeV dosage. It is not realistic to attempt to extrapolate the results of these tests to the expected fluence levels. However, it appears risky at this point to propose Cer-Vit for a mission where high radiation dosages can be expected. Although test data on ULE fused silica are lacking, it is expected that its resistance to radiation damage will be superior to that of Cer-Vit. Crystron-Zero and Zerodur are relatively unknown quantities. Therefore, ULE fused silica is the proposed mirror material at this time, with the recommendation that appropriate radiation testing be conducted. Fused silica could be utilized as a damage-resistant alternative as necessary.

The major optical hazards anticipated will arise from proton and electron particles, although small numbers of additional particles exist. This is important since the damage to optical glass due to radiation is dependent on the energy spectrum as well as on the type of irradiating particle. Radiation damage to glass occurs by (1) ionization or excitation of the molecules in the matter irradiated, leading to bond rupture, free radicals, coloration, luminescence, etc.; (2) dislocation of any crystalline structure by ion or electron impact, giving rise to interstitial sites; and (3) contamination of the material by implantation of the bombarding particles. The electrons and protons anticipated will probably result in ionization as the prime mode of anomaly.

Devitrification of mirror materials containing metallic oxides (e.g., TiO_2 in ULE) can result in radiation-induced crystal growth wherein the resultant phase changes that occur could significantly affect such properties as thermal expansion.

Concerning the all-refracting A lens configuration and the corrector elements of the Cassegrain system, Jaffes (Behavior of Materials in Space Environments) indicates that ionization levels of 10^5 ergs per gram (about 10^3 rads) initiate some small changes in transmission. Vendors, however, have indicated that approximately 10^4 rads are required to produce noticeable variations in transmission. This 10^3 to 10^4 rad range is reiterated by Dr. W. Jahn (Radiation Resistant Glasses). Some specific data on damage to many Schott glasses are also presented in the reference, where it is indicated that those glasses having a lead content (flint) color more quickly than crowns and also degenerate less. As an additional general rule, this reference indicates that silicate glasses show less dye coloration than silicate-borate, borate, barium oxide, lanthanum oxide, or phosphate glasses. It also notes the markedly superior performance of cerium-protected BK-7 (BK-7G) to radiative loading, and notes the influence of cerium ion balance and other additives on transmission and radiation resistance.

Recalling the potentially significant Jovian dosages noted earlier,* and bearing in mind the sensitivities as given in the article by Dr. Jahn for undoped glass type, we recommend the use of doped material as a baseline, especially considering the fact that some of the worst dosages may occur near the beginning of the total mission.

The use of fused silica, which is also resistant to radiation damage, has also been considered but its use may be unacceptable due to its poor radial thermal gradient characteristics (about 3 times worse than BK-7G).

Results of radiation experiments conducted on both unstabilized and radiation-resistant optical glasses are available from Schott that show the cerium-stabilized glasses to be free from browning over the range of interest. However, it should be noted that aside from possible transmission changes, both stabilized and unstabilized glasses exhibit changes in refractive index

---

*The Space Materials Handbook, Technical Documentary Rept. No. ML-TOR-64-40, Chapter 7, Jan 1965, shows earth orbits involving the Van Allen belts to give well over 10^3 roentgens (and a similar number of rads for our optical materials) integrated over 3×10^3 hours with 100 mils of aluminum shielding. As noted earlier, our dosages should be at least comparable.

when exposed to radiation. BK-7G is an exception to typical glasses in that it suffers over a 3 times greater change in index due to radiation than does BK-7 (15×10^{-5} change in index for BK-7G versus 5×10^{-5} for BK-7 for 6×10^6 roentgens at 200 keV). Since radiation patterns are at this time expected to be relatively uniform over the lenses, this phenomenon should not contribute significantly to system degradation. Thus, doped refractive materials should prove of benefit here. The specific type would be predicated on the refractor design.

2.1.2 Optical Design Requirements

The design requirements for the candidate system are presented in Appendixes A, B, and C. The requirements for the wide angle (A) and narrow angle (B) lenses of the system are summarized below:

- Wide Angle (A) Lens

    - Focal length   200 millimeters
    - Relative aperture   f/2.64
    - MTF $\geq 65\%$ at 35 lp/mm for 400 nm $\leq \lambda \leq$ 700 nm
    - Transmittance $\geq 40\%$ for 400 nm $\leq \lambda \leq$ 700 nm

- Narrow Angle (B) Lens

    - Focal length   1,000 millimeters
    - Relative aperture   f/4.4
    - MTF $\geq 65\%$ at 35 lp/mm for 350 nm $\leq \lambda \leq$ 700 nm
    - Transmittance $\geq 40\%$ for 350 nm $\leq \lambda \leq$ 700 nm

The most critical factors limiting the choice of optical design configuration in regard to the above requirements are:

1. A long back focus is required to accommodate the switching mirror, shutter, and filter wheel, and to provide clearance between the two vidicon cameras and the two lenses. This constraint affects the A lens most severely.

2. The focal ratio (relative aperture) eliminates a number of all-reflecting and catadioptric designs from consideration. In particular, all eccentric pupil designs would not be suitable.

3. The focal length of the A lens (200 millimeters), coupled with the back focus and focal ratio requirements eliminates Cassegrain configurations from consideration for the A lens.

4. The spatial frequency of 35 line pairs per millimeter with 65 percent MTF imposes limits on optics parameters. In the narrow field case, the MTF of a perfect f/4.4 lens at 700 nanometers will be 65 percent or less at 35 line pairs per millimeter if the central obstruction diameter ratio is 0.62 or larger. The system wavefront error must be 0.10 wavelength rms or better if the central obstruction diameter ratio is 0.50. Thus the design configuration for the B lens cannot have a central obstruction diameter ratio much larger than 0.50. The faster focal ratio of the A lens makes the central obstruction problem less severe, since 35 line pairs per millimeter is a smaller fraction of its cutoff spatial frequency.

5. The requirement for 40 percent transmittance over the spectral range of 350 to 700 nanometers is difficult to meet, with most of the difficulty arising at the ultraviolet end of the spectrum. The all-reflecting and catadioptric designs will have three to five mirrors. The most desirable mirror coating, silver covered with protective coatings, tends to cut off at 360 to 370 nanometers when five mirrors are cascaded. Aluminum coatings will have a higher reflectivity at 350 nanometers, but only at the cost of substantial reduction in system transmittance at longer wavelengths. One effect of these system losses is to place an upper limit on the size of the central obstruction diameter ratio in the range 0.50 to 0.60 for the all-reflecting designs.

6. The A and B lenses must both have flat fields, because the vidicon normally has a flat faceplate and because of the lateral image displacement introduced by the switching mirror. For all-reflecting designs, this means that at least three mirrors having power must be used to reduce the Petzval sum to zero. Cassegrain designs should also be of the zero Petzval sum type, which have large central obstructions.

2.2 SYSTEM OPTICAL CONFIGURATION

Four possible lens designs were identified early in the study: an all-refracting A lens, a Cassegrain B lens, and all-reflecting A and B lenses. These were combined to produce four different system optical configurations, as follows:

Configuration 1 — All-refracting A and Cassegrain B
Configuration 2 — All-refracting A and all-reflecting B
Configuration 3 — A and B both all-reflecting
Configuration 4 — All-reflecting A and Cassegrain B

The sketches of these configurations presented in this section are schematic only and are not to scale. Full scale drawings of all four configurations are available on diazo prints (see the listing of related Itek drawings at the beginning of this report).

An extensive study was made of a number of factors to obtain the lens designs and the four different optical configurations. A discussion of the switching mirror techniques is given in Appendix D. The development of the all-reflecting three-mirror designs is described in Appendix E. Developing a complete design for the A lens refractor was considered to be beyond the scope of this study, because of the extensive effort required to select a design that has broad spectral coverage extending into the ultraviolet and is corrected adequately for secondary color. As a result, the system configurations involving an all-refracting A lens must be considered no better than provisional. A detailed discussion of transmittance for the A and B lenses is given in Appendix F, and an analysis of thermo-optical factors for the selected configurations is given in Appendix G.

In configuration 1 (Fig. 2-1) the vidicon cameras are set orthogonal to each other, and in the normal operating mode, there is no mirror between the lenses and the vidicons. When the switching mirror is inserted, the A lens must be refocused. One folding mirror is required to boresight the axes of the A and B lenses, and it has been placed in front of the A lens in configuration 1. Alternatively, the folding mirror can be placed inside the B Cassegrain. This has the advantage of producing a far more compact design, with dimensions comparable to those of configuration 2. (Its disadvantage is a reduction in transmittance of the B lens.) Fig. 2-1 indicates that the optics take up the entire 20 by 30 inches of allotted space, with one vidicon extending beyond that limit.

In configuration 2 (Fig. 2-2) the Cassegrain has been replaced by the all-reflecting B lens design. The packaging is more compact, but otherwise the mechanical properties of the configuration are similar to those of configuration 1. Its weight should be similar. Although the all-reflecting B lens has more mirrors than the Cassegrain, the added weight is offset by the folding mirror in configuration 1. The all-reflecting B lens should be superior optically, if only because it has a substantially smaller central obstruction diameter ratio (0.30 instead of 0.53). This will increase MTF and transmittance, the latter in spite of the extra mirrors.

Configuration 3 (Fig. 2-3) uses all-reflecting designs for both lenses. This combination offers several advantages so far as system configuration is concerned. It will fit entirely within the 20- by 30-inch envelope dimensions. The combination adapts naturally to the opposed camera switching mirror configuration, which eliminates the need for gross refocusing when switching

2-4
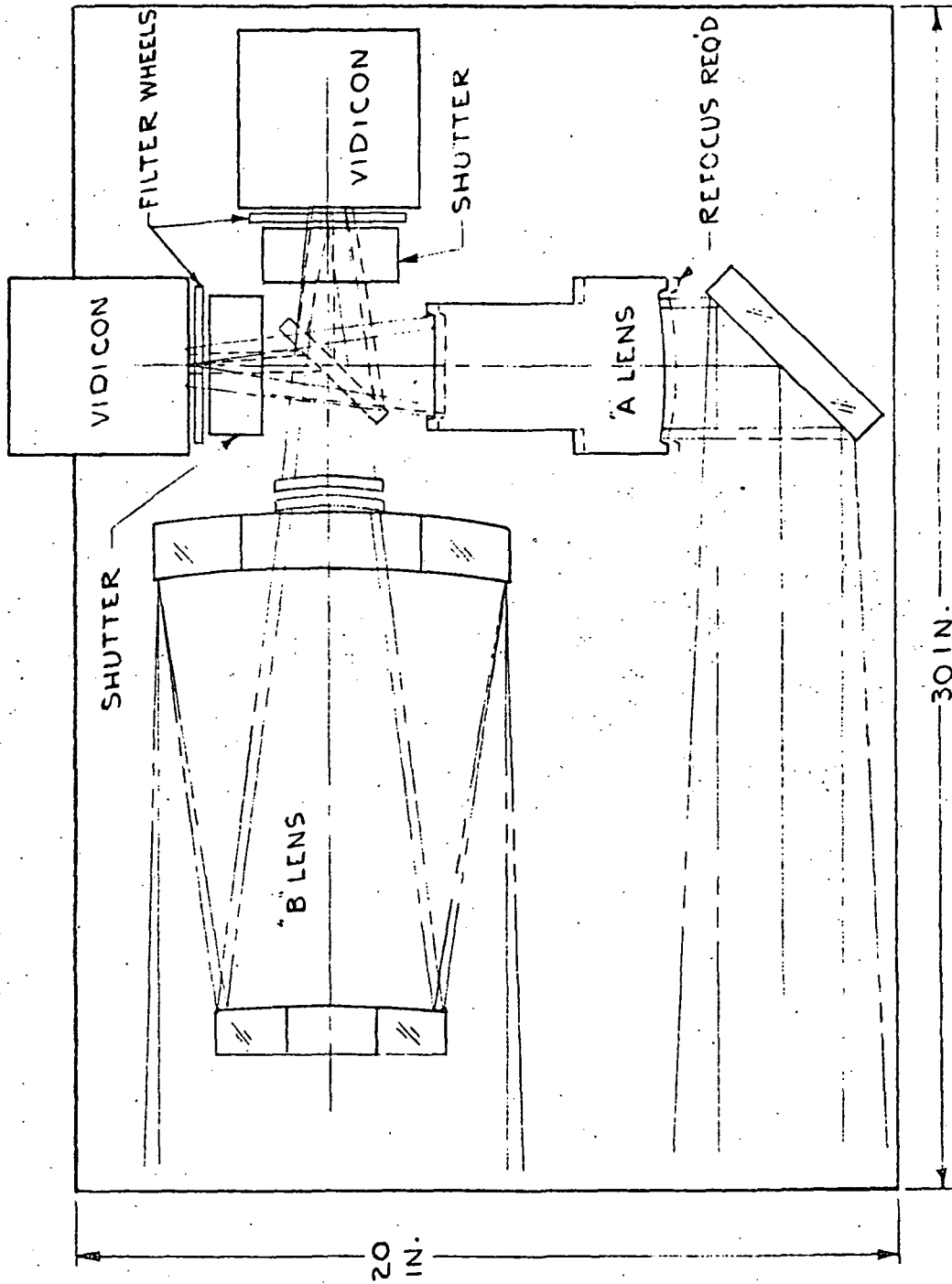
Fig. 2-1 — Configuration 1: all-refracting A lens, Cassegrain B lens with correctors; orthogonal vidicons, single switching mirror

2-5

17
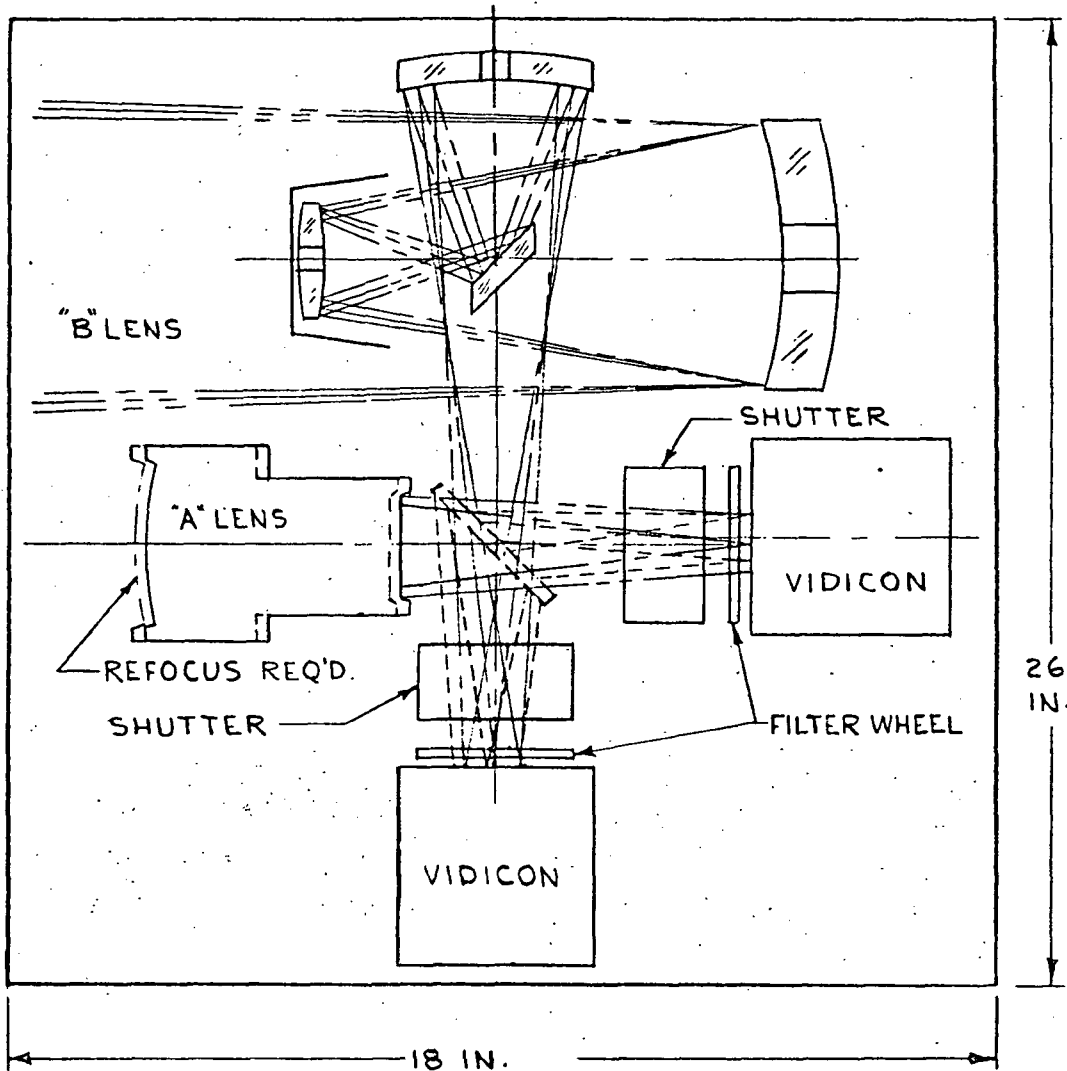
Fig. 2-2 — Configuration 2: all-refracting A lens, all-reflecting B lens; orthogonal vidicons, single switching mirror
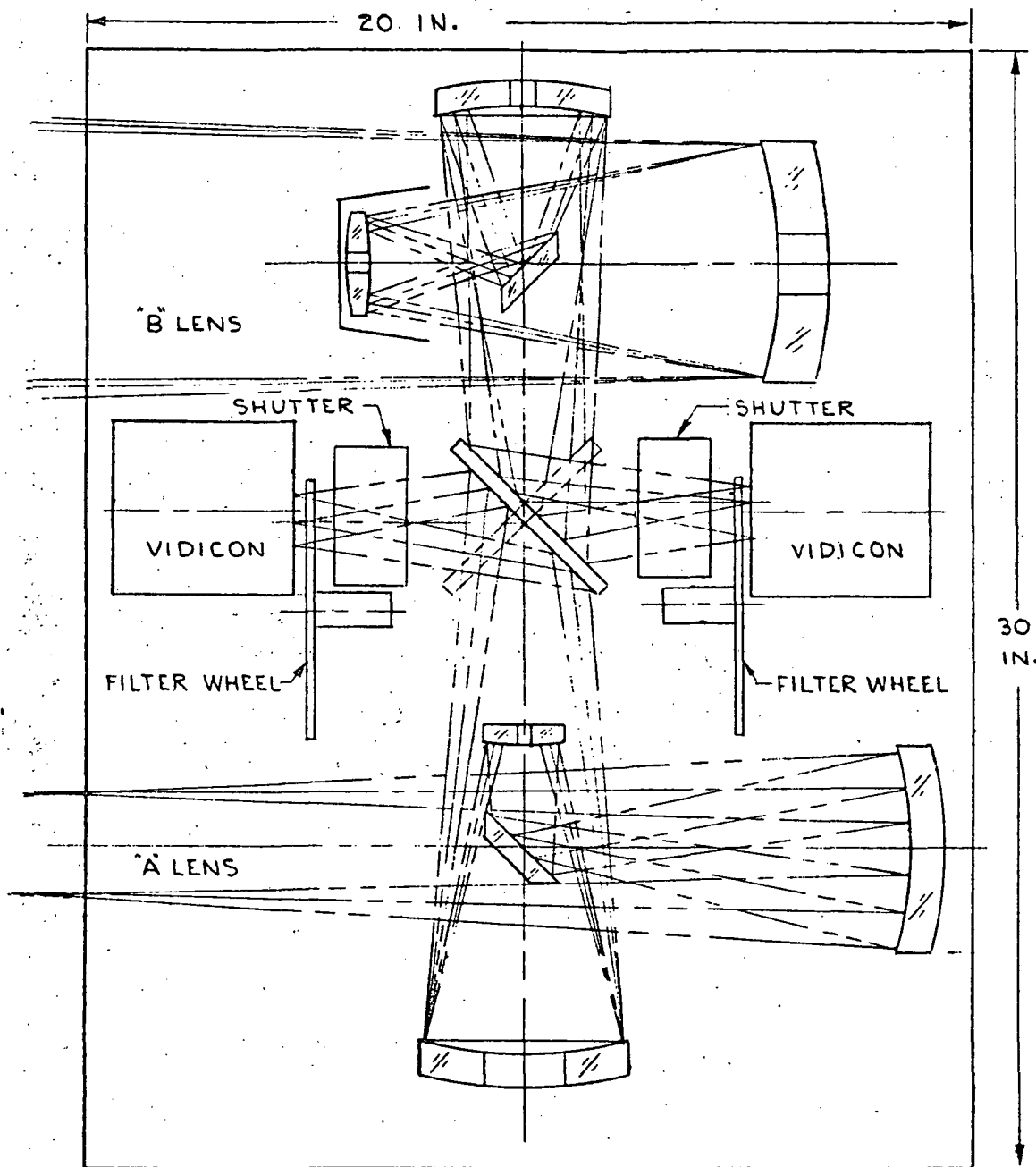
Fig. 2-3 — Configuration 3: all-reflecting A and B lenses; opposed vidicons, single switching mirror

vidicons. Each lens involves an internal relay stage, and the folding mirrors are located so that these internal relays lie on the same axis. A common structure can be made to hold these two relays plus the switching mirror assembly, shutters, and filters. The remaining optics and the two vidicons can be attached to this structure after the relays and switching mirror have been aligned.

The design incorporating a common structure for the two relays should offer some advantages so far as assembly and alignment are concerned. The three mirrors in the relays (the secondary and tertiary of the A lens and the tertiary of the B lens) have unused portions near their centers that can be cored out and fit with markers locating their optical axes. These can be used to align the mirrors on a common axis and make this axis coincident with the axis of rotation of the switching mirror. The tilt angle of the switching mirror must then be set to make the reflected optical axes perpendicular to the axis common to both relays. The axial spacing of the relay mirrors may then be adjusted to locate the two output images at the same distance from the common axis. This adjustment is somewhat less critical than other alignments, since an error can be compensated for by refocusing the first stage of each lens (the primary mirror for the A lens and the combination of primary and secondary for the B lens). Errors in the relay mirrors' axial positions cause only a magnification change after refocusing.

After the alignment has been completed, the shutters and filter wheel mechanisms may be added. The vidicons are then added and squared up with the output image surfaces. The image sensor surfaces within the vidicons should be perpendicular to the folded optical axes (parallel to each other and to the common optical axis of the relay stages) and the same optical distance from the common axis.

The final step in alignment is to attach the first stage optics of each lens to the main frame, adjust the two folding diagonals to match the optical axes, and focus the first stage optics to make the output image coincident with the vidicon image sensor surface. The axes of the first stages of the A and B lenses should be boresighted with respect to each other (the axes of the two made parallel). These two axes need not be perpendicular to the common axes of the relays, however, so long as they intersect. The diagonal mirrors can be tilted to compensate for any nonperpendicularity.

The most critical alignment will be that of the B lens primary and secondary with respect to each other, due to the extremely low focal ratio of the primary. These two mirrors should be mounted in a common structure, and the entire structure adjusted as a unit when attaching it to the main optical frame.

Configuration 4 (Fig. 2-4) is similar to configuration 3 in all respects except that the all-reflecting B lens has been replaced by a folded Cassegrain design. Because of the folding mirror in the Cassegrain, the weight of configuration 4 should be very close to that of configuration 3. Both MTF and transmittance will be lower because of the larger central obstruction of the Cassegrain. Sensitivity to misalignment should be less for the Cassegrain, however, because of its slower primary. The entire Cassegrain has to be treated as a single lens, so that assembly and alignment procedures will be somewhat different than described for configuration 3.

An alternative to configuration 4 would have an unfolded Cassegrain and would use orthogonal vidicon cameras. This has the advantage of one less mirror in the B lens, with the consequent increase in transmittance and reduction in weight. Countering this, one of the lenses would have to be refocused roughly 5 millimeters when the switching mirror is inserted. For this reason, this approach was not considered.
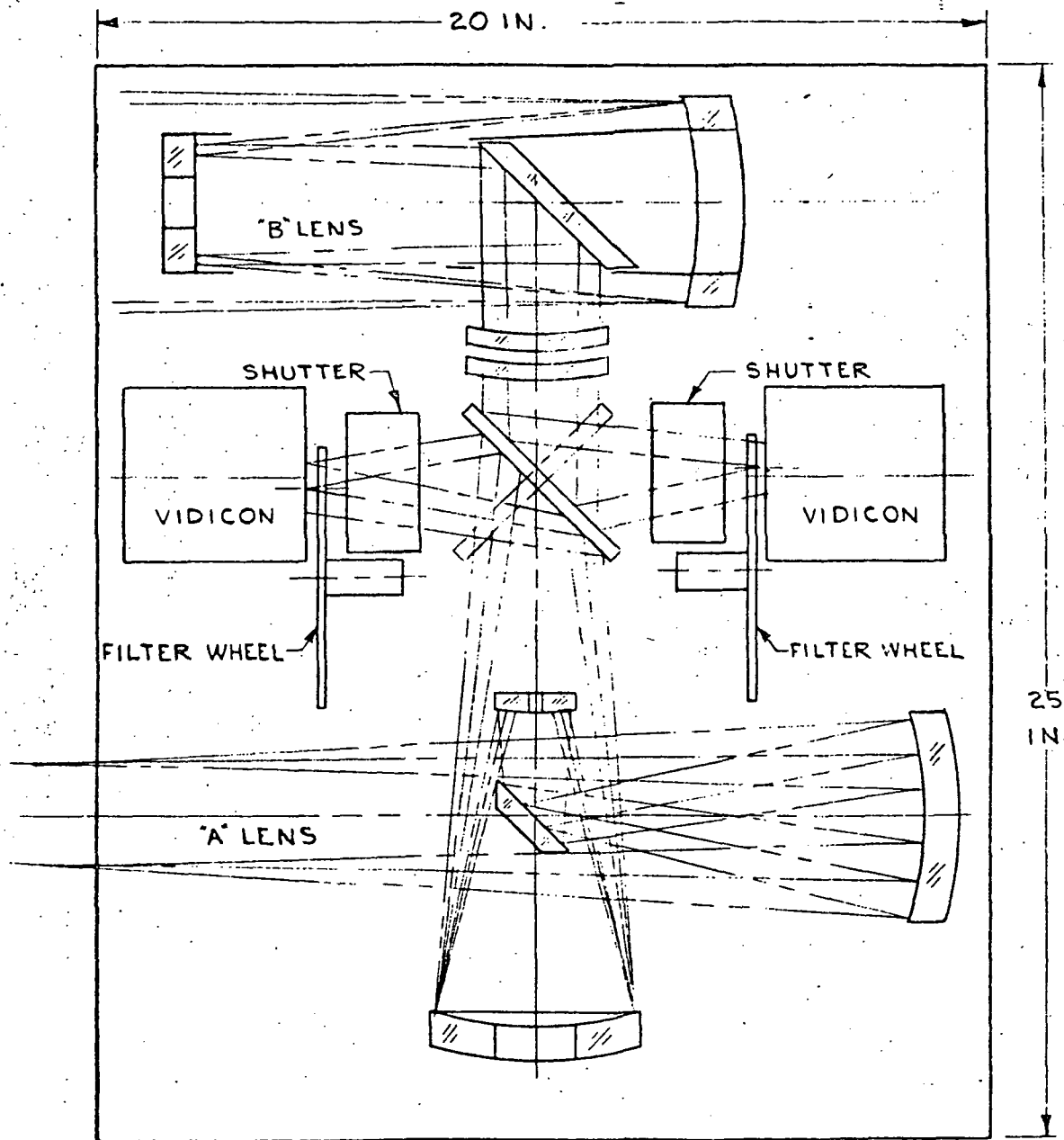
Fig. 2-4 — Configuration 4: all-reflecting A lens, Cassegrain B lens with correctors; opposed vidicons, single switching mirror

2.3 PRELIMINARY OPTICAL DESIGN

2.3.1 Background

The preliminary study phase of the program included a preliminary optical design of the configurations selected in the first-order optical configuration study. The optical design was carried far enough to establish that the proposed configurations could meet the performance specifications.

2.3.2 All-Reflecting A Lens, Configurations 3 and 4 (Figs. 2-3 and 2-4)

The radii of the three mirrors were selected to provide the desired first-order parameters as well as to correct the Petzval curvature to zero. Spherical aberration was corrected by placing a general asphere at the stop on the tertiary. A near paraboloid on the primary and a hyperboloid on the secondary enabled the field aberrations to be corrected.

Table 2-1 summarizes the performance of this system. Note that when no filter is included, the chromatic modulation at 35 line pairs per millimeter is 0.88 on axis and 0.86 at the edge of the field. To determine the effect of a filter, a 0.1-inch thick parallel plate of BK-7 glass was placed near the final image plane. After the system was recorrected for the monochromatic aberrations, it was found that the chromatic modulation at 35 line pairs per millimeter changed very little. This is true even though the chromatic optical path difference (OPD) increased to over 1 wavelength. The reason for this is that 35 line pairs per millimeter is so far from the f/2.64 theoretical cutoff (688 line pairs per millimeter at 550 nanometers) that 1-wavelength of aberration has little effect. In fact, at the edge of the field, the modulation increased slightly even though the chromatic peak-to-peak increased. This is due to the changing nature of the OPD plots.

Figs. 2-5 and 2-6 show the transverse aberration and OPD ray plots for the system without a filter. The chromatic MTF and chromatic geometrical spot diagrams are given in Fig. 2-7. A flat spectral response was assumed for the MTF. The full field values are the average of 0.45 and 90-degree target orientation. The spots are for 350, 550, and 750 nanometers equally weighted. Lens data are given in Table 2-2. The central obstruction of Table 2-1 was included in both analyses. The results of inserting the filter are shown in Figs. 2-8, 2-9, and 2-10 and Table 2-3.

2.3.3 All-Reflecting B Lens, Configurations 2 and 3 (Figs. 2-2 and 2-3)

In this system it was necessary to place a general asphere on both the primary and tertiary with a hyperboloid on the secondary. Table 2-4 gives a summary of the performance. Note that the chromatic modulation at 35 line pairs per millimeter is 0.86 at the center of the field and 0.83 at the edge. The filter was not considered in this configuration since it would introduce less aberration than in the A system due to the higher f/number. Of course, in the final design it would be accounted for.

Figs. 2-11 and 2-12 show the transverse aberration and OPD ray plots for the system. The chromatic MTF and chromatic spot diagrams are given in Fig. 2-13 and lens data are presented in Table 2-5.

2.3.4 Cassegrain B Lens, Configurations 1 and 4 (Figs. 2-1 and 2-4)

In this system it was necessary to use general aspheres on both mirrors to correct higher order aberrations. Even then, astigmatism could not be fully corrected without inserting a doublet field correction lens. To control the color introduced by these lenses, the primary and secondary were given equal curvatures. This gave zero Petzval curvature, so that to give a flat field, the corrector lenses must have zero net power. It is then possible to control the axial color by using the same glass in each element.

Table 2-1 — All-Reflecting A Lens Data, Configurations 3 and 4

	Design	Specification
Focal length	200 mm (7.874 in.)	200 mm
f/number	2.64	2.64
Half field angle	2° 45'	1° 22' by 1° 47'
Back focus	210 mm (8.3 in.)	—
Spectral range	350 to 700 nm	350 to 700 nm
Axial obstruction ratio	0.46 (diameter), 0.21 (area)	—

No Filter

	Normalized Field Point ($\bar{H}$)		
	0.0	1.0	
Percent distortion	—	0.47	—
Optical path difference			
Monochromatic (550 nm)	0.001 λ	0.49 λ	—
Chromatic	0.001 λ	0.76 λ	—
Chromatic modulation at 35 lp/mm	0.88	0.86	0.65 across field

Recorrected for 0.1-Inch Filter

Optical path difference			
Monochromatic (550 nm)	0.001 λ	0.49 λ	—
Chromatic	1.16 λ	1.20 λ	—
Chromatic modulation at 35 lp/mm	0.87	0.84	0.65 across field

LENS NO.   6   LENS OUTPUT DATA

    SYSTEM DATA

            F-NUMBER =   -2.6400564   ENTRANCE PUPIL DISTANCE =   -12.2631525
         FOCAL LENGTH =   7.8741795   EXIT PUPIL DISTANCE =   5.1181000
           BACK FOCUS =   -8.3014208   GAUSSIAN IMAGE HEIGHT =   -0.3781963
         TOTAL LENGTH =   19.1281208   DP/DV =   0
        OBJECT HEIGHT =   -7.1635 15   AXIAL BEAM RADIUS =   1.4912900
      CHIEF RAY ANGLE =   .0480300   CHIEF RAY HEIGHT =   .5889992
      AXIAL RAY ANGLE =   0

        WAVELENGTHS   LOWER   .5500   MAJOR   .5500   UPPER   .5500

    SURFACE DATA

SURFACE NUMBER	RADIUS OF CURVATURE	THICKNESS	GLASS TYPE AND/OR N(D)	V(D)	APERTURE DIAMETER
OBJECT	INFINITE	1.4915 15			
1	INFINITE	8.6000	AIR		4.2129
2	-15.7480	-7.8740	-AIR		5.0282
	CONIC CONSTANT =	-1.0322130			
3	INFINITE	-1.0000	-AIR		.8126
4	INFINITE	-1.5527	-AIR		.9904
5	-5.6511	2.2000	AIR		1.4337
	CONIC CONSTANT =	-3.6996290			
6	INFINITE	2.9181	AIR		3.1104
7	-8.9140	-5.1181	-AIR		5.0852
	CONIC CONSTANT =	0			

    ASPHERIC COEFFICIENTS
AD= 1.3600510E-05   AE= 1.6500751E-07   AF= 1.8851960E-09   AG= 2.3643530E-11

6	INFINITE	-8.3034	-AIR		3.4455
IMAGE	INFINITE				

```
* CLIC P
ID A FOLDED 3 MIRROR
         LENS NO.    6
            DRAT   9  3  1  5  0  0
CS 3 3 3 3 3 3
APS 7
WV 3.5000000E-01 4.5000000E-01 5.5000000E-01 6.5000000E-01 7.0000000E-01
CF 2.5400000E-04 SF 2.500000E-04
OBJ B  1.0000000E-15  4.8030000E-02  1.4912900E+00  5.8899921E-01
  0 CV     .000000000  AIR
  1 CAI  4.5000000E-01
  1 CV     .000000000 TH  8.6000000E+00  AIR
  2 YMT     .000000000
  2 N15  -1.00000000  -1.00000000  -1.00000000  -1.00000000  -1.00000000
  2 RD  -1.5748000E+01
  2 CC  -1.032213E-00
```

```
3 PIN    2
3 CV        .330403000 TH  -1.0009000E+00
4 PIN    2
4 CV        .300000000 TH  -1.9527000E+00
5 TH    2.200000000E+00  AIR
5 RD   -5.651100000E+00
5 CC  -3.629629E+00
5 CA1   4.500000000E-01
6 CV        .000000000 TH   2.9181000E+00  AIR
7 PIN    2
7 TH   -5.1181000E+00
7 RD   -8.814000000E+00
7  ASP     .000000000   1.360081E-05   1.650075E-07   1.895104E-09   2.364353E-11
8 YMT       .000000000
8 CA1   7.500000000E-02
8 PIN    2
8 CV       .000000000
9 CV       .000000000
END
```

Table 2-3 — Preliminary Design Data for All-Reflecting A Lens, Configurations 3 and 4, With 0.1-Inch Filter

```
LENS NO.    7                        LENS OUTPUT DATA

      SYSTEM DATA

              F-NUMBER =   -2.6400564    ENTRANCE PUPIL DISTANCE =   -12.2631525
          FOCAL LENGTH =    7.8741795        EXIT PUPIL DISTANCE =    13.1839535
            BACK FOCUS =   -0.2355673    GAUSSIAN IMAGE HEIGHT =    -0.3781968
          TOTAL LENGTH =   19.1622673                  DP/DV =            0
         OBJECT HEIGHT =   -7.143E 15      AXIAL BEAM RADIUS =     1.4912900
       CHIEF RAY ANGLE =     .0480300       CHIEF RAY HEIGHT =      .5889992
       AXIAL RAY ANGLE =            0

         WAVELENGTHS         LOWER  .3500   MAJOR  .5500   UPPER  .7000

      SURFACE DATA
```

SURFACE NUMBER	RADIUS OF CURVATURE	THICKNESS	GLASS TYPE AND/OR N(D)	V(D)	APERTURE DIAMETER
OBJECT	INFINITE	1.491E 15			
1	INFINITE	8.6000	AIR		4.2129
2	-15.7480	-7.8740	-AIR		5.0282
	CONIC CONSTANT = -1.0327050				
3	INFINITE	-1.0000	-AIR		.8126
4	INFINITE	-1.9527	-AIR		.9904
5	-5.6511	2.2000	AIR		1.4337
	CONIC CONSTANT = -3.7221720				
6	INFINITE	2.9181	AIR		3.1102
7	-8.9143	-5.1181	-AIR		5.0849
	CONIC CONSTANT = 0				

```
      ASPHERIC COEFFICIENTS
AD= 1.3563673E-05  AE= 1.6423440E-07  AF= 1.8743530E-09  AG= 2.3495410E-11
```

8	INFINITE	-8.0000	-AIR		3.4453
9	INFINITE	-0.1000	- BK7 -1.516500	64.17	.8649
10	INFINITE	-0.2356	-AIR		.8438
IMAGE	INFINITE				

```
+ CLIC P
ID A FOLDED 3 MIRROR
          LENS NO.    7
          DRAT  9 3 1 5 0 0
CS 3 1 3 1 5 3
APS  7
WV 3.5000000E-01 4.5000000E-01 5.5000000E-01 6.5000000E-01 7.0000000E-01
CF 2.540000E+04 SF 5.000000E-04
OBJ B  1.0000000E-15  4.8030000E-02  1.4912901E+00  5.8999921E-01
  0 CV    .000060000  AIR
  1 CAI  4.5000000E-01
  1 CV    .000000000  TH  8.6000000E+00  AIR
```

```
 2 YMT          .300300000
 2 N15      -1.00000000   -1.00009000   -1.00000000   -1.70000000   -1.00000000
 2 RD      -1.5746000E+01
 2 CC      -1.032705E+00
 3 PIN     2
 3 CV          .00000000 TH   -1.0000000E+00
 4 PIN     2
 4 CV          .00000000 TH   -1.9527000E+00
 5 TH       2.20000000E+00   AIR
 5 RD      -5.6511000E+00
 5 CC      -3.722172E+00
 6 CAI      4.5000000E-01
 6 CV          .00000000 TH    2.9181000E+00   AIR
 7 PIN     2
 7 TH      -5.1151000E+00
 7 RD      -8.8143000E+00
 7 ASP         .00000000   1.356367E-05   1.642344E-07   1.874353E-09   2.349541E-11
 8 CAI      7.5000000E-01
 8 PIN     2
 8 CV          .00000000 TH   -8.0000000E+00
 9 CV          .00000000 TH   -1.0000000E-01  S N BK7
10 YUT          .00000000
10 PIN     2
10 CV          .00000000
11 CV          .00000000
END
```

Table 2-4 — All-Reflecting B Lens Data, Configuration 3

	Design	Specification
Focal length	1,000 mm (39.37 in.)	1,000 mm
f/number	4.4	4.4
Half field angle	0° 40'	0° 16' by 0° 21'
Back focus	178 mm (7.0 in.)	—
Spectral range	350 to 700 nm	350 to 700 nm
Axial obstruction ratio	0.31 (diameter), 0.096 (area)	—

	Normalized Field Point ($\bar{H}$)		
	0.0	1.0	
Percent distortion	—	0.07	—
Optical path difference			
Monochromatic (550 nm)	0.001 λ	0.09 λ	—
Chromatic	0.002 λ	0.14 λ	—
Chromatic modulation at 35 lp/mm	0.86	0.83	0.65 across field

```
LENS NO.    6                          LENS OUTPUT DATA

        SYSTEM DATA

              F-NUMBER =      -4.3996197    ENTRANCE PUPIL DISTANCE =        6.0000000
          FOCAL LENGTH =      39.3683549       EXIT PUPIL DISTANCE =       -2.2855181
            BACK FOCUS =     =11.6375320    GAUSSIAN IMAGE HEIGHT =       -0.4582477
          TOTAL LENGTH =      17.6375320                       DP/DV =             0
         OBJECT HEIGHT =      =5.208E 13       AXIAL BEAM RADIUS =        4.4738600
       CHIEF RAY ANGLE =       .0116400        CHIEF RAY HEIGHT =       -0.0698400
       AXIAL RAY ANGLE =              0

        WAVELENGTHS           LOWER   .3500   MAJOR   .5500   UPPER   .7000

        SURFACE DATA

SURFACE       RADIUS OF                      GLASS TYPE                    APERTURE
NUMBER        CURVATURE      THICKNESS       AND/OR N(D)          V(D)     DIAMETER


OBJECT        INFINITE       4.474E 15

   1          INFINITE        6.0000            AIR                         9.1783

   2          -16.0866       =4.3000           -AIR                         9.0372
        CONIC CONSTANT =          0
     ASPHERIC COEFFICIENTS
 AD= 2.8252310E-05  AF= 5.7130170E-08  AF= 1.4406230E-10  AG= 4.0811500E-13

   3          INFINITE       =2.4938           -AIR                         4.6558

   4          -5.8863         2.2017            AIR                         1.6439
        CONIC CONSTANT = =10.8515000

   5          INFINITE        2.3000            AIR                          .3890

   6          INFINITE        4.2992            AIR                         1.8795

   7          -9.2930        -6.0000           -AIR                         4.8495
        CONIC CONSTANT = -0.3516143
     ASPHERIC COEFFICIENTS
 AD=         0  AF= 3.8777940E-08  AF= -2.4053090E-09  AG=                      0

   8          INFINITE      -11.6375           -AIR                         2.9541

 IMAGE        INFINITE


* CLIC 0
ID 3 FOLDED 3 MIRROR
          LENS NO.    6
          DRAT  9  3  1  5  0  0
CS 3 1 3 1 5 3
APS  2
WV 3.5000000E-01 4.5000000E-01 5.5000000E-01 6.5000000E-01 7.0000000E-01
CF 2.540000E+04 SF 2.500000E-04
OBJ 8   1.0000000E-15   1.1640000E-02   4.4738600E+00  -6.9840000E-02
  0 CV     .000000000 AIR
  1 CAI  1.4000000E+00
  1 CV     .000000000 TH  6.0000000E+00  AIR
  2 N15  -1.00000000  -1.00000000  -1.00000000  -1.00000000  =1.00000000
  2 TH  =4.3000000E+00
```

```
2 RD  =1.6086600E+01
2  ASP    .000000000  2.825231E-05  5.713017E-08  1.440623E-10  4.081150E-13
3 CAI   4.0000000E-01
3 PIN   2
3 CV      .000000000 TH  -2.4833000E+00
4 YMT      .000000000
4 AIR
4 RD  =5.8863000E+00
4 CC -1.085150E-01
5 CV      .000000000 TH   2.0000000E+00  AIR
6 CV      .000000000 TH   4.2992000E+00  AIR
7 PIN   2
7 TH  =6.0000000E+00
7 RD  =9.2833000E+00
7  ASP -3.516143E-01     .000000000  3.877794E-08 -2.405309E-09    .000000000
8 YMT     .000000000
8 CAI  3.0000000E-01
8 PIN   2
8 CV      .000000000
9 CV      .000000000
END
```

TANGENTIAL FANS   SAGITTAL FANS
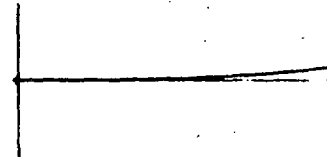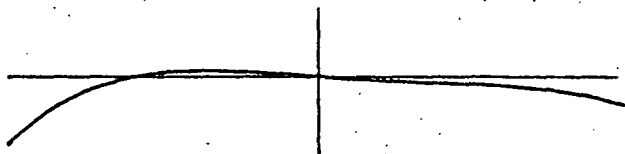
FULL FIELD
±2° 45'

0.7 FIELD

$\longrightarrow Y_{EN} \longrightarrow$

Y_{EN} ON AXIS

ENTRANCE
PUPIL   0.0003 inch

$\rightarrow X_{EN}$ TA

0.0003

$\longrightarrow X_{EN} \longrightarrow$
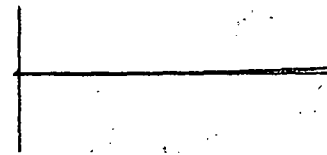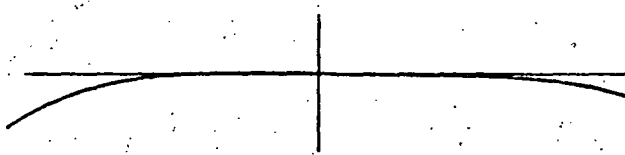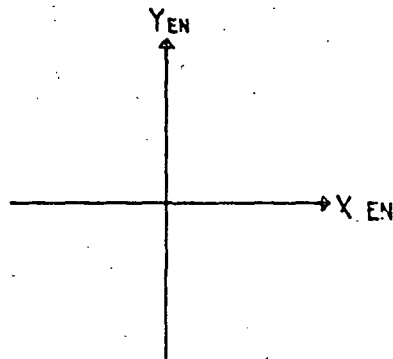
RAY TRACE   (TA = TRANSVERSE ABERRATION)

Fig. 2-5 — Transverse aberration plots for all-reflecting A lens without filter

32

TANGENTIAL FANS   SAGITTAL FANS

.35μ

.55μ

FULL FIELD

±2° 45'

.70μ

0.7 FIELD

⟵ Y_{EN} ⟶

Y_{EN}

ON AXIS

ENTRANCE
PUPIL

⟶ X_{EN} OPD

0.1000λ

0.1000

⟵ X_{EN} ⟶

RAY TRACE   (OPD = OPTICAL PATH DIFFERENCE)

Fig. 2-6 — OPD plots for all-reflecting A lens without filter

32

$\bar{H} = 0$ $\bar{H} = 0.7$ $\bar{H} = 1.0$

Airy disk diameter = 550 nm
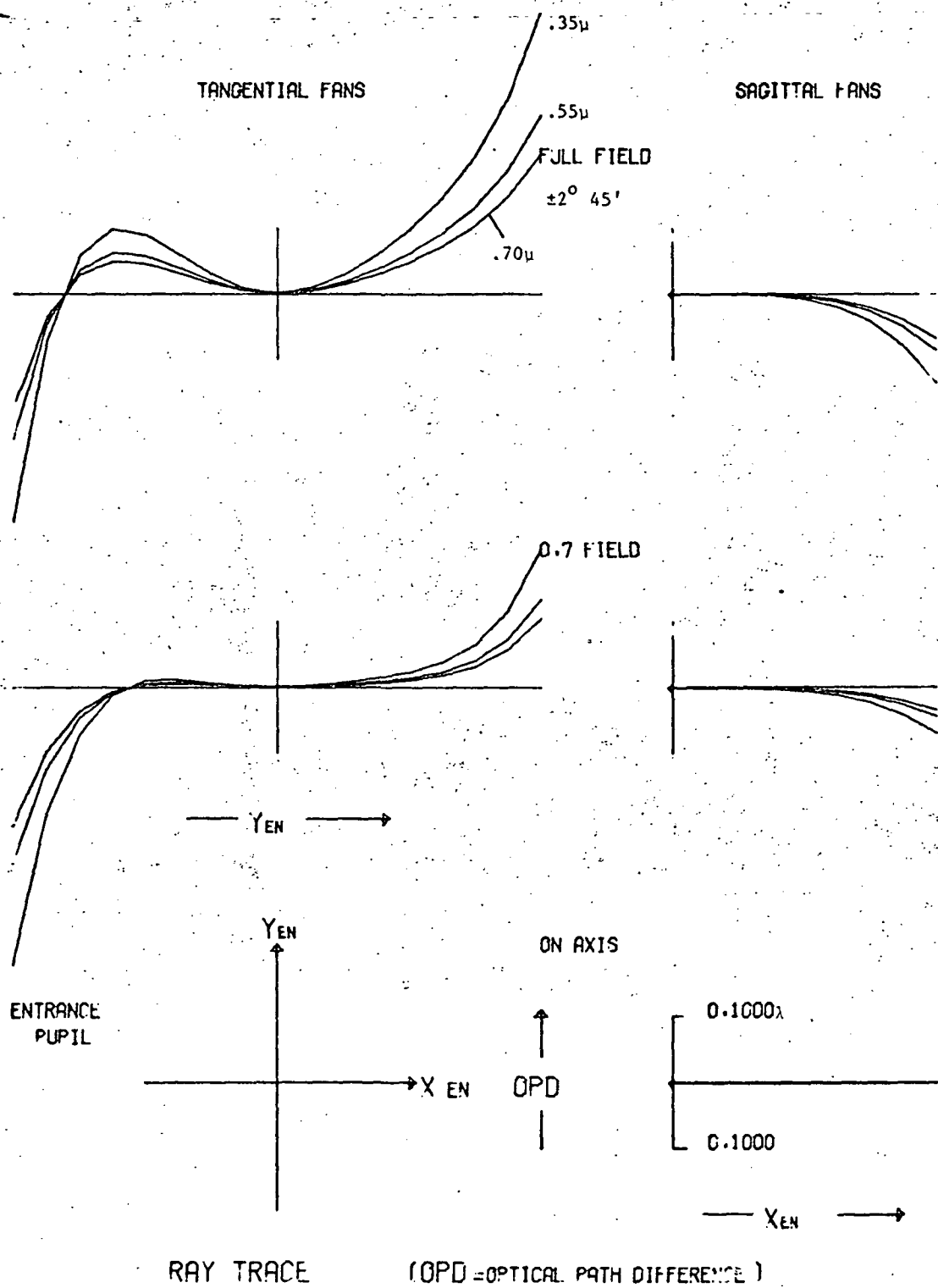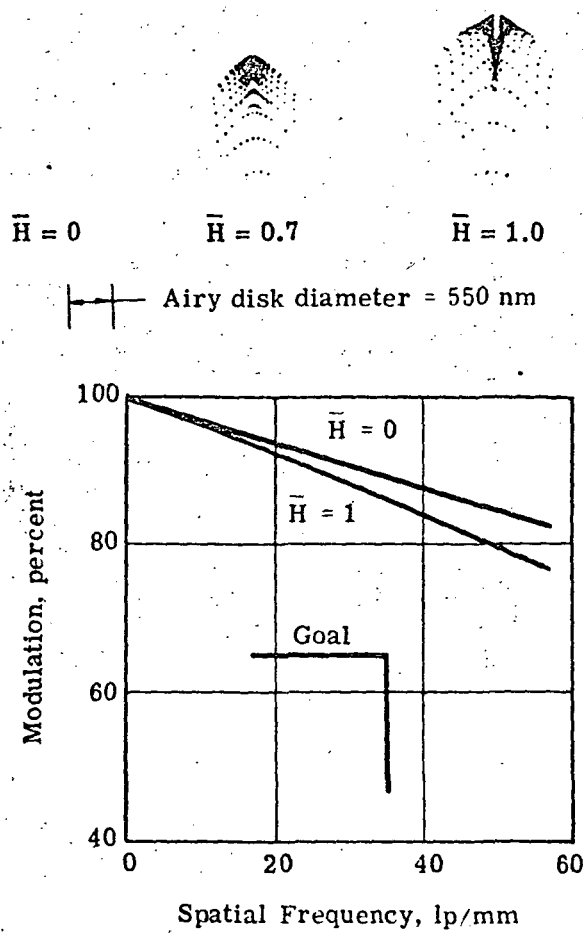
Fig. 2-7 — Chromatic MTF and geometrical spot diagrams for all-reflecting A lens without filter (350 to 700 nanometers)
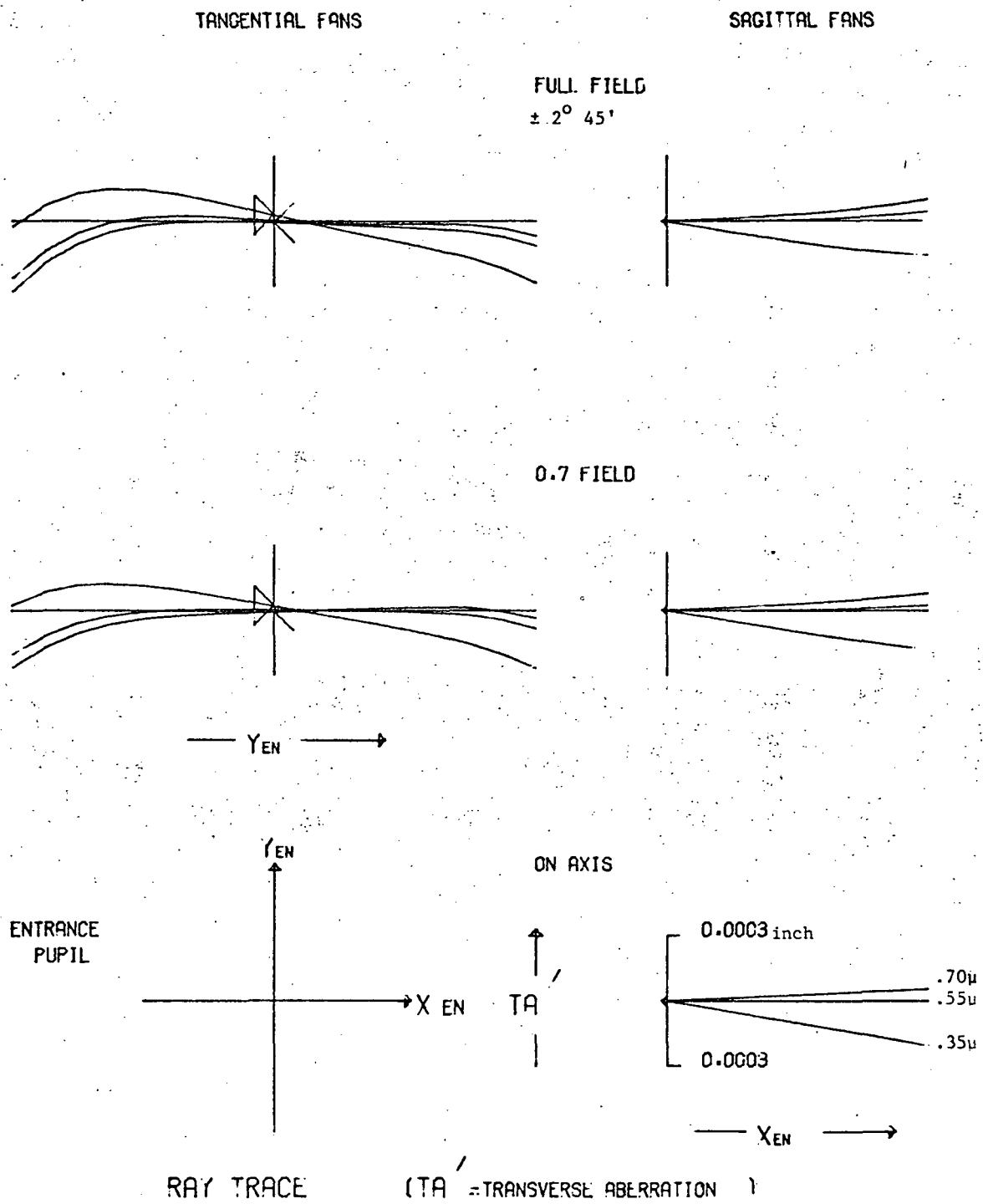
TANGENTIAL FANS   SAGITTAL FANS

FULL FIELD
± 2° 45'

0.7 FIELD

— Y$_{EN}$ —→

Y$_{EN}$ ON AXIS

ENTRANCE
PUPIL

→ X $_{EN}$ TA

0.0003 inch

.70μ
.55μ

.35μ

0.0003

— X$_{EN}$ —→

RAY TRACE   (TA = TRANSVERSE ABERRATION)

Fig. 2-8 — Transverse aberration plots for all-reflecting A lens with 0.1-inch filter

TANGENTIAL FANS   SAGITTAL FANS

FULL FIELD
± 2° 45'

C.7 FIELD
.35μ
.55μ
.70μ

Y_{EN}

Y_{EN} ON AXIS
ENTRANCE
PUPIL
                                                                .35μ

                                              0.5000 λ
                                                                .55u
                        X EN   OPD
                                                                .70u
                                              0.5000

                                                    Y_{EN}

RAY TRACE   (OPD-OPTICAL PATH DIFFERENCE)

Fig. 2-9 — OPD plots for all-reflecting A lens with 0.1-inch filter

.55μ

.70μ

.35μ

$\bar{H} = 0$ $\bar{H} = 0.7$ $\bar{H} = 1.0$

├──┤ Airy disk diameter = 550 nm

$\bar{H} = 0$

$\bar{H} = 1$

Goal

Modulation, percent

Spatial Frequency, lp/mm
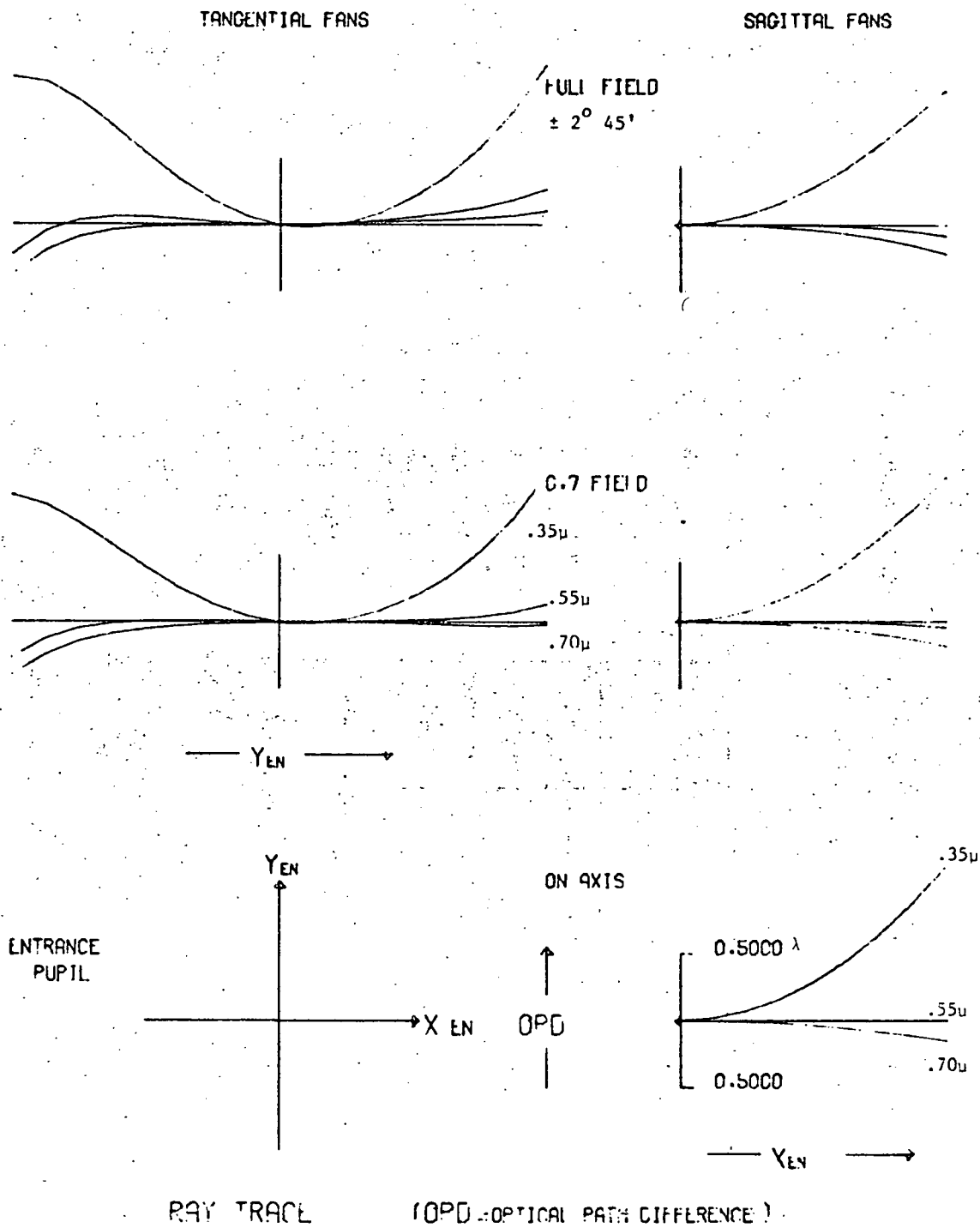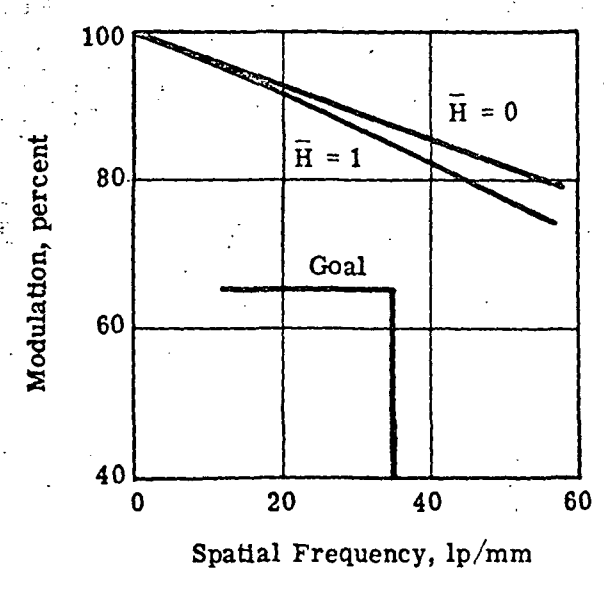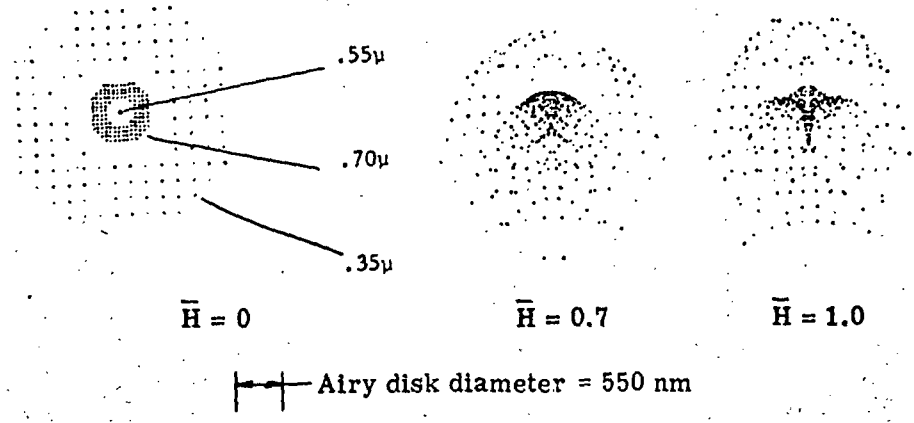
Fig. 2-10 — Chromatic MTF and geometrical spot diagrams for all-reflecting A lens with 0.1-inch filter

TANGENTIAL FANS   SAGITTAL FANS

FULL FIELD
± 0° 40'

0.7 FIELD

— Y$_{EN}$ ——→

Y$_{EN}$ ON AXIS

ENTRANCE
PUPIL   0.0003 inch

→X $_{EN}$ TA   C.0003

—— X$_{EN}$ ——→

RAY TRACE   TA TRANSVERSE ABERRATION
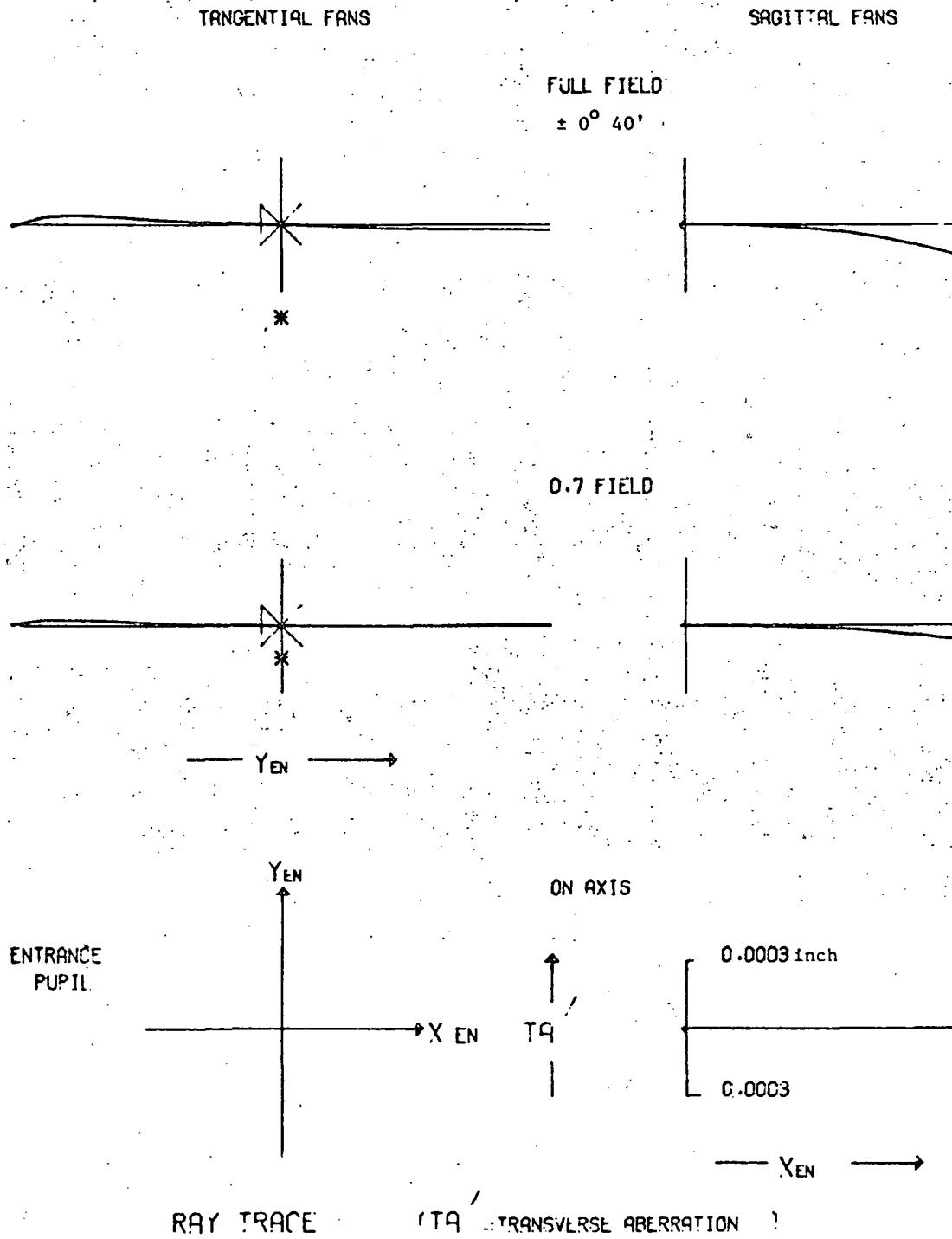
Fig. 2-11 — Transverse aberration plots for all-reflecting B lens

TANGENTIAL FANS   SAGITTAL FANS

FULL FIELD
±0° 40'

.35μ
.55μ
.70μ

C.7 FIELD

— Y_EN —→

Y_EN

ON AXIS

ENTRANCE
PUPIL

→ X_EN   OPD   0.1000 λ

0.1CCC

— X_EN —→

RAY TRACE   (OPD = OPTICAL PATH DIFFERENCE)
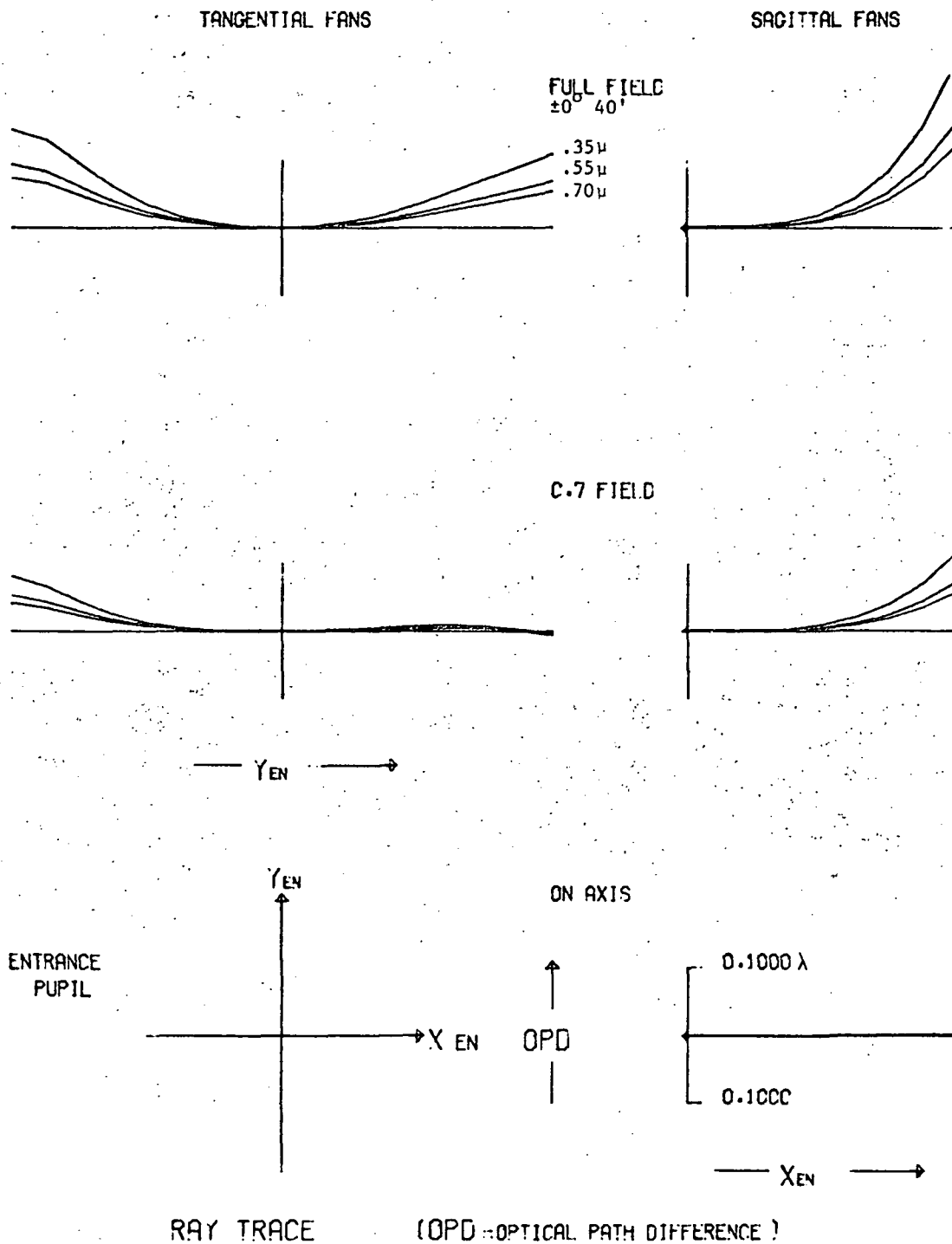
Fig. 2-12 — OPD plots for all-reflecting B lens
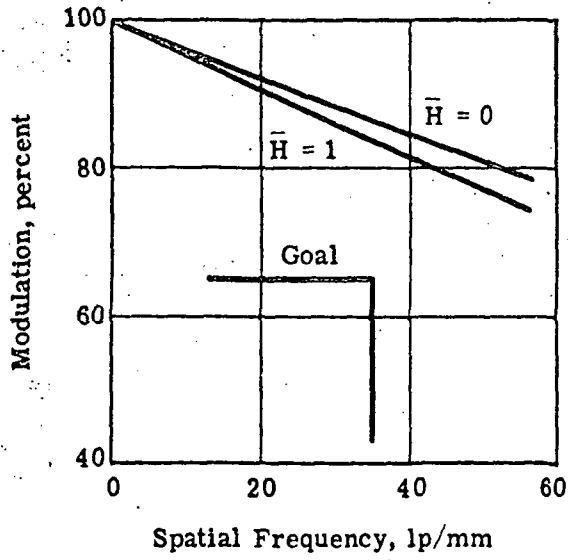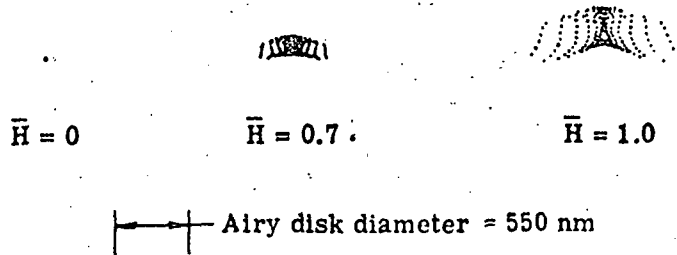
Fig. 2-13 — Chromatic MTF and geometrical spot diagrams for all-reflecting B lens (350 to 900 nanometers)

Table 2-6 summarizes the performance of this system. Note that the chromatic modulation at 35 line pairs per millimeter is 0.78 on axis and 0.72 at the edge of the field. In the final design an effort will be made to reduce the axial and lateral color without increasing the complexity of the field lens. Figs. 2-14 and 2-15 show the transverse aberration and OPD ray plots for the system. The chromatic MTF and chromatic geometrical spot diagrams are given in Fig. 2-16, and lens design data are given in Table 2-7. A scale drawing of the system is shown in Fig. 2-17.

2.3.5 All-Refracting A Lens, Configurations 1 and 2 (Figs. 2-1 and 2-2)

Design of an all-refracting lens for configurations 1 and 2 was felt to be beyond the scope of this study. Full exploration of available materials and configurations to achieve an optimized design would require lengthy expenditure of time, and system characteristics were considered of more importance than a detailed lens design. The preliminary study activities performed indicate the problem areas and suggest possible ways of overcoming them.

There are many factors affecting the design. Paramount is the wide spectral range extending into the ultraviolet (400 to 700 nanometers). This makes it extremely difficult to correct secondary color. Not only do the glasses have a very high dispersion, but many of them have low transmission at the low end of the spectral range. In order to find materials that can be used to reduce secondary color over this spectral range and still have high enough transmission, it is necessary to consider crystalline materials, e.g., calcium fluoride. But now the design task is compounded by materials that have very high coefficients of thermal expansion.

Besides the wide spectral region, the relatively fast cone angle of the system also makes secondary color the most difficult aberration to be corrected. Since secondary color is simply a longitudinal shift of the focal point with wavelength, in terms of optical path difference it is inversely proportional to the square of the f/number.

The requirement for a long back focus, at least 60 percent of the focal length, limits the design configurations. Those available from the file of conventional lens types are derivatives of the triplet, double-Gauss, and reverse telephoto.

An initial design study was undertaken to determine the seriousness of the design problem. A patent search yielded very few lenses designed for the ultraviolet. It became evident, however, that successful designs incorporated materials like fused quartz, calcium fluoride, and cesium iodide. Next, to find out how much secondary color existed in a standard design, a modified double-Gauss designed for the visible spectrum was recorrected for the desired spectral range. Thirty-eight wavelengths of secondary color resulted.

A search was made to find those materials that would be best suited to reduce secondary color and still have the high transmission required. To correct secondary color of a doublet, the partial dispersions of the two glasses must be equal. Thus by plotting reciprocal dispersion, ν, versus partial dispersion, P, it is possible to determine which glasses are the best candidates for correcting secondary color. This was done for a sampling of glasses that had a transmission of at least 80 percent at 350 nanometers, including those glasses normally used to reduce secondary color in the visible spectrum. The plot is included in Fig. 2-18. As can be seen, in order to find two materials with similar partial dispersions it was necessary to consider crystalline materials. Calcium fluoride coupled with UBK-7 or FK-6 glass are likely pairs. The materials search has not been completed. It would be advisable to continue looking for materials with maximum difference in ν (and equal P) to keep element powers as small as possible in order to reduce zonal aberrations.

In addition, a preliminary thermal analysis of three standard Itek lenses was conducted to establish the feasibility of a refractor on the basis of best performance over the specified temperature range (see Appendix G). It was found that a Petzval configuration would give the best performance, but the optics would not satisfy the mechanical packaging constraint of a 5- to 6-inch back focus.

Table 2-6 — Cassegrain B Lens Data, Configuration 4

	Design		Specification
Focal length	998 mm (39.30 in.)		1,000 mm
f/number	4.36		4.4
Half field angle	0° 40'		0° 16' by 0° 21'
Back focus	148 mm (5.85 in.)		—
Spectral range	350 to 700 nm		350 to 700 nm
Axial obstruction ratio	0.52 (diameter), 0.27 (area)		—
	Normalized Field Point ($\bar{H}$)		
	0.0	1.0	
Percent distortion	—	0.03	—
Optical path difference			
Monochromatic (550 nm)	$0.003\,\lambda$	$0.25\,\lambda$	—
Chromatic	$0.47\,\lambda$	$1.43\,\lambda$	—
Chromatic modulation at 35 lp/mm	0.78	0.72	0.65 across field

41

LENS NO. 18   LENS OUTPUT DATA

SYSTEM DATA

F-NUMBER =	4.3671823	ENTRANCE PUPIL DISTANCE =	9.7500000
FOCAL LENGTH =	39.3046407	EXIT PUPIL DISTANCE =	-19.2747712
BACK FOCUS =	5.8517492	GAUSSIAN IMAGE HEIGHT =	.4575060
TOTAL LENGTH =	18.8517492	DP/DV =	0
OBJECT HEIGHT =	-5.238E 13	AXIAL BEAM RADIUS =	4.5000000
CHIEF RAY ANGLE =	.0116400	CHIEF RAY HEIGHT =	-0.1134900
AXIAL RAY ANGLE =	0		

WAVELENGTHS   LOWER .3500   MAJOR .5500   UPPER .7000

SURFACE DATA

SURFACE NUMBER	RADIUS OF CURVATURE	THICKNESS	GLASS TYPE AND/OR V(D)	V(D)	APERTURE DIAMETER
OBJECT	INFINITE	4.500E 15			
1	INFINITE	9.7500	AIR		9.3192
2	INFINITE	.2500	AIR		9.0900
3	-41.2762	-10.8000	-AIR		9.0899

CONIC CONSTANT = -2.1410340
ASPHERIC COEFFICIENTS
AD=   0 AE= 2.9306760E-09 AF= 1.9931640E-11 AG=   0

4	-41.2762	12.4000	AIR		4.6523

CONIC CONSTANT = -34.7041400
ASPHERIC COEFFICIENTS
AD=   0 AE= 4.5432430E-07 AF= -5.8556730E-10 AG=   0

5	10.8872	.3000	BK7 1.516800	64.17	2.1593
6	37.7249	.2000	AIR		2.1270
7	-8.5294	.2000	BK7 1.516800	64.17	2.0935
8	-20.5730	0	AIR		2.0713
9	INFINITE	0	AIR		2.0663
10	INFINITE	5.8517	AIR		2.0663
IMAGE	INFINITE				

```
* CLIC P
ID B CASSEGRAIN
        LENS NO.   18
        DRAT  9 1 3 5 0 0
CS 3 1 3 1 5 3
APS  2
WV 3.5000000E-01 4.5000000E-01 5.5000000E-01 6.5000000E-01 7.0000000E-01
CF  2.540000E+04  SF  2.500000E-04
OBJ B   1.0000000E-15   1.1640000E-02   4.5000000E+00  -1.1349000E-01
   0 CV     .000000000  AIR
   1 CAI   2.3500000E+00
```

```
  1 CV       .000000000 TH   9.7500000E+00  AIR
  2 CV       .000000000 TH   2.5000000E-01  AIR
  3 N15  -1.00000000   -1.00000000   -1.00000000   -1.00000000   -1.00000000
  3 TH  -1.0800000E+01
  3 RD  -4.1276200E+01
  3  ASP -2.141034E+00    .000000000  2.930676E-09  1.983164E-11    .000000000
  4 TH   1.2400000E+01  AIR
  4 RD  -4.1276200E+01
  4  ASP -3.470414E+01    .000000000  4.343248E-07 -5.855673E-10    .000000000
  5 CV   9.1851064E-02 TH   2.0000000E-01 S   BK7
  6 CV   2.6507685E-02 TH   2.0000000E-01  AIR
  7 CV  -1.1724184E-01 TH   2.0000000E-01 S   BK7
  8 CV  -4.8607343E-02 TH    .000000000  AIR
  9 CV       .000000000 TH    .000000000  AIR
 10 YMT      .000000000
 10 CV       .000000000  AIR
 11 CV       .000000000
END
* EJOB
```

FULL FIELD
±0° 40'

0.7 FIELD

.35μ

.55μ

.70μ

Y_{EN}

Y_{EN}

ON AXIS

ENTRANCE
PUPIL

C.CCC3 inch

.35μ

X_{EN} TA

.55μ

.70μ

C.CCC3

X_{EN}

RAY TRACE   (TA = TRANSVERSE ABERRATION)
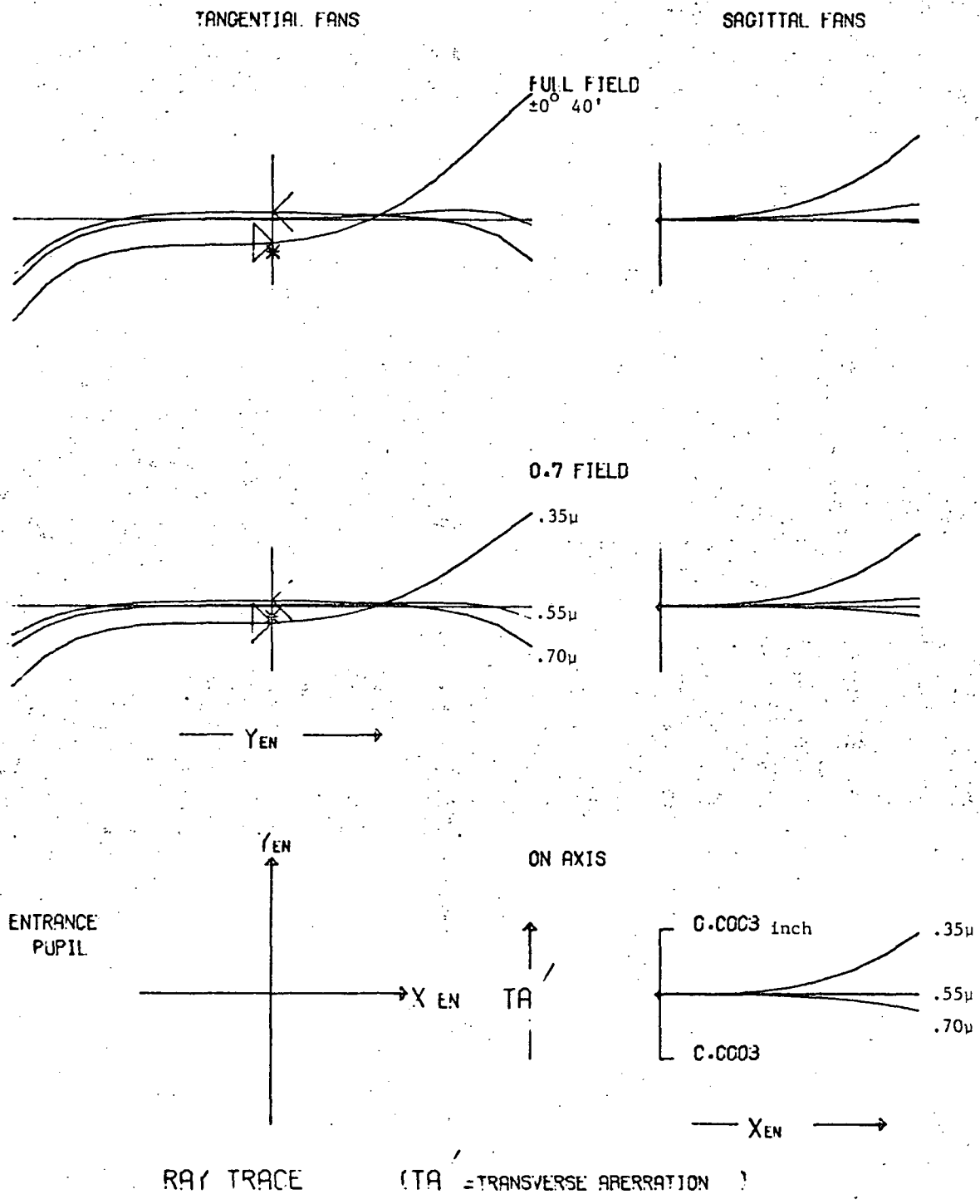
Fig. 2-14 — Transverse aberration plots for Cassegrain B lens

TANGENTIAL FANS   SAGITTAL FANS

FULL FIELD
±0° 40'

0.7 FIELD

.35μ

.55μ
.70μ

— r_EN —→

Y_EN   ON AXIS

ENTRANCE   0.5000 λ   .35μ
PUPIL
                              →X_EN   OPD   .50μ
                                                                             .70μ
                                                  0.5000

RAY TRACE   (OPD = OPTICAL PATH DIFFERENCE)   — X_EN —→
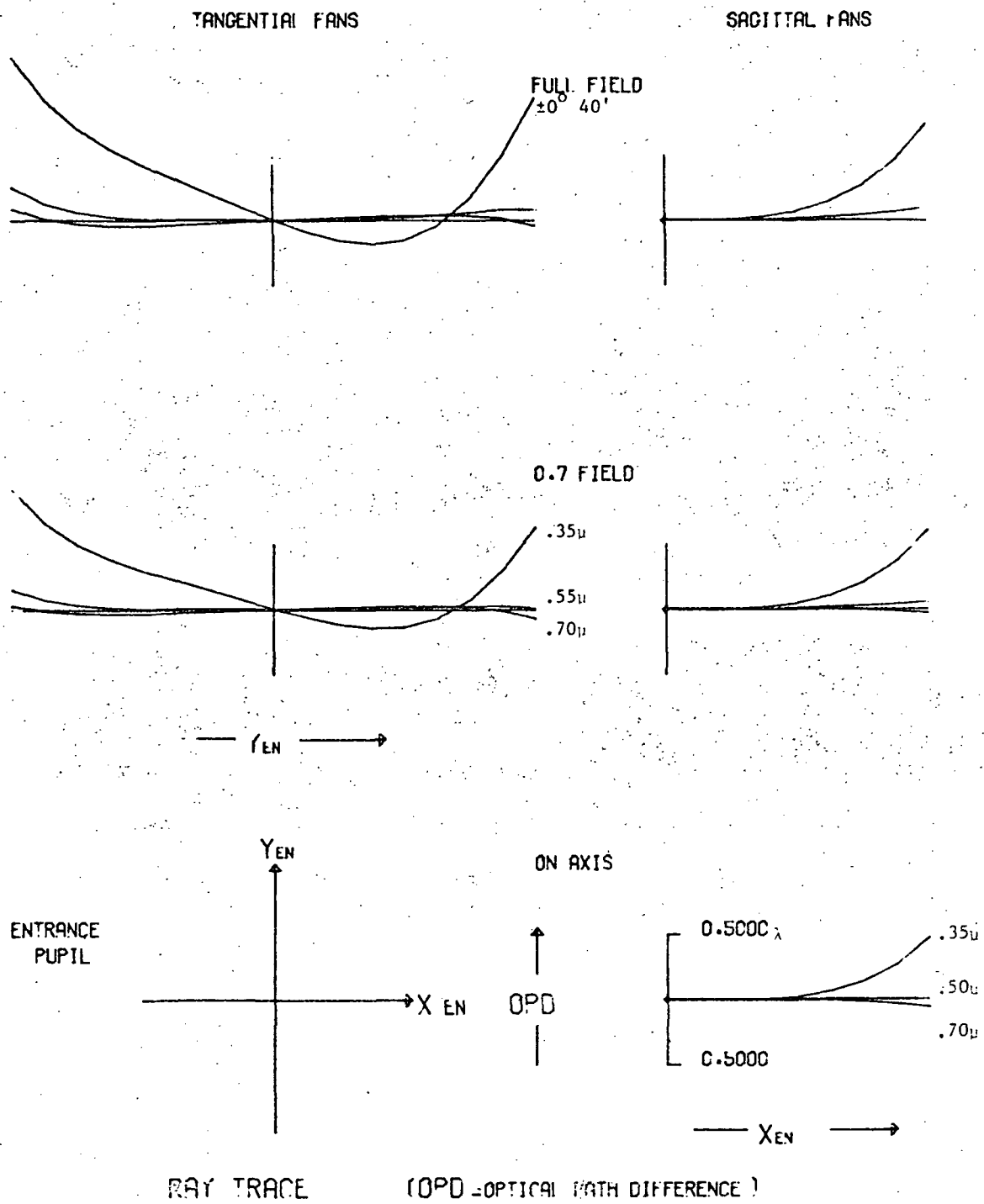
Fig. 2-15 — OPD plots for Cassegrain B lens

$\bar{H} = 0$ $\quad\quad\quad$ $\bar{H} = 0.7$ $\quad\quad\quad$ $\bar{H} = 1.0$

|←——→| Airy disk diameter = 550 nm
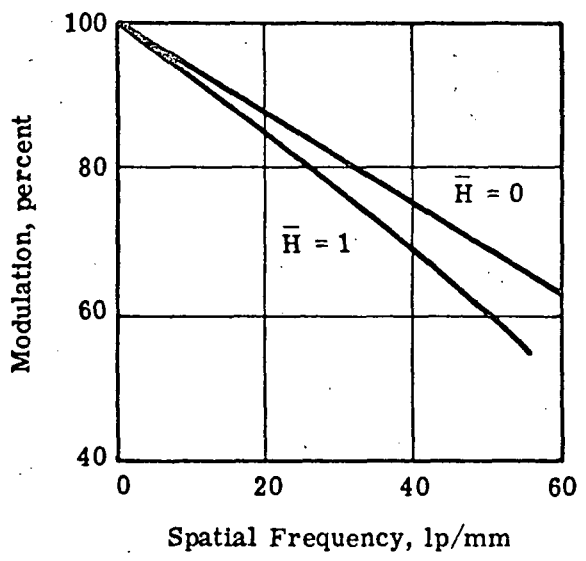
Fig. 2-16 — Chromatic MTF and geometric spot diagrams for Cassegrain B lens (350 to 700 nanometers)
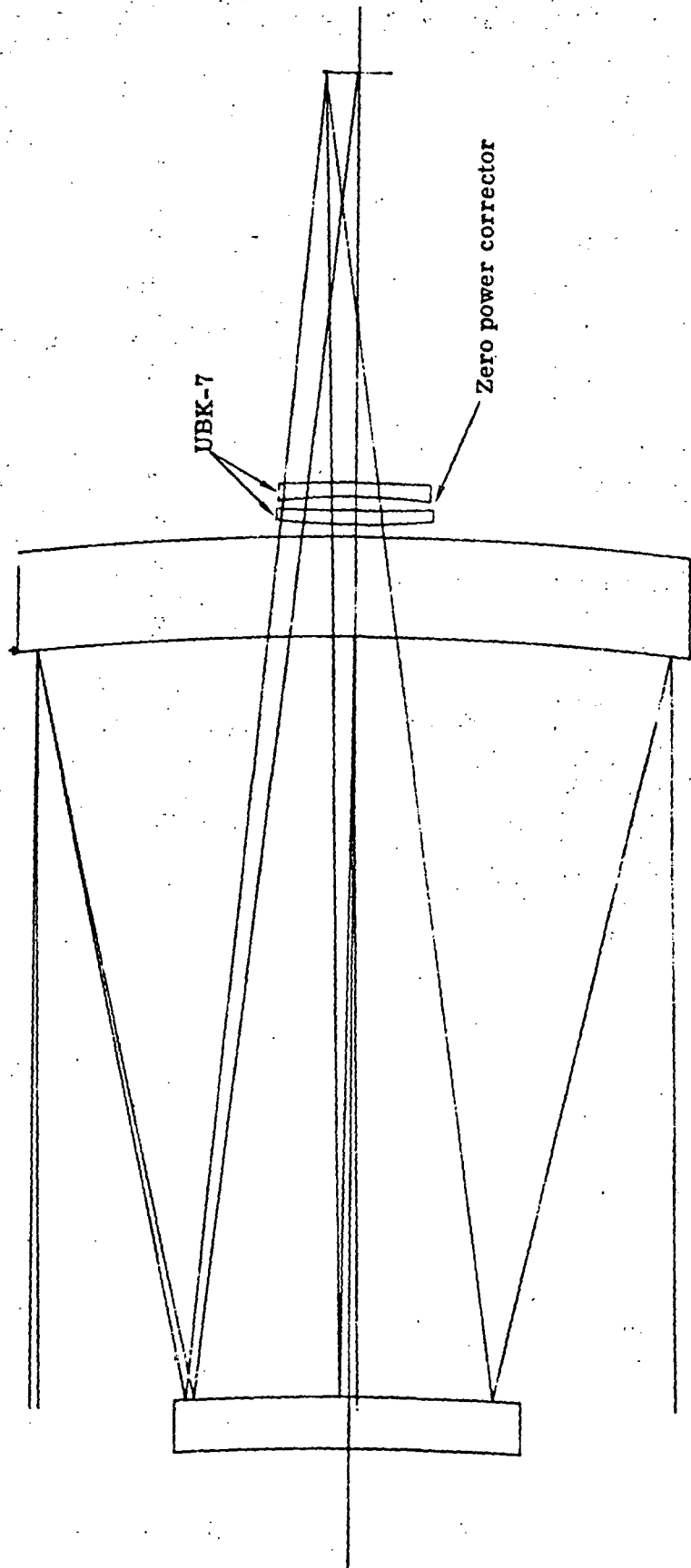
Fig. 2-17 — Scale drawing of Cassegrain B lens
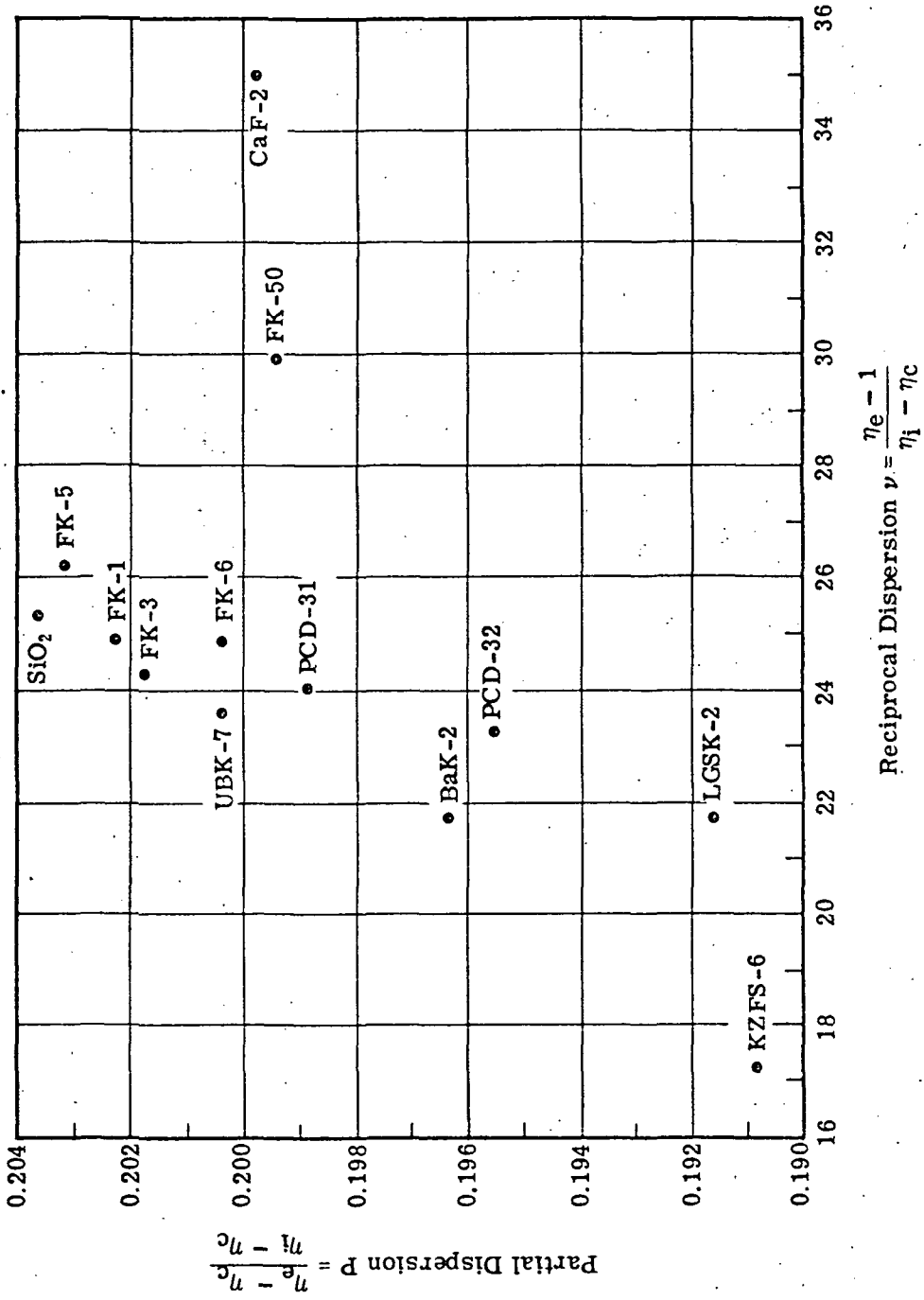
Fig. 2-18 — Reciprocal dispersion versus partial dispersion for several glass types

It was felt in the preliminary study phase that any further design effort would be based on starting with an entirely new lens employing the materials found to be best suited to reducing secondary color as well as meeting the environmental requirements. The large back focus limits the lens types to derivatives of the achromatic triplet, double-Gauss, and reverse telephoto.

2.4 PRELIMINARY STRUCTURAL CONSIDERATIONS AND WEIGHT ESTIMATES FOR CONFIGURATIONS 1 AND 3

The major emphasis during the preliminary studies was on the general structural design considerations for the optics study. These considerations are summarized in Fig. 2-19, which shows the interrelationships of major tasks with inputs and the form of expected results. Preliminary mechanical layouts were generated for both configurations 1 and 3, in addition to weight estimates for both configurations.

The preliminary layout for configuration 3 (Itek Dwg 186098) is a shell-type structure. This approach was taken in the interest of structural simplicity. The configuration consists basically of three intersecting tubes, the first holding the A lens secondary, tertiary, and B lens tertiary in alignment with the switching mirror. The second and third tubes, both on axes perpendicular to the first tube, hold the A lens primary and B lens primary with secondary.

The two vidicons are supported by a separate structure and not attached to the shell, to prevent any direct loads from the vidicons going into the lens cell. Although unattached to the cell, the vidicon support structure will tie back to the cell mounting system to prevent any relative motion between the lens and the vidicon.

The preliminary layout for configuration 1 (Itek Dwg 186097) incorporates a shell structure for the B lens Cassegrain with correctors and a truss-type structure to hold the all-refracting A lens cell, A lens diagonal, switching mirror, filter wheels, shutters, vidicons, and all drives.

The results of a preliminary weight analysis based on the layout of configurations 1 and 3 are shown in Table 2-8. Both configurations met the original 25-pound weight limitation. (The system study phase later allowed for a system weight of 30 pounds.)
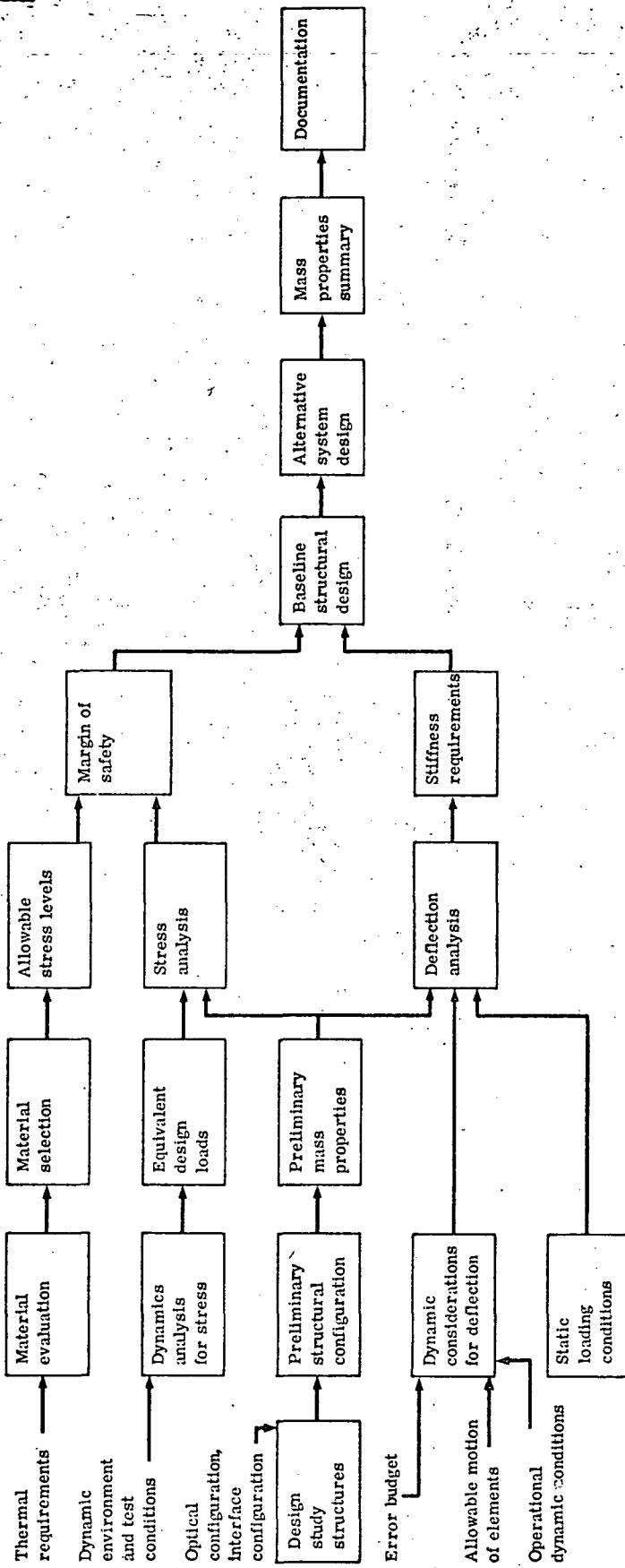
Fig. 2-19 — Structural analysis flowchart

Table 2-8 — Preliminary Weight Estimates

Item	Configuration 1			Configuration 3		
	A Lens, pounds	B Lens, pounds	Total, pounds	A Lens, pounds	B Lens, pounds	Total, pounds
Glass (ULE)	3.62	2.83	6.45	2.5	4.6	7.1
Structure (titanium)	1.8	6.2	8.0	3.35	5.4	8.75
Intermediate structure (titanium)	3.8 Includes vidicon support structure	—	3.8	1.7 Vidicon structure not included	—	1.7
Drive motor/solenoids	1.5	—	1.5	1.0	—	1.0
Filter wheels	0.41	—	0.41	0.41	—	0.41
Switching mirror	0.30	—	0.30	0.30	—	0.30
Subtotal	—	—	20.45	—	—	19.25
20% contingency	—	—	4.09	—	—	3.85
Total	—	—	24.54	—	—	23.10

3. SYSTEM STUDY PHASE—OPTICAL SYSTEM DESIGN

3.1 CONFIGURATION FOR SYSTEM STUDY

The results of the preliminary studies phase (Section 2) were presented at an Interim Design Conference at JPL on 16 March 1972. The four proposed configurations were discussed. Lens design data was not supplied for the refractor of configurations 1 and 2, since it was agreed that a detailed design of a refractor was beyond the scope of this study.

The configuration selected at the meeting for system study by JPL personnel was a modified version of Itek configuration 1. The technical directive given by JPL for the system study phase is reproduced as Appendix C, Technical Direction Memorandum No. 2, dated 23 March 1972.

The basic task of the study phase was to perform a system study of configuration 1, as shown in Fig. 3-1, with emphasis on mechanical, structural, and thermal design. The transfer mirror was to be designed to be inserted only in the event of the narrow angle (B) vidicon failure. If the event were to occur during the mission, wide angle (A) photography would be discontinued. Thus, provision for refocusing the A lens (as conceived in the preliminary phase) would not be required. It was understood that a prescription design for a refractor was beyond the scope of the study program. Thus, the requirement for the refractor design was to establish a best estimate so far as optical, mechanical, and thermal characteristics were concerned.

3.2 SYSTEM OPTICAL PRESCRIPTIONS

3.2.1 Narrow Angle (B) Lens—Cassegrain Optics and Baffling

The optics prescription for the narrow angle (B) Cassegrain for the system was presented in Section 2.3.4, and the lens data from that section apply to this discussion.

In this system it was necessary to use general aspherics on both mirrors to correct higher order aberrations. Even then, astigmatism could not be fully corrected without inserting a doublet field correction lens. To control the color introduced by these lenses, the primary and secondary were given equal curvatures. This gave zero Petzval curvature, so that to give a flat field the corrector lenses must have zero net power. It is then possible to control the axial color by using the same glass in each element.

Table 2-6 gives a summary of the performance of this system. Note that the chromatic modulation at 35 line pairs per millimeter is 0.78 on axis and 0.72 at the edge of the field. In the final design an effort will be made to reduce the axial and lateral color without increasing the complexity of the field lens. Figs. 2-14 and 2-15 show the transverse aberration and OPD ray plots for the system. The chromatic MTF and chromatic geometrical spot diagrams are given in Fig. 2-16, and scale drawing of the system is shown in Fig. 2-17.

52
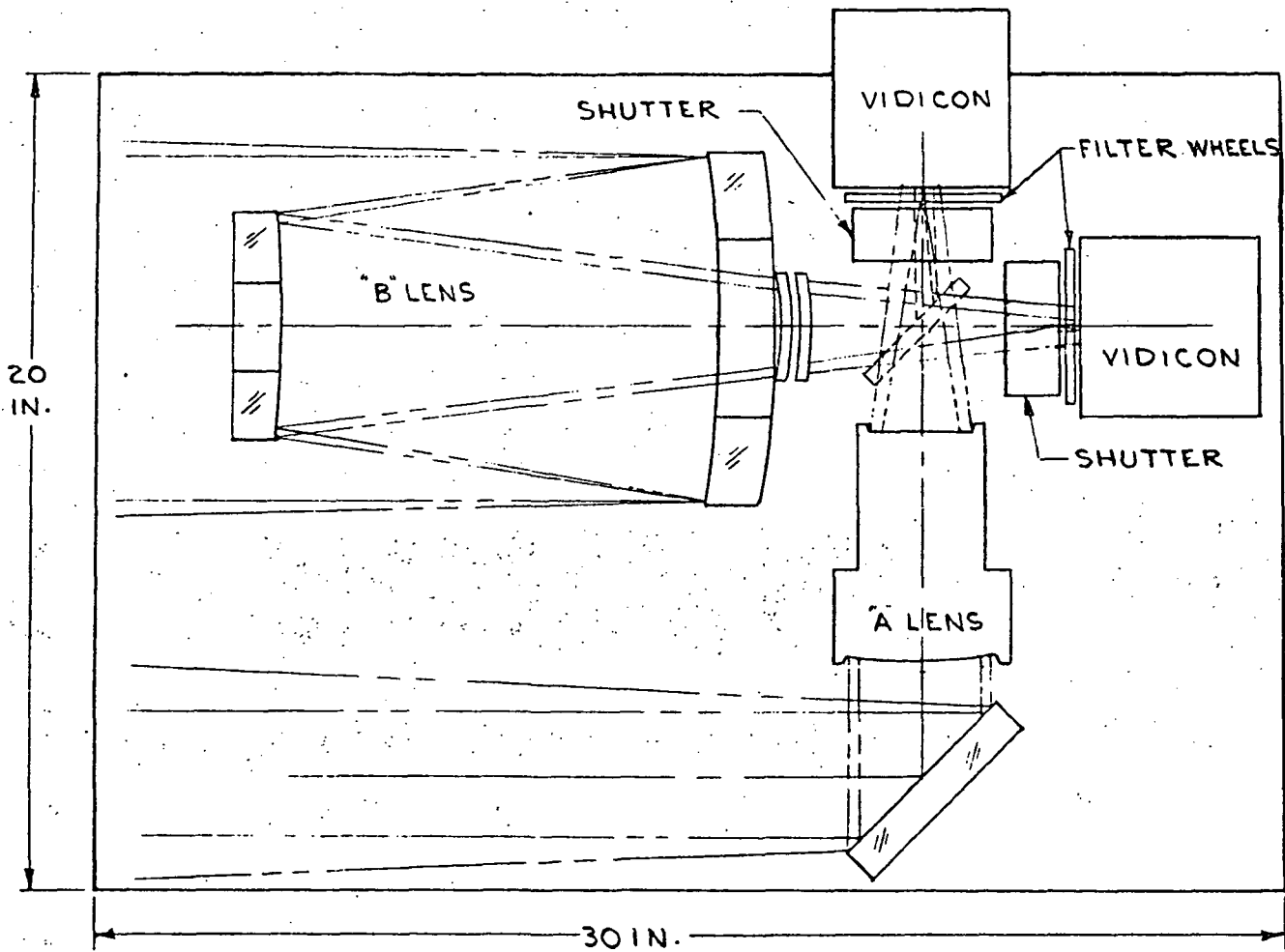
Fig. 3-1 — Configuration for system study—all-refracting A lens,
Cassegrain B lens with correctors

53

A preliminary study of the Cassegrain optics (without window) for the B lens has shown that there are two alternatives for the baffle design as shown in Fig. 3-2. Baffle 1 allows no direct light outside the field of view to reach the image format, but does allow some direct light to reach the refractive elements. Baffle 2 has a slightly larger central obstruction and allows no direct light to reach either the image format or the refractive element. The baffle 1 scheme is shown in the system mechanical layout presented in this report. Note that in both designs no baffling is required in front of the secondary surrounding the incoming beam. However, both designs allow direct light to reach the inside of the primary baffle. Scattered light from this surface could reach the image format. Two methods are possible to eliminate this if it is expected to be a problem. The first is to mount a series of fins on the inside of the primary baffle acting as stops just outside the beam. The second is to mount a cylindrical baffle outside the incoming beam and extending a short distance in front of the secondary.

A computer capability for performing a quantitative evaluation of glare in the image format is not available. However, as baffle 2 demonstrates, a baffle can be designed that makes it impossible for any direct light outside the field of view to reach either the image format or the refractive elements.

The modulation calculation for the preliminary optical designs was done with a central obstruction diameter ratio of 0.522. Baffle 1 has an obstruction of 0.555, and baffle 2 has an obstruction of 0.605. The unbaffled obstruction is 0.482. During the final design effort it will have to be determined whether or not this increase in obstruction ratio can be tolerated in conjunction with improved correction of residual aberrations to yield the required modulation.

If a window is to be employed in front of the B Cassegrain, then baffling must be considered for it. It is not possible to baffle the window so that no light from outside the field of view can reach it. However, it is possible to shield it from direct sunlight or other light under certain conditions.

It is unlikely that the optics would be pointed closer to the sun than about 45 degrees, since it would be looking at too steep an incident angle at the illuminated side of the planet. Direct sunlight could be prevented from striking the window under these conditions by erecting in front of the window a sunshade whose length is equal to the diameter of the window. It should be noted that the use of a sunshade eliminates the need for fins inside the baffle mounted on the primary.

It might be advantageous to mount the secondary directly onto the window, thus eliminating the spider. This would require a thicker window, however, and a weight comparison would have to be made.

If a window is to be placed in front of the A refractor, a sunshade should be added for the same reason as in the B optics. It need not be longer than the diameter of the window. Also, it may be possible to position the A and B systems so that the A lens is shielded from the sun by the B Cassegrain, thus providing further protection from direct sunlight.

3.2.2 Wide Angle (A) Lens—All-Refracting Optics (Preliminary Design)

From the preliminary thermal analysis of three standard Itek lenses (Appendix G), it was concluded that the apochromatic Petzval lens would give the best performance over the temperature range. Unfortunately, it could never be made to give the required back focus of 5 to 6 inches. The double-Gauss, examined in the thermal analysis (Appendix G), is shown in Fig. 3-3. Based on temperature changes alone, it had an MTF less than 65 percent. However, it has the potential of being modified to yield the required modulation and back focus. Thus, the optical design problem is to improve the performance of the modified double-Gauss while increasing its back focus. This means reducing its secondary color. To meet this end at f/2.64, special glasses will have to be employed. However, experience in designing fast apochromatic lenses has demonstrated that it should be possible to obtain the desired modulation over the required temperature range.

After the above thermal analysis was performed, a second double-Gauss lens of short focal length that is a better starting point was found. This lens, scaled to proper focal length, f/number, and field, is shown in Fig. 3-4. Even though it has slightly worse correction, its back focus is long to start with since it has no field flattener. Its transverse aberration ray plots and optical path difference ray plots are shown in Figs. 3-5 and 3-6.

Table 3-1 lists the additional activities required to obtain a preliminary design from the modified double-Gauss of Fig. 3-4. The preliminary design would be carried sufficiently far to demonstrate the feasibility of obtaining the desired modulation across a flat field.

3.2.3 Optical Coatings

A fairly complete analysis is presented in Appendix F for potential all-reflecting systems where combinations of silver and aluminum mirrors could be employed to achieve the desired 40 percent transmission over the entire spectral range. The data presented in Figs. F-1 through F-6 will be employed for the considerations presented here for the presently defined wide and narrow angle systems.

The wide angle A lens (refractor design) baseline will be considered to be represented by the double-Gauss shown in Fig. 3-4. This design has 14 air-glass surfaces in the lens (assuming no cemented surfaces) plus two refractive (air-glass) surfaces at the filters. In addition, a fold mirror will be required. This is assumed to be a protected silver design. The data in Fig. F-3 indicate that the 400-nanometer transmittance of a 16-surface plus one mirror optical train would be about 75 percent, while the 700-nanometer value would be about 70 percent. These transmittance values neglect variations in the substrate indicies to higher values, which may increase the transmittance at the middle of the spectral range while lowering it near the extremes. The special glasses suggested for this lens will probably be of higher index. The estimated transmittance values will, however, be somewhat similar to the average of most lenses. An additional loss due to real surface effects should reduce the transmission still further by about 10 percent. Over and above these losses, absorption in the glass will produce a further reduction of about 20 percent in the blue region and perhaps about 10 percent in the red. If we cascade these data, we obtain a resultant transmission of about 54 percent in the blue (400 nanometers) and about 57 percent in the red (700 nanometers) for the all-refracting lens. A more complete analysis can be performed after the design is complete. However, the present indications are for significantly greater than minimum performance over the 400- to 700-nanometer spectral range.

The narrow angle Cassegrain B lens baseline will be considered to be the design shown in Fig. 3-1. One additional refractor is present in the filter wheel, increasing the number of refractor surfaces to six. A cursory review, which includes three refractors (six surfaces) and two protected silver mirrors, yields transmittances of approximately 83 percent at the 400- and 700-nanometer extremes. Additional losses must be included to account for absorption and real surface effects. These would produce reductions to about 74 percent without considering either the central obscuration or lower transmittance values in the 350- to 400-nanometer region. A further reduction would occur if the switching mirror were required to shift the image to the wide angle vidicon.

Some improvement may be obtainable from multilayer designs. However, broad bands, especially to 350 nanometers, preclude normal commercial designs. The possibility of multilayers would have to be reviewed during a final design phase. All angles in both designs appear sufficiently small, thereby precluding any significant variations in transmittance.

If a window were to be included in either design, an additional reduction in transmission would be experienced. It would be possible, however, in the Cassegrain design to locate the secondary on the window. This approach has been employed successfully in other Itek-produced optical systems.

No interior fins are required
if this area is baffled.

Region 1

Baffle 1: Obstruction diameter ratio = 0.555.
Direct light can reach lenses.

Interior fins may be desired to prevent
diffusely scattered light from reaching
lens unless region 1 is baffled.

Direct light
on lens

Baffle 2: Obstruction diameter ratio = 0.605.
No direct light can reach lenses.

Interior fins may be desired to prevent
diffusely scattered light from reaching
lens unless region 2 is baffled.

Region 2

No interior fins are required
if this area is baffled. Note
that this baffle is not necessary
to keep direct light from lenses.

Fig. 3-2 — Baffling techniques
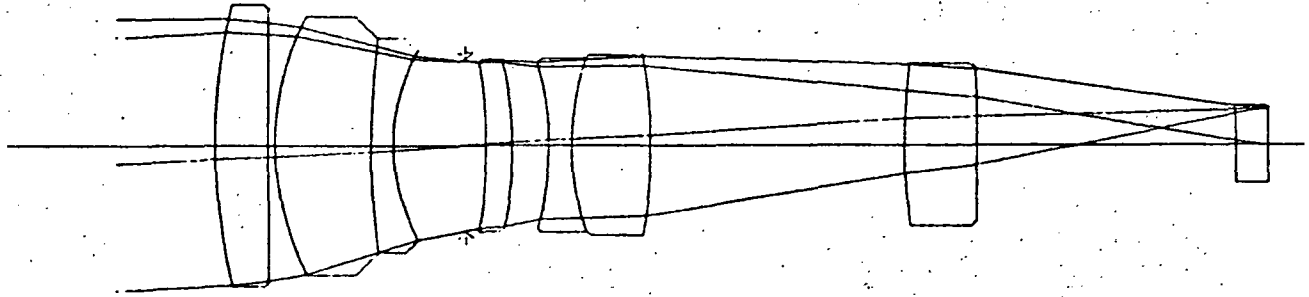
Fig. 3-3 — Modified f/3.0 double-Gauss used in thermal analysis
(scaled to proper field)
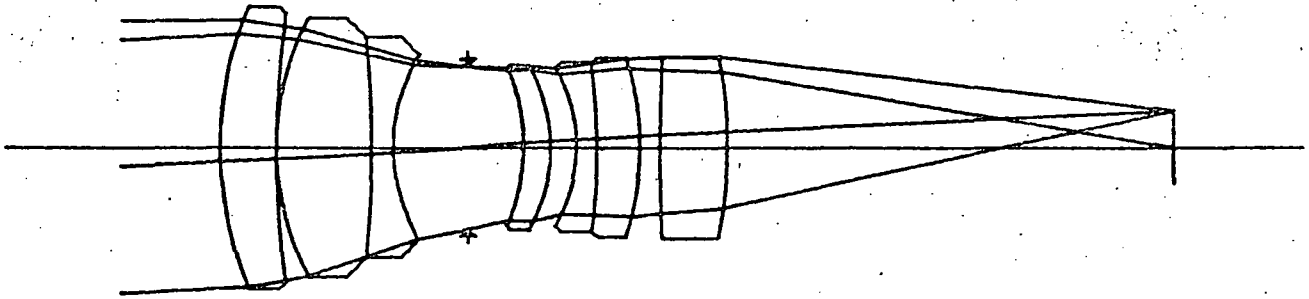
Fig. 3-4 — f/3.0 double-Gauss used as starting point for A lens design

57

TANGENTIAL FANS   SAGITTAL FANS

FULL FIELD

0.7 FIELD

Y_{EN}

Y_{EN} ON AXIS

ENTRANCE PUPIL

X_{EN} TA′

.48u

0.0010 inch

.69u

.58u

0.0010

X_{EN}

RAY TRACE   (TA′ =TRANSVERSE ABERRATION)
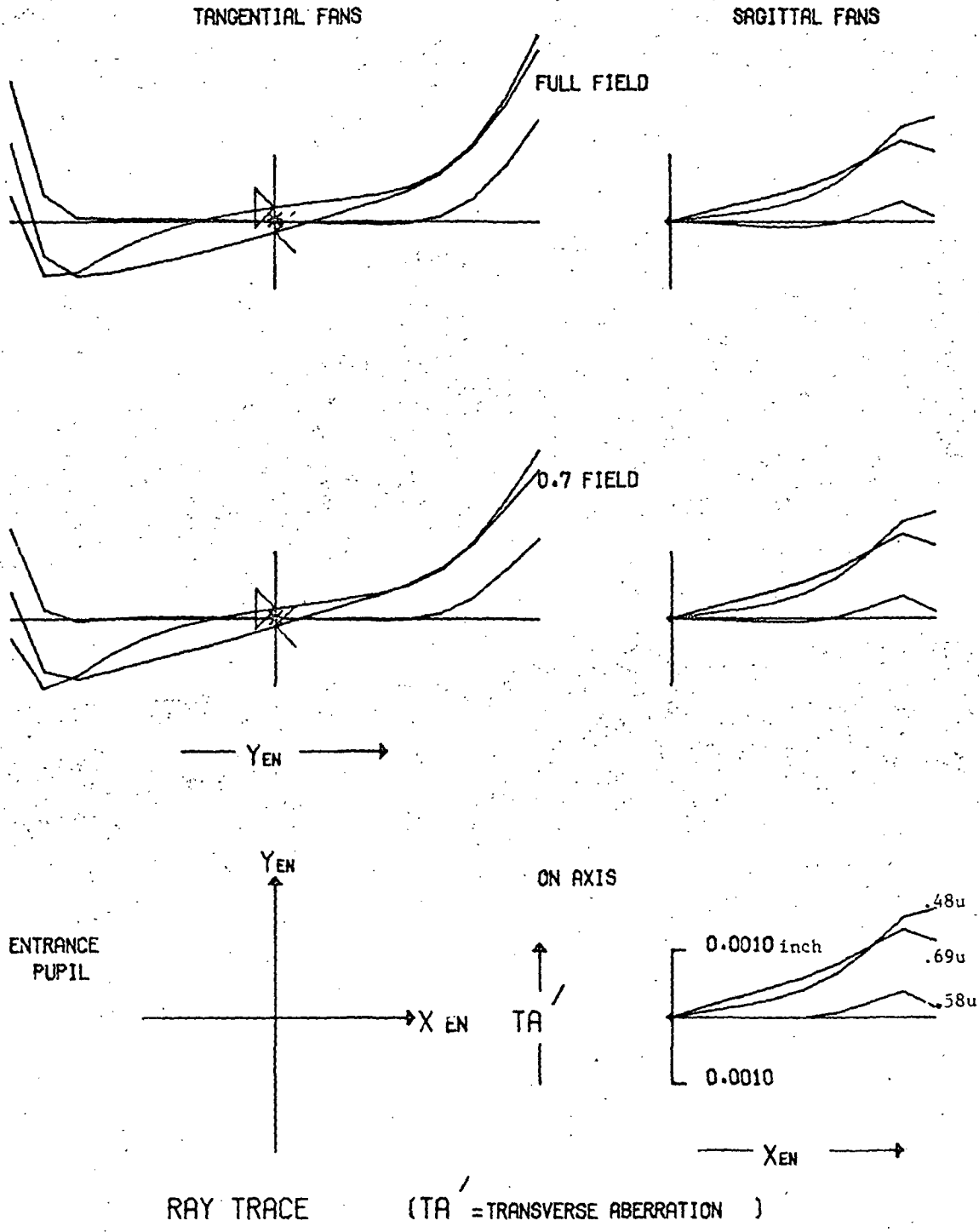
Fig. 3-5 — Transverse aberration plots for lens in Fig. 3-4

TANGENTIAL FANS   SAGITTAL FANS

FULL FIELD

0.7 FIELD

$\longrightarrow Y_{EN} \longrightarrow$

Y_{EN} ON AXIS

ENTRANCE   .48u
PUPIL   .69u

                                                2.0000 λ   .58u
$\rightarrow X_{EN}$ OPD
                                                2.0000

                                            $\longrightarrow X_{EN} \longrightarrow$

RAY TRACE   (OPD = OPTICAL PATH DIFFERENCE)
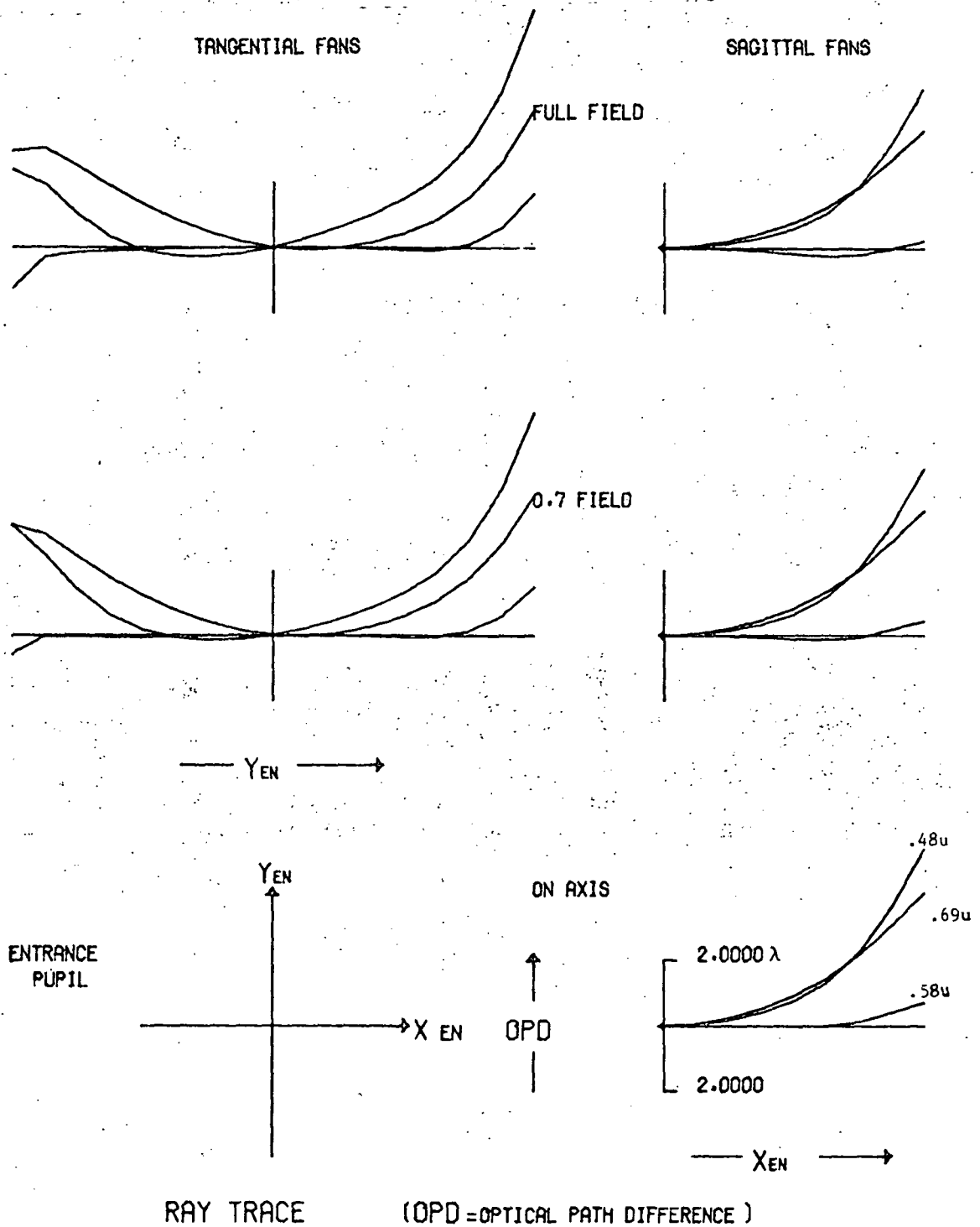
Fig. 3-6 — OPD plots for lens in Fig. 3-4

Table 3-1 — ROM Estimate and Preliminary Design Effort for Modified Double-Gauss A Lens

Design Goals

f/number	f/2.64
Focal length	7.874 inches
Back focus	5 to 6 inches
Half field	2.75 degrees
Wavelength	400 to 700 nanometers
Performance	65% modulation at 35 lp/mm across a flat field

Preliminary Design Effort

- Optical Design
  - Start with f/2.64 achromat
  - Convert to apochromat to reduce secondary color
  - Increase back focus
  - Vary three colors used in color correction to optimize white light modulation
  - Thermal interface

- Thermal Design
  - Thermal soak analysis
  - First-order athermalization

Certain space environment conditions have not been discussed previously as they pertain to substrates (Section 2.1.1). These are treated briefly below with some references applicable to coatings. The three general classes of degradation that could occur are erosion, radiation damage, and contamination.

Only the outer elements would be susceptible to erosion (wearing away of material due to the action of particulate matter) because of direct contact with the space environment. Previous[*,†] tests including a sensitive thermal control coating that was designed to exhibit marked changes for small losses in the 10-nanometer-thick outer germanium film showed no change due to erosion. This test was conducted on the OSO-I for a period of over 16 months.

Radiational effects have been analyzed by numerous observers with somewhat ill-defined results. The major question appears to be the source of on-station degradation when it occurs, either radiational damage or contamination. Indications that prelaunch conditions and film preparation have a bearing on the lifetime of externally positioned samples has been postulated.[‡] Other mirror surfaces of vacuum deposited silver have exhibited good stability in a rear surface configuration when exposed to laboratory simulated Van Allen proton, artificial electron belt, solar wind proton, solar ultraviolet, and other selected environmental radiation combinations. The coatings showed most change in the solar absorption. Other simulated tests exposed antireflection coatings to 1.2×10^6 radians, with no phosphorescence or transmittance change resulting from the exposure. It now appears that the antireflection coatings exhibit good radiation resistance and that changes in mirror coatings may be due largely to contamination effects and not direct radiation damage. The observed effects of contamination are generally restricted to the ultraviolet region and therefore will have a greater impact on the narrow angle B Cassegrain lens. Photopolymerization of contaminant films by various irradiation conditions can produce very difficult to remove absorbing films. These films and others not necessarily affected by radiation will cause either scatter centers or lower reflectance at minima on protected mirror coatings. It should be noted that the effect of reduced minima should be lower for the proposed silver mirror than for the aluminum design.

Finally, the most logical approach to contamination reduction is to employ present technology to the fullest in eliminating to the greatest extent possible all sources of contamination.

3.2.4 System Error Budget

A system error budget was estimated for the B Cassegrain optics to assist in defining the allowances for the factors contributing to optical performance degradation. The criterion for establishing the error budget was the requirement that system performance not degrade to less than 50 percent MTF at 35 line pairs per millimeter. The total allowable defocus (and equivalent rms wavefront) error was computed from the difference of the design MTF values discussed in Sections 3.2.1 and 3.2.2 and the 50 percent MTF value (see Fig. 3-7).

The Cassegrain lens as currently configured has a total defocus error budget of ±0.0027 inch, based on on-axis modulation data. However, it is estimated that optimization of the lens design will raise the modulation at best focus to 83 percent and will maintain this performance across the field. If it is assumed that the entire modulation curve is raised proportionately, this should provide a final total defocus error budget of approximately ±0.0030 inch.

---

[*] L. Drummeter and G. Hass, Solar Absorptance and Thermal Emittance of Evaporated Coatings, Physics of Thin Films, Vol. 2, p. 305, 1964.

[†] D. McKeown and M. G. Fox, Measurement of Surface Erosion From Discoverer 26, ARS Journal, p. 954 (June 1962).

[‡] J. B. Heaney, Results From the ATS-3 Reflectometer Experiment, Astronautics and Aeronautics, Vol. 23.
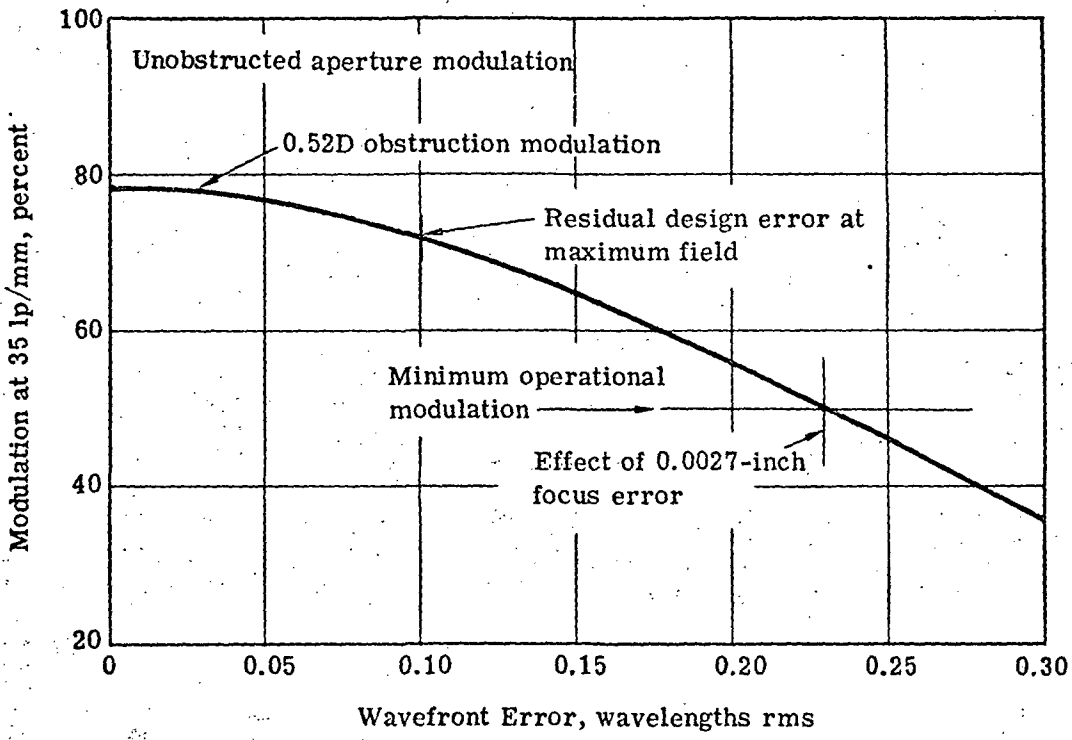
Fig. 3-7 — Cassegrain modulation as affected by wavefront error

Table 3-2 gives the preliminary error budget for the Cassegrain optics. The error budget is believed to represent a realistic first iteration allocation. The operational contingencies are assumed to be 0.10 wavelength rms, which will decrease with further study.

Table 3-3 shows the results of the study of operational sensitivities for the B Cassegrain. The total rss value of 0.190 wavelength was taken as that part of the error budget that would be present during operation but could not be removed by assembly adjustments (i.e., handling, launch, thermal, focus, long term aging, and contingencies).

Those perturbations marked with an asterisk were affected only by a temperature change of 40 °C, allowing for final assembly to be done at 20 °C (−20 to +35 °C temperature range). ULE was used for the mirrors and UBK-7 for the lenses. It was assumed that the dn/dt for UBK-7 was similar to that of BK-7.

3.3 THERMO-OPTICAL CONSIDERATIONS FOR SYSTEM DESIGN

3.3.1 Athermalization

The system selected as the baseline consists of the Cassegrain with correctors for the narrow angle (B) lens and an achromatic double-Gauss, all-refracting system for the wide angle (A) lens.

The Cassegrain lens as currently configured has a total defocus error budget of ±0.0027 inch, based on on-axis modulation data. However, it is estimated that optimization of the lens design will raise the modulation at best focus to 83 percent and will maintain this performance across the field. If it is assumed that the entire modulation curve is raised proportionately, this should provide a final total defocus error budget of approximately ±0.0030 inch.

According to Table G-6, a worst case thermal soak will produce a defocus effect of 0.0025 inch in the Cassegrain lens if an all-Invar (free-machining Invar) or equivalent ($\alpha = 1.5 \times 10^{-6}/°C$) structure is used in conjunction with a low expansion mirror material ($\alpha \approx 0.03 \times 10^{-6}/°C$). In order to provide a reasonable error allocation to other system error sources, the low expansion mirror/all-Invar (or equivalent) structure combination was established as the design guideline. The thermal soak defocus error for this combination can be further broken down as follows:

Error Source	Defocus, inches
Expansion between primary and secondary mirror	0.0021
Expansion between primary and vidicon (back focus expansion)	0.0003
Mirror expansion	0.0001
Total	0.0025

It is obvious that the most critical area for soak athermalization is the connecting structure between the primary and secondary mirrors. However, because of the already tight overall tolerances, the back focus structure must also be of Invar or its equivalent (e.g., a titanium back focus structure would increase the defocus due to back focus expansion to 0.0018 inch, increasing the total lens defocus error to 0.0039 inch, which exceeds the total defocus error budget). An athermalizing technique for the back focus structure that can meet the requirements is discussed in Section 3.4.

Table 3-2 — Preliminary Cassegrain Wavefront Error Allocation*
($\lambda = 550$ nanometers)

Error Source	Error Magnitude, wavelengths rms	Remarks
Residual design aberration	0.050	At maximum field
Surface manufacturing errors, primary, secondary, field lenses, filter, coatings, glass quality, etc.	0.03	
Mounting strains	0.03	For lightweight mirror with large hole in center
Assembly, alignment, and initial focus setting	0.09	
Handling and launch sets (structures)	0.02	
Thermal focus error	0.13	0.0015-inch focal shift
Long term aging of materials producing focal shifts, misalignments	0.10	Difficult to estimate, little data available
Other errors and contingencies	0.10	
RSS	0.23	MTF = 50 percent

*Based on straight rss of all individual errors.

Table 3-3 — Preliminary Operational Sensitivity Values

Element	Perturbation	Wavefront Deformation, wavelengths rms
Primary	Radius:*,† −0.00005 inch	0.005
	Axial shift: 0.00038 inch	0.091
	Decenter: 0.00076	0.015
	Tilt: 0.00019 radian	0.057
Secondary	Radius:*,† −0.00005 inch	—
	Axial shift: 0.00038 inch	0.118
	Decenter: 0.00076 inch	0.053
	Tilt: 0.00019 radian	0.042
First lens	First radius:* 0.003 inch	0.037
	Second radius:* 0.010 inch	0.010
	Axial shift: 0.00076 inch	0.026
	Δn:* 0.00004	0.007
	Decenter: 0.0038 inch	0.007
	Tilt: 0.00038 radian	0.007
Second lens	First radius:* 0.0024 inch	0.044
	Second radius:* 0.0057 inch	0.017
	Axial shift: 0.00076 inch	0.026
	Δn:* 0.00004	0.014
	Decenter: 0.0038 inch	0.023
	Tilt: 0.00038 radian	0.015
RSS		0.190

* Determined by 40 °C drop in temperature only.
† Taken together since they are of the same radius and material.

The thermo-optical characteristics of the achromatic double-Gauss lens-(rated to 8-inch focal length at f/3), investigated in Appendix G, were used to construct an error budget for the A lens and to estimate its athermalization characteristics. The double-Gauss shows a total defocus error budget of 0.0026 inch based on on-axis modulation data in Appendix G. A worst case thermal soak will produce a defocus effect of ±0.0014 inch on this lens with an all-titanium cell structure. Since the B lens design guidelines have already dictated that the back focus structure be all-Invar or its equivalent, and since the vidicon must be parfocal with the A and B lenses, thermal expansion of the A lens back focus will be less, and so the A lens will have a lower sensitivity to thermal soaks than noted. Therefore, it appears that the A lens will need no further athermalization. Sufficient slack should exist in the budget to allow for manufacturing errors and provide for small thermal gradients. This would be studied in additional detail in future phases.

3.3.2 Effects of Temperature Gradients on Optical Performance

Although no detailed examination of gradients was performed, it is appreciated that gradients are critical and should be minimized. An effort was made to size the effects of both axial and radial temperature gradients. The results are shown in Tables 3-4 and 3-5. Table 3-4 shows the defocus caused by a radial and an axial temperature gradient on the primary mirror of the B (Cassegrain) lens. Table 3-5 shows the defocus caused by radial and axial temperature gradients on the first three elements of the A (achromatic double-Gauss) lens. Since elements 2 and 3 of the double-Gauss lens are cemented together, a 1 °C axial gradient and a 1 °F radial gradient was assumed to be across the combination of the two elements. In these gradient analyses, the elements are assumed to be unconstrained and stress-free. The radial and axial gradients appear to have little effect on defocus.

3.3.3 Window Considerations

It may be desirable to use a window as a protective cover for the optics and to provide additional thermal stability.

The use of a window on the B lens will serve to reduce temperature gradients on the optics, particularly the primary mirror. However, the window itself then becomes subject to temperature gradients. Therefore, the effects of the window on image quality will depend to a large extent on what temperature gradients the window will be subjected to. The use of a low expansion material such as ULE fused silica for the mirror makes the primary relatively insensitive to gradients, and, in general, indicates that the use of a window would only degrade the overall thermal performance of the reflecting system.

The use of a window on the A lens (an all-refracting system) will also serve to reduce the temperature gradients on the optics. However, unlike the low expansion mirrors, the refracting lens elements are not insensitive to temperature gradients. As a result, the relative effects of the window on the overall thermal performance of the system are difficult to predict without a detailed thermal analysis of the system.

3.4 STRUCTURAL DESIGN

3.4.1 General Description and Requirements

A conceptual structural design and first-order structural analysis was completed, with the design based on configuration 1 of the preliminary optical study. The system consists of an all-refracting wide angle (A) system, a narrow angle (B) Cassegrain system, and two vidicons (see Fig. 3-1). Requirements that control the structural design include:

1. Maximum weight of 30 pounds, excluding vidicons

Table 3-4 — Cassegrain B Lens Sensitivity
to Temperature Gradients on Primary Mirror

Condition	ΔT, °C	Defocus, inches
Radial gradient	1, edge hot	< −0.0001
Axial gradient	1, front cool	−0.0002

Notes: 1. Mirror material is solid ULE fused
silica, 0.5 inch thick.
2. Base temperture = 7.5 °C.
3. λ = 550 nanometers.
4. Sign convention for defocus:
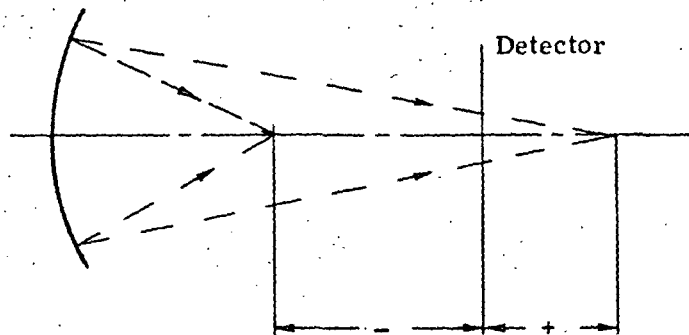
Table 3-5 — Achromatic Double-Gauss A Lens Sensitivity to Temperature
Gradients on First Three Elements

Condition	Element	Material	ΔT, °C	Defocus, inches
Radial gradient	1	SK-19	1, edge hot	<0.0001
	2	BaFN-10	1, edge hot	0.0002
	+3	SF-2		
Axial gradient	1	SK-19	1, front cool	<0.0001
	2	BaFN-10	1, front cool	−0.0005
	+3	SF-2		

Notes: 1. Base temperature = 7.5 °C.
2. $\lambda = 550$ nanometers.
3. Sign convention for defocus:
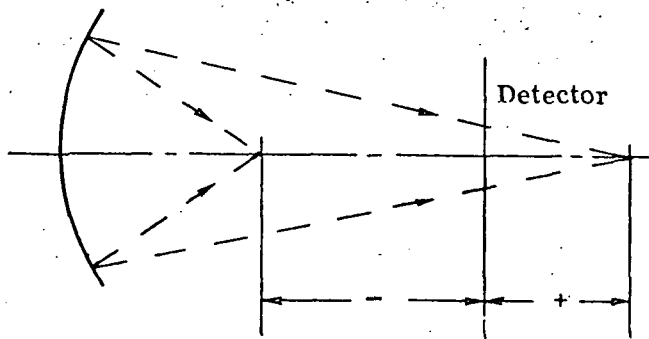
2. Operating soak temperatures between −20 and +35 °C, with no gradients presently defined

3. Dynamic environments as listed in TOPS-3-300A:

Boost acceleration	$+15 \atop -4$ } g axial
	± 4 g lateral
Sine vibration	5 to 30 hz, 4 g
	30 to 2,000 hz, 10 g
Random vibration	0.2 g/hz, 100 to 1,100 hz
	12 db/octave rolloff above
	1,100 hz
Acoustics	150 db overall level
Pyrotechnic shock	See TOPS-3-300A, Fig. 2

4. Athermalization technique incorporated into structure

5. Capability to undergo gravity release without performance degradation.

All these requirements, in addition to the assumptions listed below, were considered in the structural design:

1. The vidicons can be repackaged (without decreasing their size) to accommodate simple interfacing with our structure.

2. Boresight errors between the two systems and decenter errors of the vidicons will be calculated but not minimized to the smallest possible values. This approach is taken since tolerances on these values are not available and controls could be added later.

3. Both lens systems will include provisions for the mounting of protective windows. However, the windows themselves and their effect on system performance will not be considered in this report.

4. Mechanical covers to protect the instrument against harsh environments will be mounted on the same platform to which the system will be mounted (i.e., the space platform), and is not considered part of the optical system design

Structural materials for the system are limited to aluminum and Invar, and stainless steel for the flexures. Invar 36 is used in all structures that control spacing between optical elements where athermalization is required. Super-Invar was not used here because of instability of the expansion properties of the material over long periods of time. Aluminum was chosen for the remainder of the structure for a variety of reasons. Among these are high strength to weight ratio, ease of fabrication, and cost.

Detailed design may reveal advantages that can be gained by the substitution of magnesium or titanium for parts of the aluminum structure. Magnesium may offer a worthwhile weight saving in parts with low stress levels, and titanium offers a relatively low thermal expansion coefficient combined with desirable structural properties that may provide advantages as a transitional structure between aluminum and Invar components.

Selection of the design concept was heavily influenced by the high levels of sinusoidal vibration the unit must survive and the requirement for very small dimensional changes between elements during temperature changes. The high sine levels required that special consideration be given to efficient load paths, especially where those paths passed through the Invar metering

material. High stresses in the metering material will cause permanent set and affect focus. The requirement to desensitize the structure to temperature changes was too severe to allow the use of either Invar or super-Invar alone as a metering material. The principle employed to athermalize the structure is shown in Fig. 3-8.

As the relatively long, low α Invar rods expand, the short, high α aluminum path expands an equal amount in the opposite direction. Such a system can maintain the critical dimensions much better than Invar alone and is limited only by the stability and linearity of the material α's in the soak range. Both these properties are very good in the range of interest. The α's for aluminum and Invar 36 have a ratio of about 14:1. Therefore, to maintain the 6.5-inch critical spacing dimension, a 7-inch Invar 36 rod would be used with two 1/4-inch aluminum paths.

As stated previously, Invar 36 is used in preference to super-Invar for its stable α characteristics. This athermalization concept is equally well suited for dimensional control both in the Cassegrain (where the aluminum paths are the spiders or bezels) and between the major components (vidicons, refractor, etc.) of the system.

The design concept shown in Fig. 3-9 was developed using this athermalization technique. The system is supported by a rigid aluminum base that bolts to the space platform at three places. The Cassegrain telescope is rigidly attached to this base and forms the reference point for the other three major system components. These other components are connected to the Cassegrain by a pair of Invar crosslike structures (one above the other) which maintain their dimensional relationships independent of temperature changes. Each of these other three components (two vidicons and the refractor group) are connected to the aluminum base by a pair of stainless steel blade-type flexures. These flexures are oriented to allow differential motion between the aluminum base and the system components. The transfer mirror and its mechanism are connected to the lower Invar frame to maintain its dimensional position with the rest of the components.

The shutter assembly, filter wheel, and filter wheel actuator are all connected directly to the face of the vidicon. This minimizes the number of connections between the floating, dimensionally controlled system and the aluminum base and also saves some weight.

The design concept provides a favorable arrangement of load paths. The Cassegrain is the heaviest component and is bolted directly to the base. The blade flexures are very stiff when loaded in shear along their width or in compression. The blade flexures and the Cassegrain hard mount are arranged such that less than half the inertial forces generated during vibration must pass through the Invar structure regardless of the direction of load input.

3.4.2 Thermal Considerations in Structural Design

As the temperature varies within the soak range, the motion of the aluminum base will create forces tending to move the A system and vidicon sideways along the x axis (Fig. 3-9). Since the blade flexures are stiff in this direction, the result will be a slight bending of the Invar rods, resulting in a slight decenter of the A vidicon in relation to the B telescope when used in the contingency mode. The amount of the decenter is

$$\pm 3.12(13.5 \times 10^{-6})(49.5) = 0.0021 \text{ inch}$$

It is assumed that this amount of decenter is acceptable.

The design of the aluminum base and the component pickup points is also influenced by thermal considerations. If the base structure and pickup points are not symmetrical about two axes, there will be a tendency for the components to rotate as the structure expands and contracts. In our case, the components are mounted on flexures oriented such that most of the twisting force created in the base cannot pass through the flexures and affect the components. In keeping with this, an attempt was made to keep the base structure only approximately symmetrical.
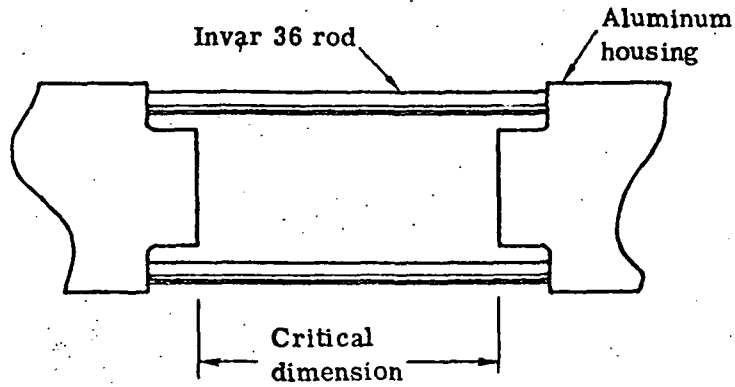
Fig. 3-8 — Athermalization principle
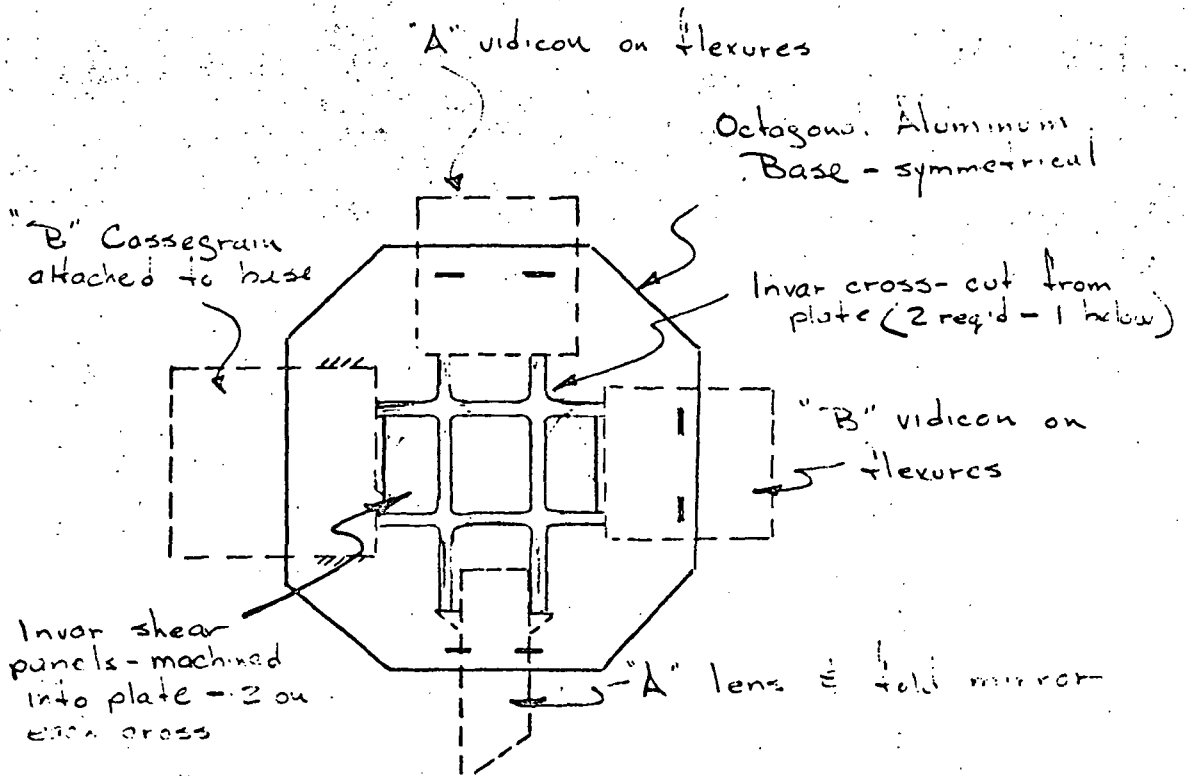
Fig. 3-9 — Athermalization scheme—Invar spacer (cross) with
Cassegrain attached to base

3-21

Another thermal consideration concerns the mounting of the fold mirror in the A system and the allowable boresight error. To minimize weight, the fold mirror is mounted in an aluminum cell with the components of the A lens group. As temperature variations occur, the outer edge of the fold mirror bracket will expand and contract, tilting the fold mirror. The extreme ranges of this tilt or boresight error calculate to be ±0.00066 radian. If this is intolerable, it may be reduced or eliminated by using Invar in combination with aluminum to hold the mirror. This will add slightly to system weight.

The final thermal consideration involves the rotational forces applied to the components as the flexures deflect to compensate for base expansion. This rotational force is reacted to by the Invar mounting rods and results in some small differential deflection of these rods. The result is a small rotation of the component itself. The tilt resulting from this phenomenon is calculated at 3.2×10^{-7} radian for each component (except the B telescope, which is rigidly attached).

3.4.3 Structural and Dynamic Analyses

A first-order structural analysis of the system was completed to solve for the effects of environments listed in Section 3.4.1. Allowable stresses in Invar members were limited to half the microyield strength, or 7,100 psi. Allowable stresses for the aluminum structure were based on a safety factor of 1.4 applied to the ultimate material strength. Analysis was limited to the effects of the sine vibration environment, since these are judged to be the most severe in the intermediate frequency range. The intermediate range is of interest to us here because the highest stresses will be associated with the lowest modes of this relatively stiff structure; these are estimated to lie between 100 and 500 hz. The random vibration spectrum was studied and found not to exceed the sine environment, except for frequencies above 884 hz. For all cases, resonance amplification factors were assumed to be 20 to 25. These transmissibilities are understood to be high, but should not be considered conservative because of the low damping inherent in the flexures and the slender Invar rods.

The results of the calculations are shown in Table 3-6. In all cases the stresses are either below the allowable limit or close enough to be acceptable with some design optimization.

In the process of calculating the structural loads, it became obvious that the slender Invar rods connecting the B system would be overstressed when the unit was vibrated along its y axis. This occurs because both the A lens system and the A vidicon are mounted on flexures that cannot react to forces along the y axis. The load path then is through the Invar rods of the B system in bending, and out through the B components into the base. In order to withstand the loads associated with this condition, it is necessary to add shear panels, as shown in Fig. 3-9. These panels lower the stresses to an acceptable level and at the same time provide a convenient mounting platform for the transfer mirror assembly.

3.4.4 Structural Design of Cassegrain B Lens

The structure of the Cassegrain includes an aluminum outer tube, a secondary spider, Invar metering rods, and the mount for the primary mirror. Spacing of the primary and secondary elements is maintained by three Invar metering rods connecting at the outside of the secondary spider. The position of the secondary is maintained during temperature changes by decoupling the secondary spider from the aluminum outer tube with flexures that have little resistance to relative axial motion. The flexures are designed to be stiff in the lateral direction to provide an adequate load path between the secondary and the outer tube during periods of high lateral loading.

The primary mirror is a solid ULE fused silica design. ULE has been chosen because of its stability in a radiation environment. Cer-Vit is a candidate material for the primary. However, there is insufficient information regarding stability of the material under our anticipated radiation

Table 3-6 — Calculated Stress Levels for Sine Vibration (PSI)

	Direction of Vibration Input		
	x	y	z
Invar rods (1)	7,000	5,090	0
Invar rods (2)	1,350	5,200	0
Flexures (3)	33,400	0	20,000
Flexures (4)	0	33,400	20,000
Flexures (5)	26,700	0	16,000
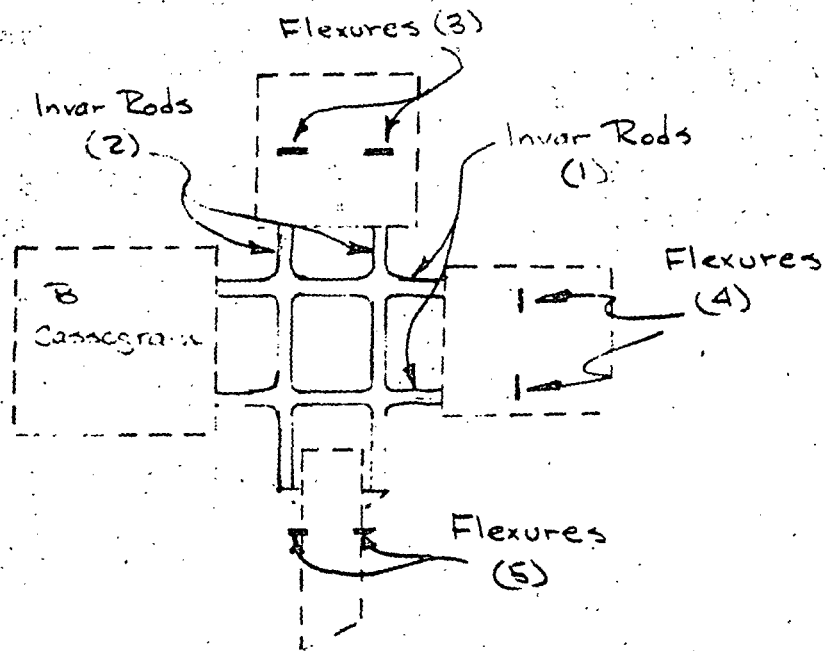
levels. Cer-Vit is a more desirable material structurally, because the criterion for determining the thickness of the blank is based on gravity release, and Cer-Vit has a slightly better stiffness-to-weight ratio than ULE. This would allow use of a slightly thinner Cer-Vit blank and a weight saving. Lightweighting of the blank was considered but did not offer significant weight savings over the solid blank. This becomes obvious if we consider the dimensions of the piece (9.25-inch outside diameter × 4-inch inside diameter), and that a lightweighted design would require inner and outer closure rings, and a minimum faceplate thickness of about 0.30 inch for fabrication. If a lightweight mirror were fabricated of either ULE or Cer-Vit, it would be machined from the back surface rather than built up as a sandwich type monolith.

The primary mirror is mounted by edge potting into an aluminum bezel. The potting would not be configured into a continuous ring, since this would produce a stiff bond that would induce moments into the glass as temperature changes occurred. Instead, the potting would be applied as three or four strips of material, with air spaces between. The potting material would be a silicone type. The exact potting material and configuration would require analysis of the whole mirror/potting/bezel system under different temperature conditions to determine what combination of stiffnesses and dimensions produced minimum effects on the mirror surface.

3.5 CANDIDATE SYSTEM DESCRIPTION

3.5.1 General Description

The proposed candidate optical system shown in Fig. 3-10 is based on the mechanical layout drawing (Itek Drawing 915175, 2 sheets) developed under this study (Fig. 3-11), and includes the design features developed during the system study phase. The total optical system weighs (excluding vidicons) approximately 30 pounds and has overall dimensions of 26.6 by 19.5 by 12.3 inches.

The narrow angle B lens is a Cassegrain telescope utilizing a low thermal expansion Invar substructure to maintain an allowable spacing between the ULE secondary and primary elements under thermal soak shifts from −20 to +35 °C. The primary and secondary mount assemblies are made of Invar, as well as the Invar metering rods between these assemblies. The outer shell of the telescope is aluminum and is rigidly fixed to the aluminum base. The B lens corrector group elements are of UBK-7 and are also housed in an Invar mount.

Adjustment provisions are supplied to allow proper alignment of the primary, secondary, and corrector group elements.

The link between the B lens assembly and the A and B vidicons and the A lens assembly is with an Invar cross structure. This structure maintains the allowable spacing between lens assemblies and vidicons over the soak temperature range. The two vidicons and the A lens assemblies are mounted to the base by means of stainless steel flexures. In addition, differential screw adjustments are provided for the two vidicons and the A lens assembly for use in system optical alignment.

The A lens assembly is a refractor lens of a double-Gauss configuration. The refractor optics presented in this study is an estimate, since a detailed refractor design was considered beyond the scope of the study.

A transfer mirror mechanism provides for the transfer of the B lens image to the A vidicon. In this mode, the A optics would not be monitored. The transfer mirror assembly has differential screw adjustments for alignment, and is mounted to the Invar cross structure. It should be recognized that because of the transfer mirror scheme, the shutters and filter wheels on the B vidicon must be capable of operating with either the A or the B lens.

Note: Differential screw adjustment provided for A and B vidicons and A lens assembly
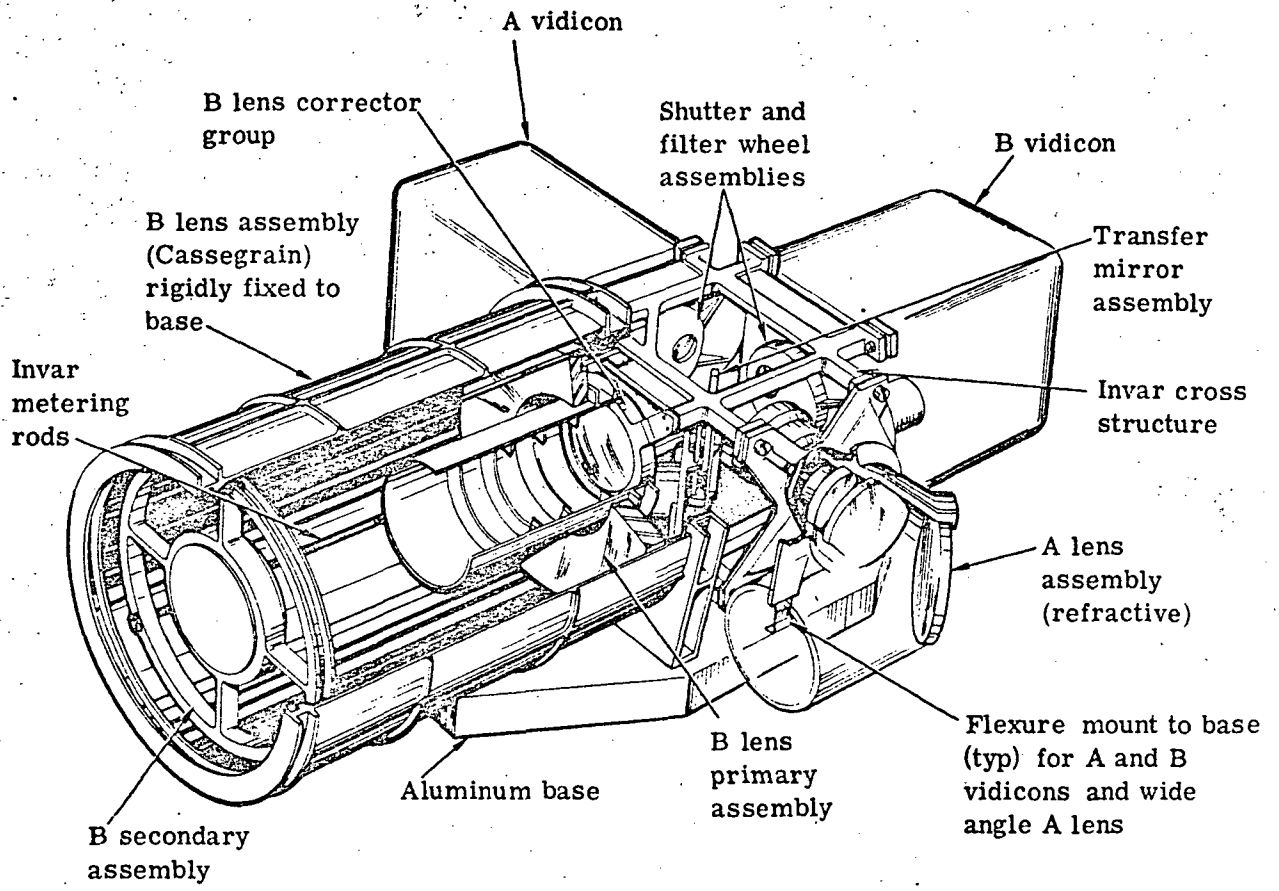
Fig. 3-10 — Candidate optical system

3-25

3.5.2 Transfer Mirror Mechanism

An exploded view of the transfer mirror mechanism is shown in Fig. 3-12. The mirror is translated up (into the optical path) by means of a Scotch-yoke mechanism. This mechanism consists of a slot on the mirror assembly and a rotating arm with a bearing that travels in the slot. The arm is driven by a torque motor. Rotational motion from the torque motor is thus transformed into translational motion of the mirror assembly.

The torque motor rotates 120 degrees. The pivot arm and slot dimensions are designed to ensure that the mirror is totally out of the optical path before torque motor excursion, and in the optical path when the motor is actuated to rotate 120 degrees. The torque motor can be actuated to move the mirror either in or out of the optical path. A brake mechanism is coupled to the torque motor to ensure no movement of the mirror when the torque motor is not being actuated.

Smooth and precise motion of the mirror assembly is assured with the use of three ball bushings mounted to the mirror assembly that travel on shafts fixed to the torque motor housing.

3.5.3 Weight and Center of Gravity Information

The 30-pound weight limit for the optical package (less vidicons) was understood to be an important design constraint and influenced several facets of the design. Among these were:

1. No bezel for the primary mirror of the Cassegrain
2. Minimum gauge metal in baffles and Cassegrain tube (0.020 to 0.030 inch).

The total calculated weight for the system (less vidicons and protective windows) is 27.3 pounds. This allows us a 10 percent contingency without exceeding the 30-pound limit. The weight breakdown is shown in Table 3-7.

The center of gravity of the package, less vidicons, is located at

$$X = -1.5 \text{ inches}$$
$$Y = -0.7 \text{ inch}$$
$$Z = 2.7 \text{ inches}$$

referenced from an origin at the intersection of the A and B system lines of sight, i.e., the center of the Invar frames. The Z axis is positive toward the B telescope, the Y axis is positive toward the A vidicon, and the X axis is positive away from the base. The axis system and center of gravity location in the plan view are shown in Fig. 3-13.

3.5.4 Fabrication

A Lens Assembly

The optics cells and the assembly of the A lens are typical of the type of lenses normally used in conventional optical systems designed and fabricated at Itek. No problems are anticipated during the fabrication cycle of this lens.

B Lens Assembly

The B lens assembly is a Cassegrain system consisting of a primary, a secondary, and two field elements. This system has a faster f/number than is normally used in Cassegrain systems and therefore utilizes a general aspheric surface figure on both the primary and secondary rather than the conventional parabola-hyperbola combination. Because of the general aspheric surface, the measurement of the surface errors requires specialized test techniques, although the fabrication techniques are conventional.
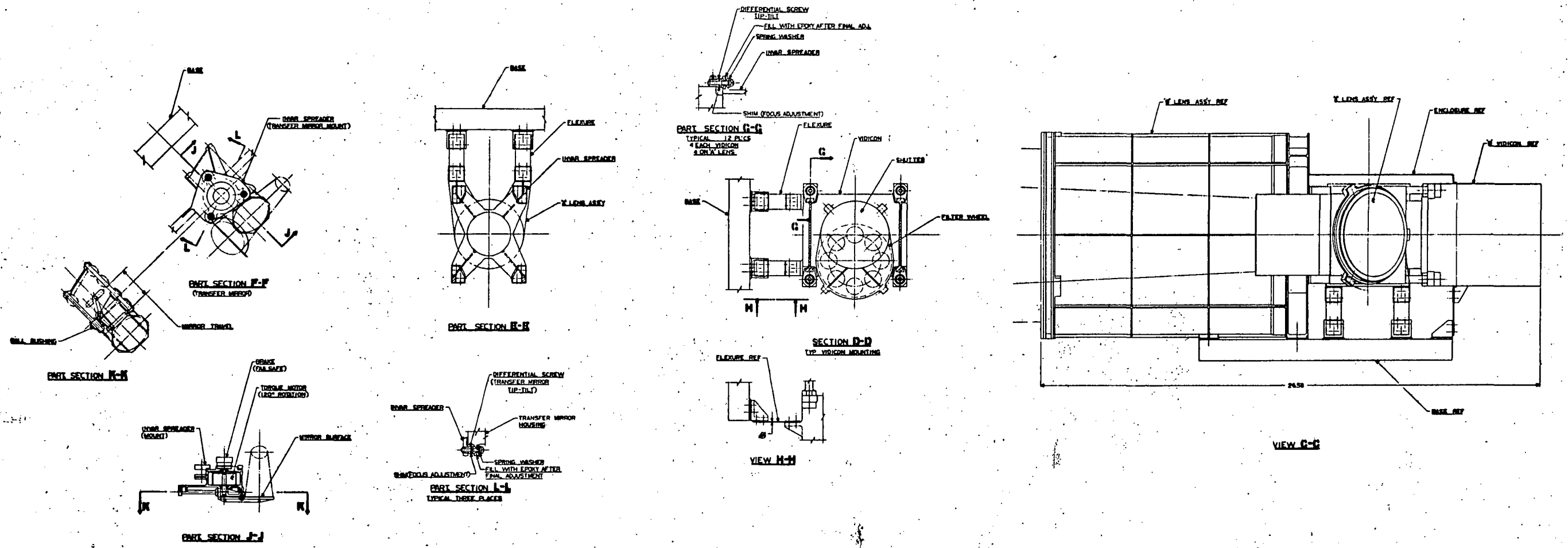
Fig. 3-11 — Layout of candidate system (Cont.)
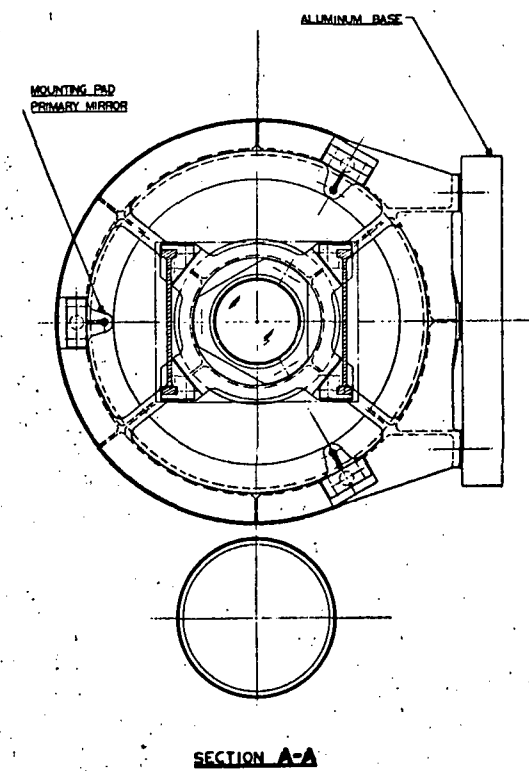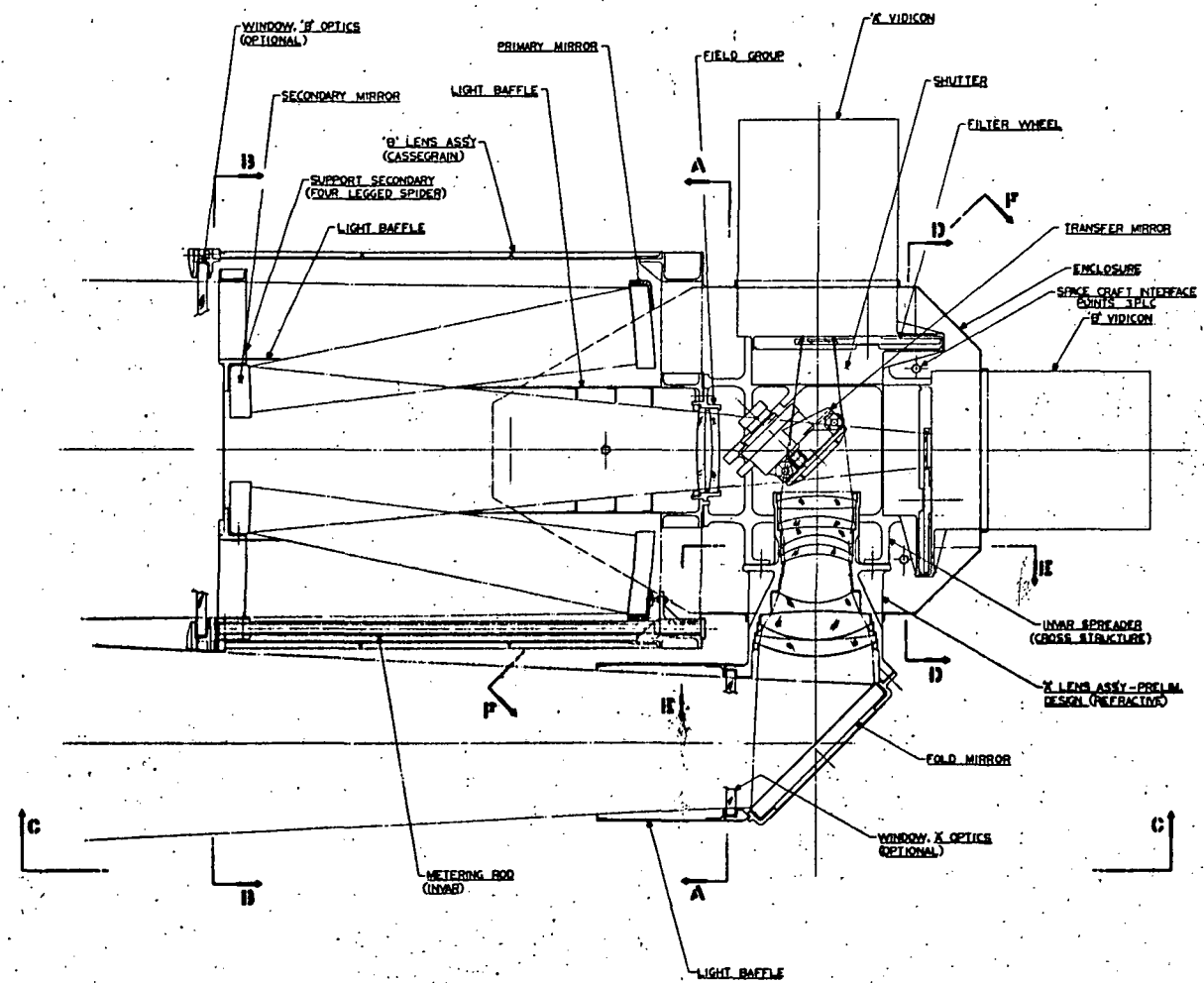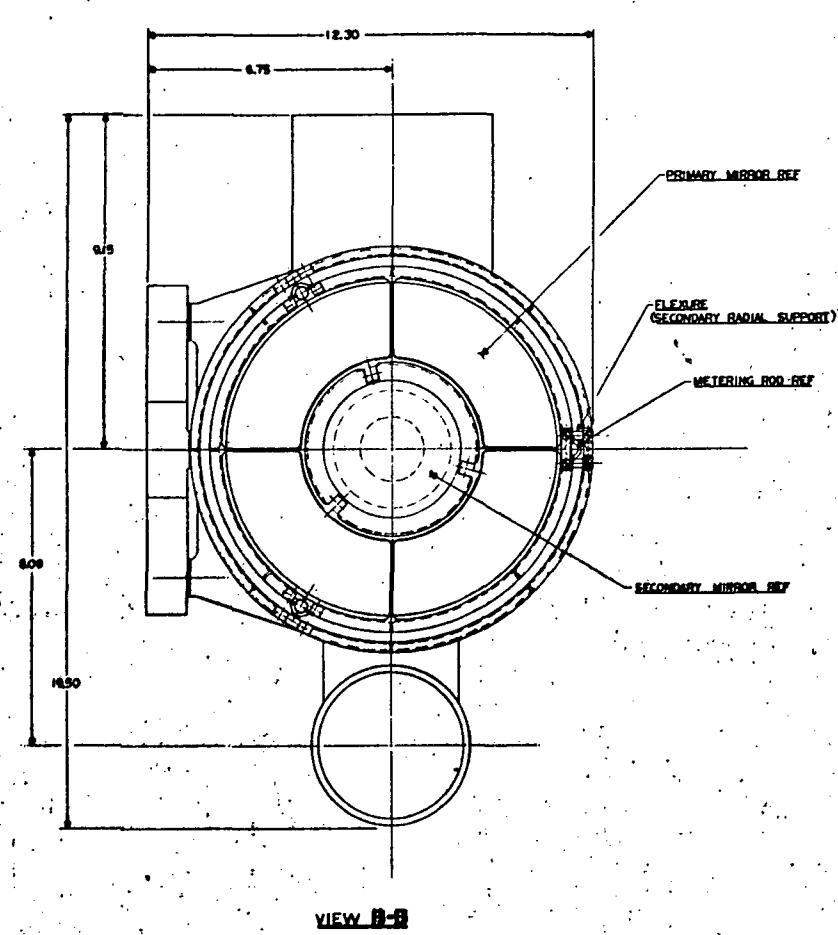
Fig. 3-11 — Layout of candidate system
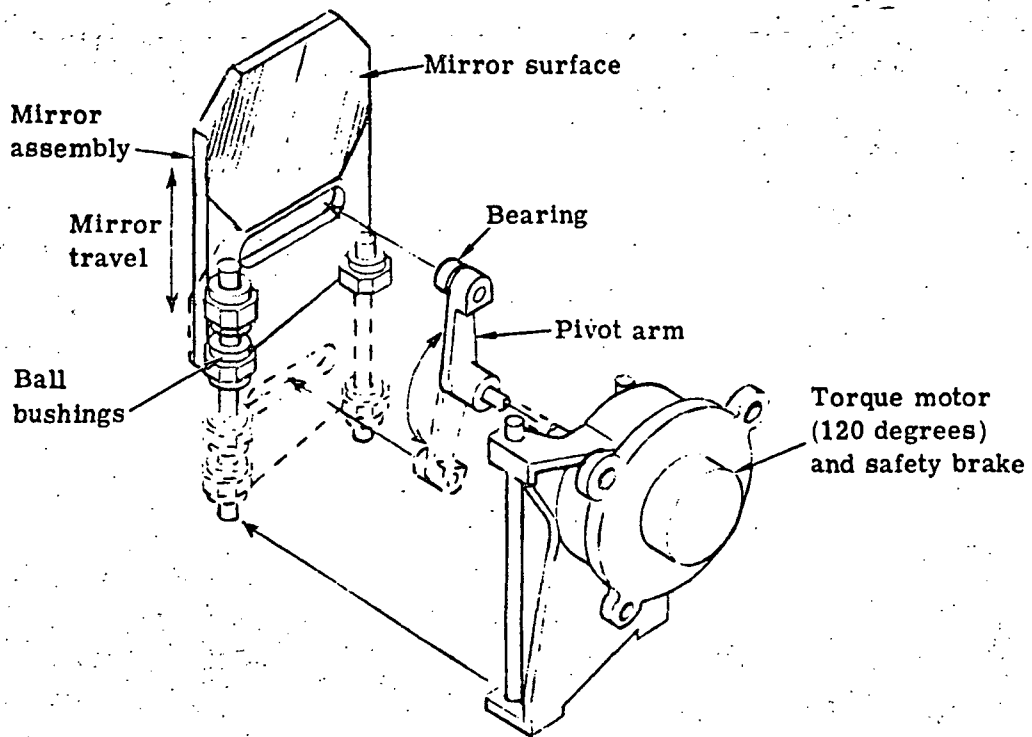
Fig. 3-12 — Transfer mirror mechanism

Table 3-7 — Total System Weight

	Weight, pounds
A optics	4.4
B optics	8.7
Intermediate structure (base, Invar frames, etc.)	9.6
Filter wheels, shutters, and filter drive motors	1.5
Differential screws (15)	0.6
Transfer mirror with motor	1.1
Miscellaneous hardware, etc.	1.4
Total estimated weight	27.3
Total budget	30.0
Estimated weight	27.3
Remainder for contingencies	2.7 (= 10%)

79

+Y

+Z ← ⊕ +X (up)

Center of gravity coordinate system

System c.g.
(without vidicons)
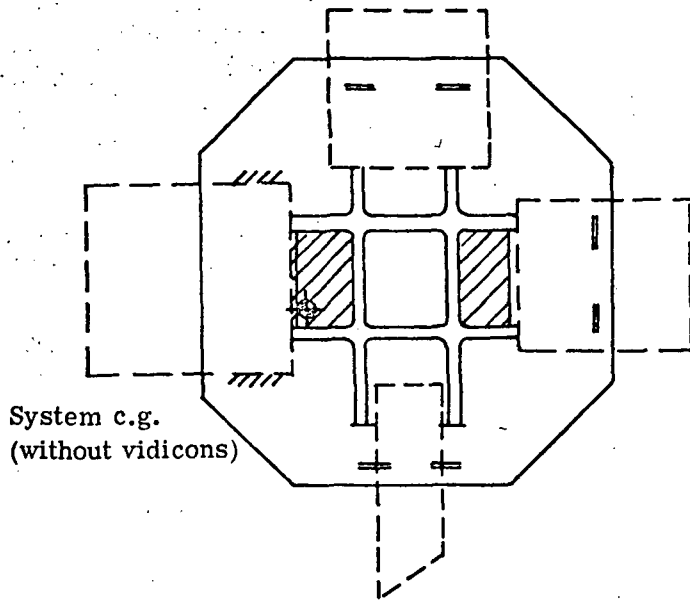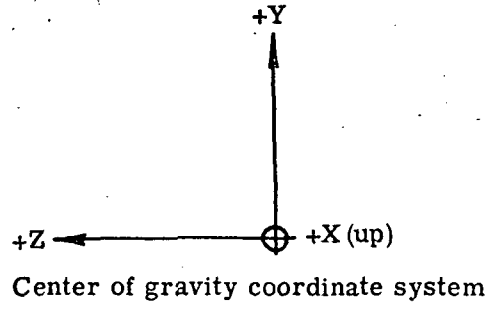
Fig. 3-13 — Center of gravity diagram

Primary Mirror Fabrication

The measurement technique is dependent on the departure of the final aspheric surface from a parabola and the surface tolerance required. Assuming a 1/10 wavelength ($\lambda = 632.8$ nanometers) surface tolerance and a departure of less than 3 wavelengths, the primary would be fabricated using the autocollimation technique shown in Fig. 3-14. If the aspheric surface is greater than 3 wavelengths from the best fit parabola, the use of a null lens in conjunction with a laser unequal path interferometer (LUPI) test would be desirable (see Fig. 3-15).

Secondary Mirror Fabrication

· Surface figure measurement techniques for the secondary are also dependent on departure from a true hyperbola and the accuracy to which the surface must be manufactured. Assuming a 1/10 wavelength ($\lambda = 632.8$ nanometers) surface figure tolerance and the optical surface within 3 wavelengths of a true hyperbola, the measurement of the secondary surface would be made using a concave master test plate. This test plate would be fabricated using an auxiliary spherical mirror in a Silvertooth configuration (Fig. 3-16).

If the departure from a true hyperbola is greater than a few wavelengths, the measurement of the secondary may be accomplished by making the master concave test plate and verifying its figure using a LUPI and a null lens (see Fig. 3-17) or by final figuring the secondary in the optical system (see Fig. 3-18). The latter has a disadvantage in that the primary must be completed before proceeding with the final figuring of the secondary. The use of a test plate master makes the process of fabricating the secondary completely independent of the primary.

3.5.5 System Alignment

The alignment procedure is as follows:

1. Align the elements of the Cassegrain as a subassembly. Adjustments will be made to the secondary mirror, which will then be potted in place.

2. Align the A refractor group with its fold mirror as a subassembly. Pot the fold mirror in place.

3. Mount the upper and lower Invar spacer frames in a precision fixture on an alignment table. The fixture will provide crosshairs on the four vertical faces formed between the upper and lower Invar frames, such that two crosshairs will define the light path of the B system and the other two will define the A system.

4. Using alignment telescopes and the crosshairs for sighting, the B telescope is mounted to the Invar framework.

5. Using another alignment telescope and the other pair of crosshairs, align the A lens unit perpendicular to and through the axis of the B system.

6. Focus and square the B vidicon on the B telescope. Image readout of the vidicon itself will be employed to assist in this operation.

7. Insert the transfer mirror and adjust to make the reflected B line of sight coincident with the A vidicon line of sight. The same alignment telescope will be employed as used for A cell alignment.

8. Focus and square the A vidicon on the reflected B beam.

9. Focus the A image on the A vidicon by translating the A lens unit with shims.

This completes the alignment. The alignment may be checked by alternately reading out A and B system images using a collimator.
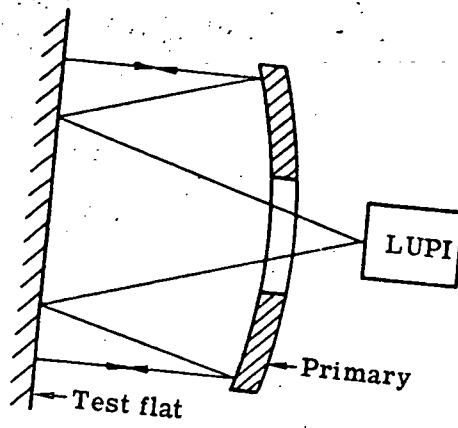
Fig. 3-14 — Autocollimation test
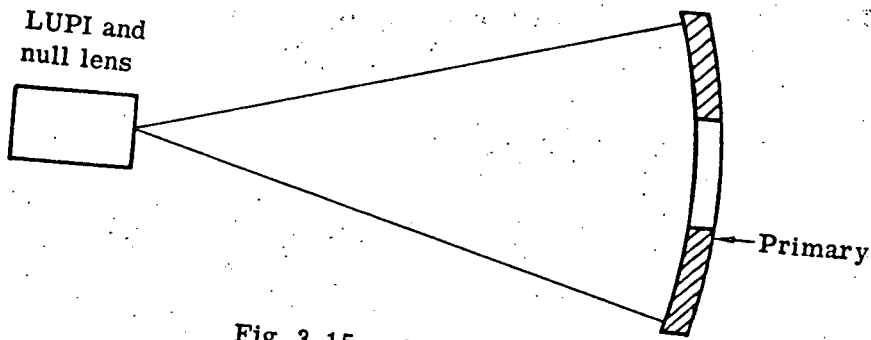

Fig. 3-15 — Null lens test
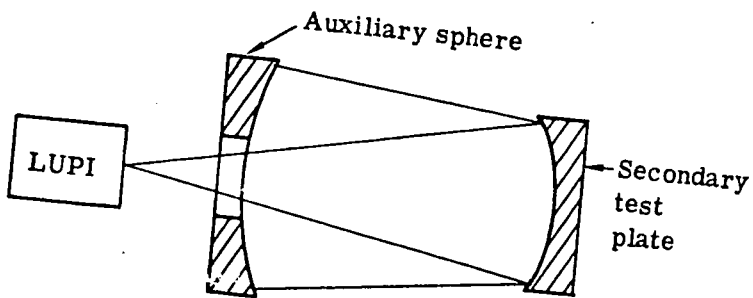
Fig. 3-16 — Silvertooth test for secondary test plate

3-34
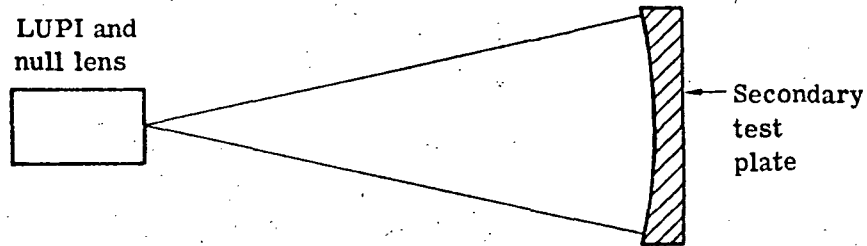
Fig. 3-17 — NUPI test for secondary test plate
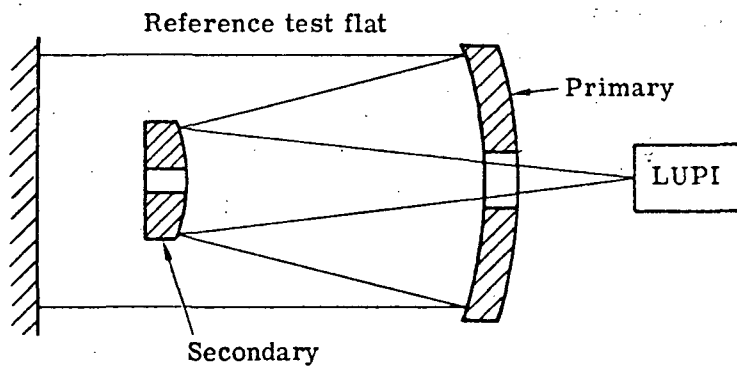
Fig. 3-18 — Completed optical system used for final figuring of the secondary

The mechanics involved in making tip, tilt, and translational adjustments can be described with reference to Fig. 3-19. The adjusting procedure for a single unit is as follows:

1. Loosen the locking nuts on three of the differential screws so that the Belleville washer is partly compressed and exerts only slight compressive forces on the assembly. This will ensure that the spherical washers can rotate easily within the Invar frame such that axial adjustments of the differential screw will not introduce bending moments in the Invar.

2. Remove the locking nut on the fourth differential screw unit so that the unit can move freely on the screw and the other three adjusting assemblies can control the position of the unit.

3. Adjust the three active differential screw assemblies for proper tip-tilt of the unit. Lock the differential screws in place with the setscrews provided.

4. If translational motion of the unit is required, the three locking nuts must be backed off farther and shims inserted as shown. Identical shims are placed in each of the three differential screw assemblies.

5. Tighten the locking nuts.

6. Adjust and tighten the fourth differential screw.

7. Pot all assemblies.

3.6 ADDITIONAL STUDIES

3.6.1 Alternative Optics Study

B Cassegrain

It was thought beneficial to examine the possibility of an alternative B system, for comparison, with the following first-order parameters:

	Base Design	Alternative Design
Focal length	1.0 meter	2.0 meters
f/number	f/4.37	f/8.7

It is not possible to scale the base design to the alternative design parameters and maintain the modulation of 65 percent at 35 line pairs per millimeter. The reason for this, as shown in Fig. 3-20, is the central obstruction coupled with the high f/number. Since it is not possible to reduce the size of the obstruction and hold the required 8-inch back focus with a flat field, an unobstructed aperture design must be employed.

The second reason for not using a scaled base design is that the system length would be too large. Even with adjustment of the parameters, the length from secondary vertex to image plane could not be made shorter than about 33 inches to hold the back focus to 8 inches with a flat field. This is shown in Fig. 3-21.

Fortunately, the relatively slow f/8.7 lends itself readily to an eccentric pupil design. This is a system that has an axis of symmetry for all the elements, and the aperture stop is decentered far enough from the axis of symmetry to eliminate any obstructions.

A three-mirror design allows all aberrations to be corrected on a flat field. One configuration is a primary and secondary forming a real image which is relayed at nearly 1:1 by the tertiary. A final fold is employed to provide the necessary back focus. A preliminary design has shown it
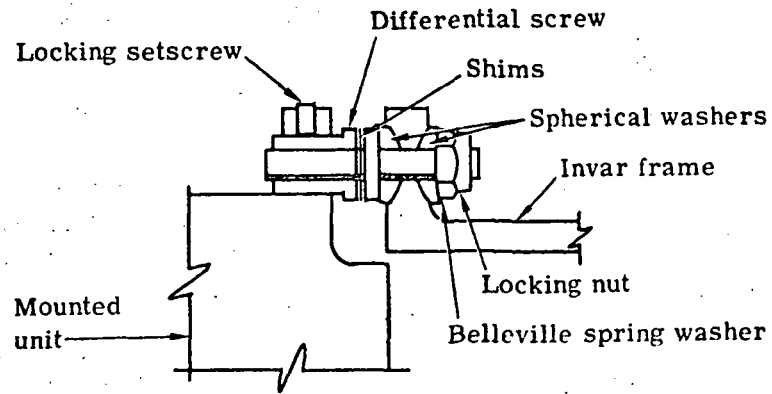
Fig. 3-19 — Differential screw adjusting unit
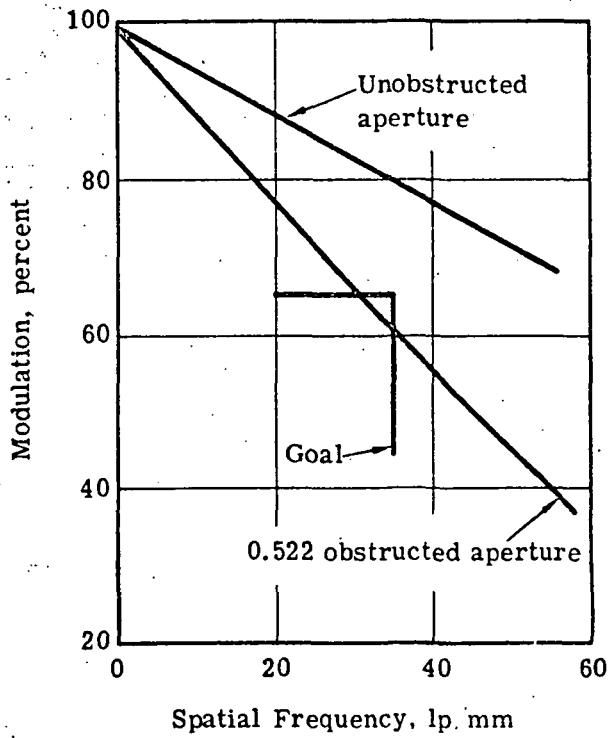
Fig. 3-20 — MTF of B Cassegrain alternative
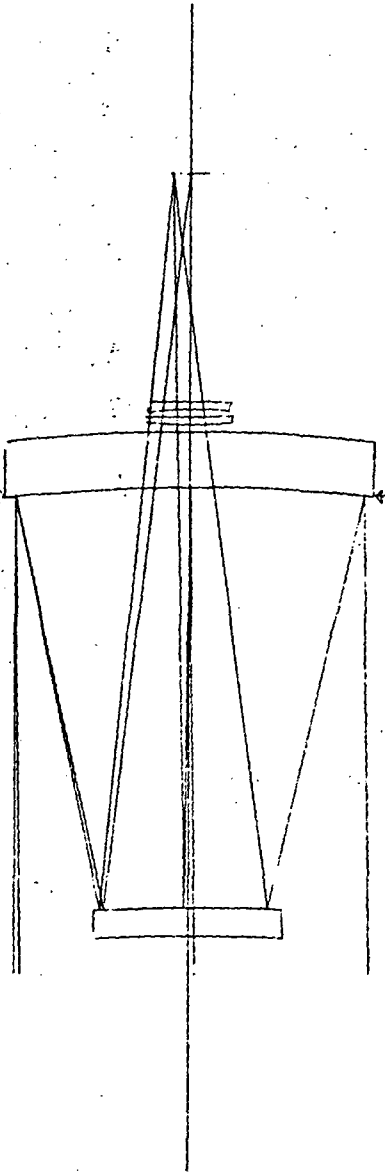
(a) Base design—focal length = 1 meter, f/4.37
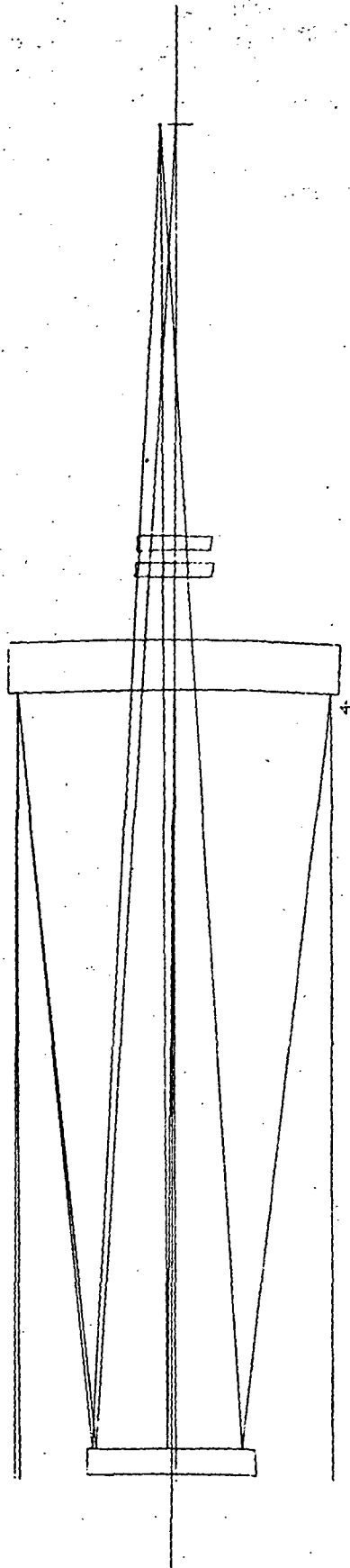
(b) Alternative design—focal length = 2 meters, f/8.7 (scaled from base design)

Fig. 3-21 — Lens diagrams for base design and alternative design

is possible to obtain diffraction limited performance across the field. Thus, the unobstructed aperture MTF shown in Fig. 3-20 should be possible in a nominal design. No account has been taken of fabrication or assembly tolerances. An optical drawing of the proposed configuration is given in Fig. 3-22.

Since the field correction is achieved without the need of refractive elements, the problem of scattered light from these elements is eliminated. Also, perfect color correction is obtained. However, once the Cassegrain base design is fully corrected for color, it will have about the same modulation at 35 line pairs per millimeter as the alternative design. Also, no advantage seems to be gained in package size.

The alternative design will weigh more since it has two more mirrors, including a fold mirror, and each mirror would not have its central zone removed. However, part of the gain is offset by the elimination of the fold mirror in front of the A refractor. The alignment tolerances will be tighter for the unobstructed aperture design than for the Cassegrain base design. This is because the speed of the primary measured from the axis of symmetry if f/1.0 in the unobstructed aperture, whereas it is f/2.2 in the Cassegrain. Fabrication will also be more expensive because of the nature of the eccentric sections of the rotationally symmetrical aspheres.

In conclusion, the base design appears to be superior to the alternative design. Both give about the same modulation but the alternative is heavier and more costly to fabricate.

A Refractor

The alternative A system, examined for comparison, had an increased f/number, from f/2.64 to f/4.0. Its focal length remained unchanged at 200 millimeters. Table 3-8 shows the modulation at 35 line pairs per millimeter for a perfect system for various f/numbers and spectral bands. This shows that 35 line pairs per millimeter is so far from the cutoff frequency that the change in f/numbers and spectral bands shown have little effect on the modulation. What does affect the modulation is the degree of correction. For example, 1/2 wavelength of third-order spherical aberration will still give a modulation of over 75 percent at the given f/numbers. It is expected that residual secondary color should still allow a modulation of 65 percent to be obtained. Of course, the larger the f/number and the narrower the spectral band, the easier it is to correct secondary color.

The factors to consider in going to f/4.0 are better correction is possible, it is less expensive to design (perhaps 20 to 30 percent), the tolerances are looser, the weight is less (a function of the square of the f/number), and the thermal degradation is less. Of course this would be at the expense of longer exposures. Since it is expected that the required modulation can be obtained at f/numbers smaller than 4.0, the only advantages of going to f/4.0 are the reduction in cost of design and fabrication and in weight. For example, the weight of an f/4.0 design should be 56 percent of an f/3.0 design.

3.6.2 B Cassegrain Aperture Versus Weight

Assuming that the focal length is fixed so that the weight varies as the square of the aperture, there is a fairly limited range of f/numbers over which the B Cassegrain could be made to operate. Fig. 3-23 shows the f/number as a function of weight. The weight has been normalized to 1.0 at the base design f/number of 4.37. The upper limit in f/number is about 6.0 and is determined by the modulation requirement. Even this may be too large to allow reasonable tolerances. The lower limit in f/number is about 4.37 and is determined by the total package weight requirement. In conclusion, a thorough tolerance and error budget analysis would have to be performed to determine if the f/number could be increased sufficiently (to about f/6.0) to reduce the B Cassegrain weight to 50 percent of its value for the base design. This would provide a weight reduction of about 4 pounds.
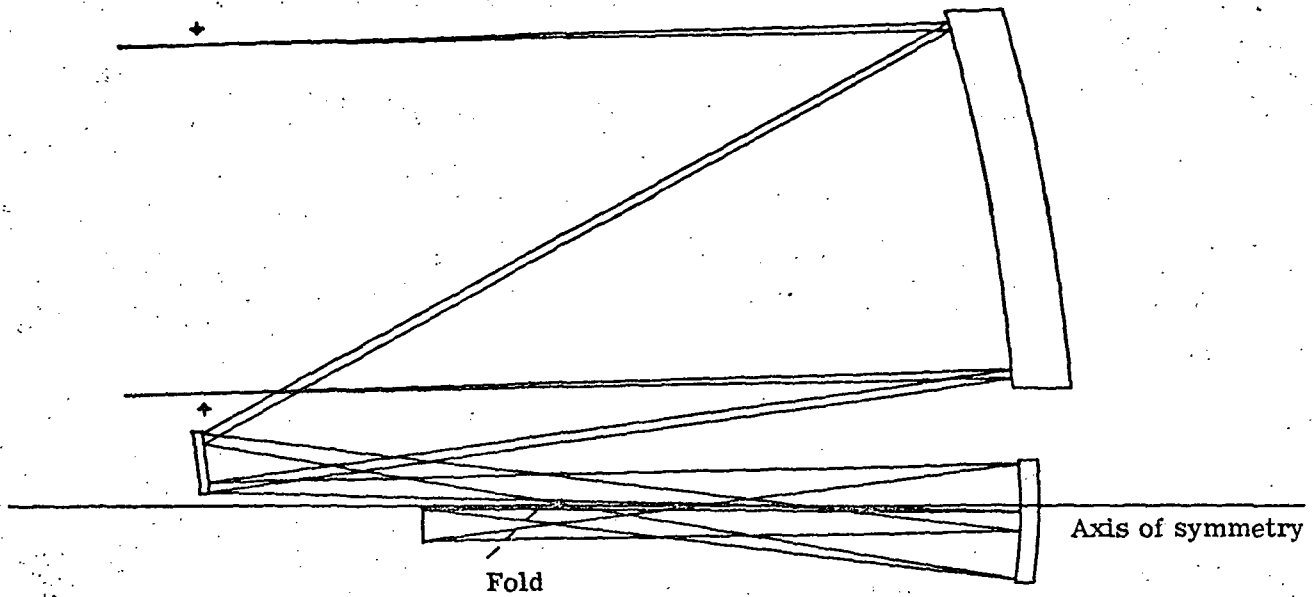
Fig. 3-22 — Alternative eccentric pupil, three-mirror design—focal
length = 2 meters, f/8.7

Table 3-8 — Perfect System Modulation
at 35 Line Pairs Per Millimeter

	Wavelength, nanometers		
f/number	400-700	450-700	500-700
f/2.64	93.4%	93.1%	92.9%
f/3.0	92.6%	92.3%	91.9%
f/3.5	91.4%	91.0%	90.6%
f/4.0	90.2%	89.8%	89.3%
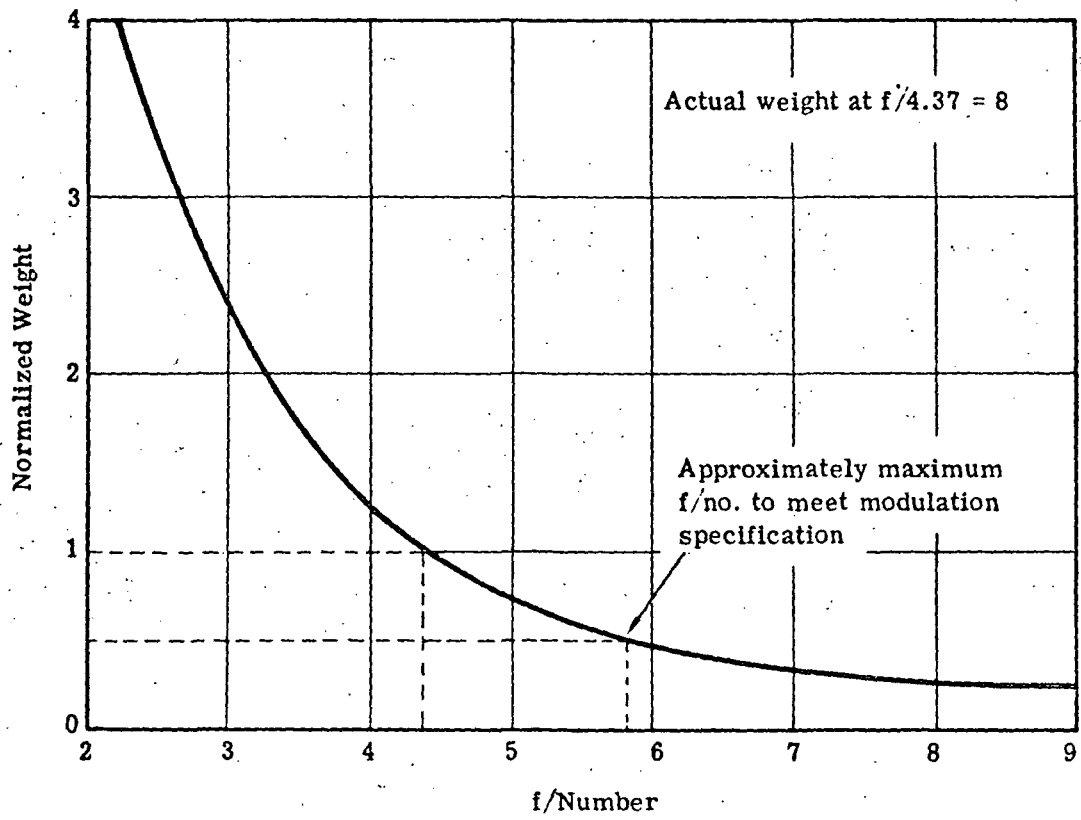
Fig. 3-23 — Aperture versus weight for B Cassegrain

4. CONCLUSIONS

Under JPL contract 953320, Itek Corporation performed an optics study to establish a candidate optical system design for the television imaging subsystem on outer planet missions. This system is applicable for use on the proposed NASA Mariner Jupiter/Saturn 77 Mission. The study was performed over the 6-month period from January through June 1972.

The candidate optical system contains both a wide angle (A) and narrow angle (B) lens with the following performance parameters:

- Wide Angle

    - Focal length   200 millimeters
    - Relative aperture   f/2.64
    - MTF   ≥65% at 35 lp/mm for 400 nm ≤ λ ≤ 700 nm
    - Transmittance   ≥40% for 400 nm ≤ λ ≤ 700 nm

- Narrow Angle

    - Focal length   1,000 millimeters
    - Relative aperture   f/4.4
    - MTF   ≥65% at 35 lp/mm for 350 nm ≤ λ ≤ 700 nm
    - Transmittance   ≥40% for 350 nm ≤ λ ≤ 700 nm

The candidate system is presented in Itek Drawing 915175. The narrow angle (B) lens is a Cassegrain with field correctors, and the wide angle (A) lens is a refractor (double-Gauss). A detailed design was developed for the Cassegrain. However, only a preliminary design was developed for the refractor since it was established that a detailed refractor design was beyond the scope of the study effort.

An additional feature of the system is a transfer mirror mechanism that allows image transfer from the narrow angle (B) lens to the vidicon initially used for the wide angle (A) lens. This image transfer feature adds an operational redundancy to the optical system in allowing for narrow angle viewing if the narrow angle vidicon were to fail. In this failure mode, photography in the wide angle mode would be discontinued. The desirability of this redundancy feature is due to the expected utilization of the narrow angle (B) lens for approximately 85 percent of the TV imaging time on outer missions on the order of 4 years or more duration.

The structure of the candidate system consists mainly of aluminum, with substructures of Invar used for athermalization. The narrow angle (B) lens assembly is fixed to an aluminum base, with the wide angle (A) lens and the A and B vidicons tied to the Cassegrain by an Invar cross structure. The A and B vidicons and the A lens assembly are tied to the base by stainless steel flexures. The total optical system weighs (excluding vidicons) approximately 30 pounds and has overall dimensions of 26.6 by 19.5 by 12.3 inches.

The selection of the proposed candidate configuration evolved from the evaluation of a number of preliminary optical configurations. Lens configurations considered for the narrow angle (B) lens included Cassegrain and three-mirror all-reflecting designs. Lens configurations considered for the wide angle (A) lens included refractor and three-mirror all-reflecting designs. First-order optical analyses and subsequent lens designs were performed to determine the optimum optical configuration for each lens. Thermo-optical analysis was used to aid in the selection of possible optical configurations as well as define the structural material and configuration requirements for supporting the optical elements. Materials selection for optics required consideration of environmental factors including long term stability in a vacuum, thermal characteristics, and radiation. Materials selection for structural materials included consideration of the dynamic environmental conditions, thermal characteristics, and strength versus weight. Mechanical design factors involved designing a reliable transfer mirror mechanism and integrating Mariner-type shutter and filter wheel mechanisms into the system.

5. RECOMMENDATIONS

Itek believes that this study effort has established a realistic and technically advantageous approach for the optical system design for the Mariner Jupiter/Saturn 77 Mission. The system provides a compact unit of both a narrow angle and a wide angle lens that meets the specified optical performance requirements. The transfer mirror mechanism provides a backup means of narrow angle TV imaging, which is highly advantageous on extended missions of 4 years or more duration. The system design has not only incorporated the functional requirements specified, but is of a design that can be put into practice within the current state of the art.

A number of additional activities are recommended by Itek in order to evaluate the proposed system capabilities in more depth. These additional activities could be considered as a preliminary design phase, and include: continued work on the wide angle (A) lens refractor design, thermo-optical analysis in relation to the use of a window and radial temperature gradient considerations, refinement of the system error budget, system thermal analysis with consideration of anticipated external heat loads and losses (both from the environment and the spacecraft), and refinement of the mechanical/structural design.

The recommended activities to establish a preliminary design for the modified double-Gauss A lens (beyond the estimate used in this study) are the following:

- Optical Design
  - Start with f/2.64 achromat
  - Convert to apochromat to reduce secondary color
  - Increase back focus
  - Vary three colors used in color correction to optimize white light modulation
  - Thermal interface

- Thermal Design
  - Thermal soak analysis
  - First-order athermalization

The activities related to thermo-optical analysis, thermal analysis, and refinement of system error budget would provide inputs to better predict optical performance and also refine the mechanical/structural design. In general, the recommended preliminary design activities would define the system to a degree that overall system parameters would be established in sufficient detail to design and build a working laboratory model (breadboard).

The design and building of an optical system breadboard is a desirable next step for the evaluation of the functional capabilities of the proposed optical system. The breadboard would consist of the wide angle and narrow angle optics assemblies, as well as the transport mirror mechanism. The performance of these components would verify the basic design approach and provide design experience that would be used for subsequent design stages. The preliminary design activities discussed in the preceding paragraph could be done prior to, or concurrently with, breadboard design and fabrication activities.

6. NEW TECHNOLOGY STATEMENT

After a comprehensive review of published reports, meeting minutes, conversations with key engineers who worked on the project, and a review of engineering notebooks and other Itek-generated documentation, it has been determined that there was no reportable new technology generated under the subject contract as defined in the NASA Procurement Regulations and associated instruction booklets.

Appendix A

TECHNICAL REQUIREMENTS FOR OUTER PLANET MISSION
TELEVISION SUBSYSTEM OPTICS STUDY

TECHNICAL REQUIREMENTS

FOR

OUTER PLANET MISSION

TELEVISION SUBSYSTEM

OPTICS STUDY

JET PROPULSION LABORATORY

PASADENA, CALIFORNIA 91103

I. INTRODUCTION

This document contains a functional description of the A (wide angle) and B (narrow angle) optics for the Outer Planets (OP) Mission. It is the intent of this study, initiated and enumerated in detail in this document, to result in an optical system design. Although concentric Cassegrain designs have been used in the figures presented, they should be interpreted only symbolically and by no means as a constraint on the final design. However, departures from traditional design approaches must offer clearly documented advantages to offset the risks inherent in new technology development.

II. FUNCTIONAL DESCRIPTION OF OPTICS

A. Wide Angle Optics (A)

The wide angle (A) optics is a 300 mm focal length system operating at a fixed relative aperture of f/4.0. As a goal, the spectral transmittance will be flat over a wavelength region extending from 350 to 900 nanometers. The image is formed on a vidicon imaging tube with a flat image plane. It has an 11.3 x 11.3 millimeter active raster containing 500 scan lines. Each line is divided into 500 picture elements or pixels.

It is desirable to keep all optical power elements reflecting to preserve a flat response over the 550 nanometer wide transmission band. However, the use of a catadioptric or refracting system may be necessary. In making design judgements here, consideration should be given to the size of a star image and the necessity to contain it within a 22.5 micron pixel at all points within the field.

Pertinent design parameters are summarized below for A optics:

1.	Focal Length	300 mm
2.	Relative Aperture	f/4.0
3.	Field of View	2.2° x 2.2°
4.	MTF	$\geq 65\%$ at 25 lp/mm for 350 nm $\leq \lambda \leq$ 900 nm
5.	Transmittance	$\geq 40\%$ for 350 nm $\leq \lambda \leq$ 900 nm
6.	Back Focal Length	Compatible with subsystem requirements, Section III.

B. Narrow Angle Optics (B)

The narrow angle (B) optics is an all reflecting objective lens. It has a one-meter focal length and operates at a fixed relative aperture of f/5.6. As in the case of A optics, it will operate in conjunction with a vidicon imaging tube (with a flat image plane) which has a 500 x 500 pixel format in an 11.3 millimeter square raster. The field of view is 0.65° x 0.65° and the spectral bandwidth extends from 350 to 900 nanometers.

Both on-axis and eccentric pupil designs should be investigated and
compared on the basis of image quality, structural integrity, and
packaging advantages.

Pertinent design parameters are summarized below for B optics:

1.	Focal Length	1 m
2.	Relative Aperture	f/5.6
3.	Field of View	0.65° x 0.65°
4.	MTF	$\geq 65\%$ at 25 lp/mm for 350 nm $\leq \lambda \leq$ 900 nm
5.	Transmittance	$\geq 40\%$ for 350 nm $\leq \lambda \leq$ 900 nm
6.	Back Focal Length	Compatible with subsystem requirements, Section III.

C. Wide Angle Optics (A alternate)

Same as A. above except:

1.	Focal Length	0.2 m
2.	Relative Aperture	f/4.0
3.	Field of View	3.3° x 3.3°

D. Narrow Angle Optics (B alternate)

Same as B. above except:

1.	Focal Length	2.0 m
2.	Relative Aperture	f/8.7
3.	Field of View	0.33° x 0.33°

III. OPTICS SUBSYSTEM

The candidate configuration for the optical subsystem is sketched in
Figure #1. Figure #2 depicts the sensor package sized for a single unit multi-
camera system. The subsystem is described below:

A. Single Unit - Two Camera Subsystem

This configuration, as depicted in Figure #1, is a two camera unit
containing both A and B optics, their filter wheels, vidicons, and a
retractable double surface diagonal mirror for interchanging optics
and vidicons. Such a system, properly configured allows for both
redundance (in that the image from either A or B optics may be

JET PROPULSION
LABORATORY
CALIFORNIA INSTITUTE
OF TECHNOLOGY

PREPARED BY	DATE	REPORT NO.
CHECKED BY	DATE	PROJECT

TITLE

FIGURE #1

SINGLE UNIT TWO CAMERA SUBSYSTEM

VIDICON 1 F.W. 1
VIDICON 2
FOCAL PLANE
SHUTTER
2 F.W. 2
A-OPTICS
B-OPTICS
TO BE DETERMINED
30"
20"
10" DIA.
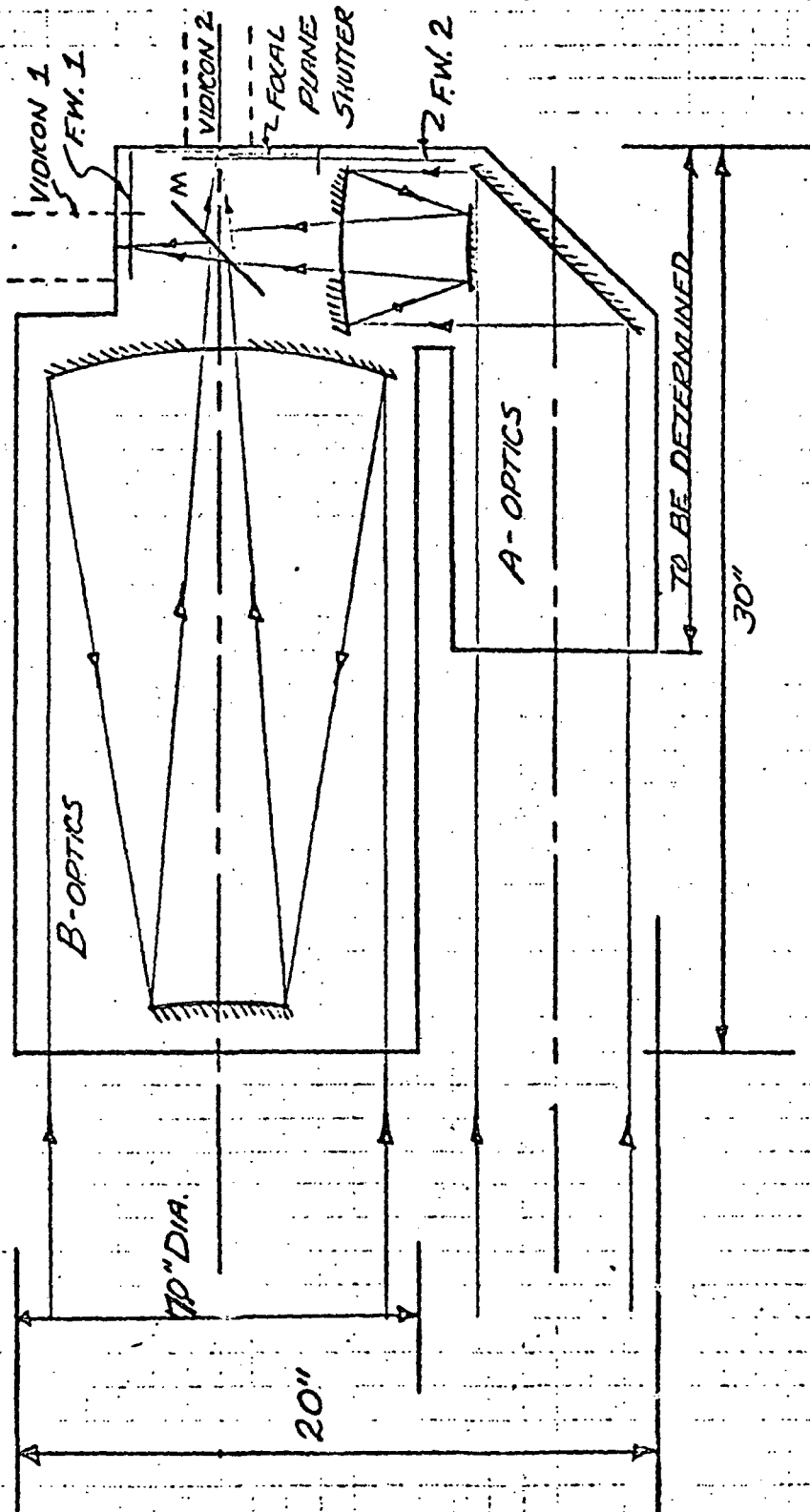
L.M.S.
9-29-71

NOTES

1. Maximum weight 25 pounds

2. Dimensions show representative maximum
   values

JET PROPULSION
LABORATORY
CALIFORNIA INSTITUTE
OF TECHNOLOGY

PREPARED BY   DATE   REPORT NO

CHECKED BY   DATE   PROJECT

FIGURE #2

VIDICON ASSEMBLY

SIDE

TOP

FRONT

L

7"

5"
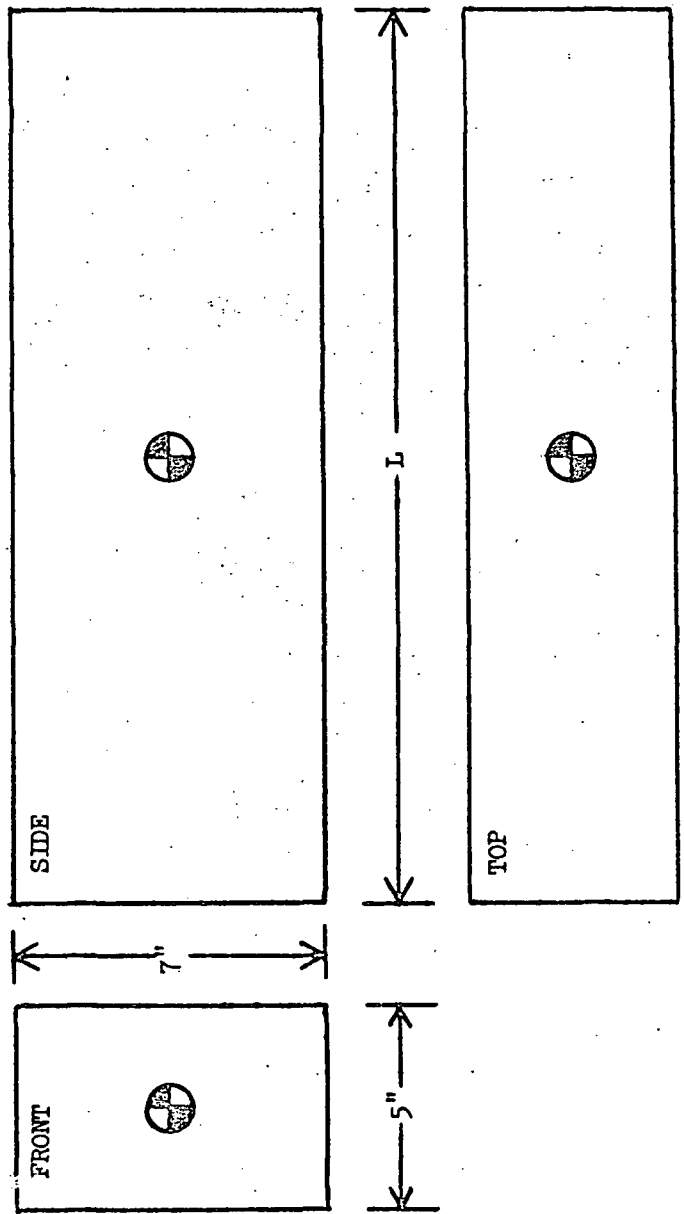
NOTES:

L = 11" Vidicon 1 (SIT); Weight = 18 pounds

= 8.5" Vidicon 2 (SI); Weight = 12 pounds

= C.G. Located at Center of Package

focused on either of the two tubes) and selective use of the appropriate vidicon at different times during the photographic mission.

With reference to Figure #1 the A optics, primary mirror of B optics and the mounts for both vidicons are contained within a single chassis. This chassis also supports A and B filter wheels, transposing mirror (M), a focal plane shutter in front of vidicon #2 and a diagonal flat which directs the light along a common line of sight to A optics. Mirror (M) may be translated out of the cavity to that the relationship between optics and vidicon may be interchanged. Since the vidicon exhibit different spectral responses, the filter sets for each will be individually designed and constrained to a location behind mirror (M) in the optical train. The relation between filter wheel and vidicon is invarient. Structural considerations for the subsystem as well as mirror (M) translating mechanisms will be determined by the contractor during the course of this study.

The entire subsystem package, exclusive of sensors (camera heads) shall not exceed the 30 x 20 x 12 inch envelope indicated in Figure #1. The weight of this package shall not exceed 25 pounds.

A summary list of design parameters are tabulated below for the single unit - two camera subsystem:

1. Subsystem Configuration - See Figure #1

2. Pointing - A and B optics shall point in parallel directions

3. Operating Modes - Two distinct combinations are required and shall be provided for. These are:

    a) M in $\begin{cases} \text{A optics/vidicon \#2} \\ \text{B optics/vidicon \#1} \end{cases}$

    b) M out $\begin{cases} \text{A optics/vidicon \#1} \\ \text{B optics/vidicon \#2} \end{cases}$

4. Optics - For both A and B a conservative design, utilizing reflective elements shall be employed. Schmidt correctors may be utilized. Field correcting elements in the exit beam are not desirable, due to severe veiling glare requirements and should be avoided.

5. Structural/Thermal Requirements - The design shall define the requirements placed on the system resulting from the stated environmental requirements. Additionally, exposure to expected environments shall not degrade the system performance, achieved in bench adjustment of the system, to less than 50% MTF at 25 lp/mm.

6. Packaging - The design must include optics mounting,
    structural support elements, transposing mirror assembly
    and compatibility with defined environmental requirements.

7. Filter Wheels - Provision for spectral filtering in the exit
    beams of A and B optics shall be provided for. Filter wheels
    are anticipated and shall contain, for the purposes of this
    study, six filter positions. The filter wheels are constrained
    to follow the retracting mirror (M) in the optical path.

8. Shutters - A mechanical shutter of the focal plane type is
    required in front of vidicon #2. Vidicon #1, which is
    electronically shuttered will not require mechanical gating.
    Shutter design by the contractor is not required and shall
    not be considered a part of this study; however, a cylindrical
    cavity $1\frac{1}{4}$" deep whose diameter is 3 inches shall be provided
    in front of the vidicon for this device.

9. Weight - The total weight of the optics subsystem exclusive
    of the vidicons, their electronics and housing, shall not
    exceed 25 pounds. Weight reduction is important and should
    be emphasized through all phases of the study program. See
    Section IV. for additional considerations.

10. Baffling - The design of light baffles will be performed
    by the contractor during the course of this study. It is
    necessary that the design guarantee less than 0.05 percent
    veiling glare from light originating at any point in the
    field of view.

11. Focusing - Provision for focusing must be studied by the
    contractor, mechanisms defined, and the focusing method to
    be utilized during subsystem assembly thoroughly described.
    Provision for refocusing by remote operation during the
    mission lifetime may be required and if identified should be
    included in this study.

12. Center of Gravity - The center of gravity of the optics sub-
    system with sensor assemblies (Figure #2) mounted shall be
    computed by the contractor. It is desired that the C.G. fall
    as close as possible to the back of the subsystem.

13. Spacecraft Interface - The two camera single unit optical
    subsystem depicted in Figure #1 will be mounted on the space-
    craft scan platform. The location and structural character-
    istics of the mounting feet shall be investigated by the con-
    tractor and described as part of the mechanical design.

14. Environmental Restrictions - Although detailed drawings are
    not required from the contractor as a part of this study, it
    is necessary that the results of this investigation be com-
    patible with:

a) Mechanical - See Document No. TOPS-3-300-A

b) Thermal Vacuum - Vacuum operation within the temperature range 35°C to -60°C is required.

IV. STUDY PLAN

To determine as much as possible about the various units, at both component and subsystem levels, in the limited time available, it will be necessary to follow a well-organized study plan. Such a plan shall be generated by the contractor and approved by JPL prior to actual design and analysis.

In the event of conflicts between TOPS-3-300-A and this document, this document shall govern.

Appendix B

JPL TECHNICAL DIRECTION MEMORANDUM NO. 1

→TECHNICAL DIRECTION MEMORANDUM

JET PROPULSION LABORATORY
California Institute of Technology
4800 Oak Grove Dr. / Pasadena, Calif. 91103

TO: (NAME OF CONTRACTOR)	CONTRACT NO.
ITEK Corporation	953320

(ADDRESS OF CONTRACTOR)	TDM NO.
10 Maguire Road, Lexington, Massachusetts 02173	1

THIS TDM IS ISSUED PURSUANT TO THE CONTRACT ARTICLE ENTITLED "AUTHORITY OF JPL REPRESENTATIVES."

PURPOSE:

☐ APPROVAL ☐ DISAPPROVAL ☐ CLARIFICATION ☒ RECOMMENDATION

THE CONTRACTOR IS DIRECTED AS FOLLOWS:

A. Change Functional Description of Optics as follows:

<u>Par. II-A Wide Angle Optics</u>

1. Focal Length — 200 mm
2. Relative Aperture — $f/2.6$
3. Field of View — $2°-45' \times 3°-35'$
4. MTF — $\geq 65\%$ at 35 lp/mm for $350 \leq \lambda \leq 700$ nm
5. Transmittance — $> 40\%$ for $350 \leq \lambda < 700$ nm
6. B.F.L. — Compatible with subsystem requirements, Sec. III

<u>Par. II-B Narrow Angle Optics</u>

1. Focal Length — 1000 mm
2. Relative Aperture — $f/4.4$
3. Field of View — $0°-33' \times 0°-43'$
4. MTF — $\geq 65\%$ at 35 lp/mm for $350 < \lambda < 700$ nm
5. Transmittance — $\geq 40\%$ for $350 < \lambda < 700$ nm
6. B.F.L. — Compatible with subsystem

B. Change Optics Subsystem as follows:

<u>Par. III-A-5</u>

Exposure to expected environments shall not degrade system performance, achieved in bench adjustment of the system to less than 50% MTF at 35 lp/mm.

THE DIRECTIONS GIVEN HEREIN ARE WITHIN THE GENERAL SCOPE OF WORK OF THE ABOVE NUMBERED CONTRACT, AND SHALL NOT CONSTITUTE A BASIS FOR ANY CHANGE IN ANY OF THE CONTRACT PROVISIONS OR REQUIREMENTS RELATING TO QUANTITY, QUALITY, FEE, ESTIMATED COST, FIXED PRICE, DELIVERY OR PERFORMANCE SCHEDULE, OR ANY OTHER TERMS OF THE CONTRACT. BY YOUR ACCEPTANCE OF THIS TECHNICAL DIRECTION MEMORANDUM, YOU AGREE THAT NO CLAIMS FOR CHANGE OR ADJUSTMENT IN ANY OF THE TERMS OR PROVISIONS OF THE ABOVE NUMBERED CONTRACT WILL BE BASED UPON THE DIRECTIONS GIVEN HEREIN.

IF YOU TAKE EXCEPTION TO ANYTHING CONTAINED IN THIS MEMORANDUM, DO NOT PROCEED WITH THE DIRECTIONS, AND NOTIFY THE JPL AUTHORIZED REPRESENTATIVE WHOSE SIGNATURE APPEARS BELOW OF SUCH FACT AS SOON AS POSSIBLE, BUT IN ANY EVENT, NO LATER THAN THREE (3) DAYS FROM THE DATE THIS MEMORANDUM IS RECEIVED.

SIGNED *Leonard M Snyder*	1-27-72	THE CONTRACTOR ACCEPTS THIS TECHNICAL DIRECTION MEMORANDUM WITHOUT EXCEPTION. SIGNED *Selwyn Alpert*	2/3/72
AUTHORIZED REPRESENTATIVE	DATE	AUTHORIZED REPRESENTATIVE	DATE
LEONARD M SNYDER		SELWYN ALPERT	
PRINT NAME		PRINT NAME	
JPL TECH MGR		PROGRAM MANAGER	
TITLE		TITLE	
JET PROPULSION LABORATORY		CONTRACTOR	

TECHNICAL DIRECTION MEMORANDUM

JET PROPULSION LABORATORY
California Institute of Technology
4800 Oak Grove Dr. / Pasadena, Calif. 91103

TO: (NAME OF CONTRACTOR)	CONTRACT NO.
ITEK Corporation	953320

(ADDRESS OF CONTRACTOR)	TDM NO.
	1

THIS TDM IS ISSUED PURSUANT TO THE CONTRACT ARTICLE ENTITLED "AUTHORITY OF JPL REPRESENTATIVES."

PURPOSE:

☐ APPROVAL ☐ DISAPPROVAL ☐ CLARIFICATION ☐ RECOMMENDATION

THE CONTRACTOR IS DIRECTED AS FOLLOWS:

Continued

    <u>Par. III-A-8</u>

    Mechanical shutter is required in front of both vidicons.

    <u>Par. III-A-9</u>

    Optics package, exclusive of sensors, shall not exceed 30 lbs.

    <u>Par. III-A-14</u>

    Vacuum operation within range 35°C to -20°C is required.

C. Change Drawing as follows:

    <u>Figure #2</u>

    Vidicons #1 and #2 are identical. Dimensions are 6" x 4 3/8" x 5 1/2".
    The weight is 8 lbs.

THE DIRECTIONS GIVEN HEREIN ARE WITHIN THE GENERAL SCOPE OF WORK OF THE ABOVE NUMBERED CONTRACT, AND SHALL NOT CONSTITUTE A BASIS FOR ANY CHANGE IN ANY OF THE CONTRACT PROVISIONS OR REQUIREMENTS RELATING TO QUANTITY, QUALITY, FEE, ESTIMATED COST, FIXED PRICE, DELIVERY OR PERFORMANCE SCHEDULE, OR ANY OTHER TERMS OF THE CONTRACT. BY YOUR ACCEPTANCE OF THIS TECHNICAL DIRECTION MEMORANDUM, YOU AGREE THAT NO CLAIMS FOR CHANGE OR ADJUSTMENT IN ANY OF THE TERMS OR PROVISIONS OF THE ABOVE NUMBERED CONTRACT WILL BE BASED UPON THE DIRECTIONS GIVEN HEREIN.

IF YOU TAKE EXCEPTION TO ANYTHING CONTAINED IN THIS MEMORANDUM, DO NOT PROCEED WITH THE DIRECTIONS, AND NOTIFY THE JPL AUTHORIZED REPRESENTATIVE WHOSE SIGNATURE APPEARS BELOW OF SUCH FACT AS SOON AS POSSIBLE, BUT IN ANY EVENT, NO LATER THAN THREE (3) DAYS FROM THE DATE THIS MEMORANDUM IS RECEIVED.

SIGNED	DATE	THE CONTRACTOR ACCEPTS THIS TECHNICAL DIRECTION MEMORANDUM WITHOUT EXCEPTION.	
Leonard M Snyder	1-27-72	SIGNED *Selwyn Alpert*	2/3/72
AUTHORIZED REPRESENTATIVE.	DATE	AUTHORIZED REPRESENTATIVE	DATE
LEONARD M SNYDER		SELWYN ALPERT	
PRINT NAME		PRINT NAME	
JPL TECH MGR		PROGRAM MANAGER	
TITLE		TITLE	
JET PROPULSION LABORATORY		CONTRACTOR	

CONTRACTOR ACKNOWLEDGMENT COPY

JPL 2084-S (REV 5-69)

Appendix C

JPL TECHNICAL DIRECTION MEMORANDUM NO. 2

TECHNICAL DIRECTION MEMORANDUM

JET PROPULSION LABORATORY
California Institute of Technology
4800 Oak Grove Dr. / Pasadena, Calif. 91103

TO: (NAME OF CONTRACTOR)	CONTRACT NO.
ITEK Corporation	953320

(ADDRESS OF CONTRACTOR)	TDM NO
10 Maguire Road, Lexington, Massachusetts 02173	2

THIS TDM IS ISSUED PURSUANT TO THE CONTRACT ARTICLE ENTITLED "AUTHORITY OF JPL REPRESENTATIVES."

PURPOSE:

☐ APPROVAL   ☐ DISAPPROVAL   ☐ CLARIFICATION   ☒ RECOMMENDATION

THE CONTRACTOR IS DIRECTED AS FOLLOWS:

I. Optics Subsystem

   A. Remainder of study limited to Configuration I. (Ref. ITEK OED-4-72-31, 9320; page 4).
      1. Finalize optical design (see II A and B below).
      2. Perform materials selection.
      3. Perform mechanical/structural design.
      4. Perform athermalization design/analysis.

   B. Optical switch
      1. Mirror to be retracted from cavity during normal A-B photographic sequences.
      2. Mirror to be inserted <u>only</u> in the event of the narrow angle (B) vidicon failure. If this event occurs during the mission, wide angle (A) photography will be discontinued making refocusing of that lens unnecessary. (Provision for cycling during ground tests must be provided).

II. Optics Components

   A. Place primary design emphasis on narrow angle optics.
      1. Spectral region 350 - 700 nm.
      2. MTF $\geq$ 65% across 1 degree field.
      3. Transmittance $\geq$ 40% (design goal).

   B. Place secondary emphasis on wide angle optics.
      1. All refractor optics.
      2. Spectral region 400 - 700 nm.
      3. Incorporate "off-the-shelf" optics with minimum redesign. If none exist, replace with best estimate as far as optical, mechanical and thermal characteristics are concerned.

   C. The construction of an accessible intermediate image in the narrow angle optical train prior to refractor elements is desired but not an absolute requirement.

SIGNED	THE CONTRACTOR ACCEPTS THIS TECHNICAL DIRECTION MEMORANDUM WITHOUT EXCEPTION.
Selwyn Alpert 29 MAR 72	SIGNED _Leonard M. Snyder_ 23 MAR '72
AUTHORIZED REPRESENTATIVE DATE	AUTHORIZED REPRESENTATIVE DATE
SELWYN ALPERT	LEONARD M SNYDER
PRINT NAME	PRINT NAME
PROGRAM MANAGER	PROGRAM MANAGER
TITLE ITEK CORP	TITLE
	CONTRACTOR

CONTRACTOR COPY

JPL 2084-S (REV 5-69)

Appendix D

SWITCHING MIRROR TECHNIQUES

Appendix D

SWITCHING MIRROR TECHNIQUES

Three switching mirror configurations for changing lenses have been considered. These techniques, illustrated in Figs. D-1, D-2, and D-3, have been given the descriptive titles, orthogonal camera switching techniques (Fig. D-1), opposed camera, single mirror switching technique (Fig. D-2), and opposed camera, double mirror switching technique (Fig. D-3). The orthogonal camera technique was taken directly from the original customer technical requirements paper, and the other two are modifications that reduce or eliminate image displacements inherent in the first design.

In the orthogonal camera switching technique, the vidicon cameras are located at right angles to each other, and light reaches them directly from the lenses in their nominal operating configuration. When the A and B lens images are to be switched to the alternate vidicons, the switching mirror is inserted as shown by the dashed lines in Fig. D-1.

If the switching mirror is of finite thickness, at least one of the images will be displaced laterally and defocused by a distance equal to $\sqrt{2}$ times the thickness of the mirror (for the front surface mirror). This displacement can be eliminated by using a pellicle mirror, but pellicle films cannot be considered high reliability components under the environmental conditions of a Jupiter/Saturn probe. The magnitude of the image displacement depends on how thin the mirror substrate can be made without being subject to environmentally induced changes in shape or becoming too fragile. For the present, it is assumed that the thickness will be on the order of 3.54 millimeters, which produces a defocus of 5 millimeters and a lateral displacement of 5 millimeters.

The lateral displacement can be tolerated, but the defocus must be compensated for. If the switching mirror, the A and B lens axes, and the vidicons are positioned as shown in Fig. D-1, the defocus can be confined entirely to one lens. An all-refracting A lens will be small enough to move bodily, but refocusing the all-reflecting lenses a distance of 5 millimeters may be problematical. Until the focus problem can be studied in more depth, the orthogonal camera configuration will be considered for use only with an all-refracting A lens.

The major advantage of the orthogonal camera configuration is that in the nominal operating position, the switching mirror is removed completely from the optical path. This means that the cameras and lenses can be boresighted accurately for navigation without the additional possible error in the mirror switching mechanism. Transmission will also be somewhat higher. One of the two lenses must have an additional 90-degree fold in it to boresight the lenses with respect to each other.

The opposed camera, single mirror switching technique illustrated in Fig. D-2 eliminates the defocus of the orthogonal camera technique. The A and B lenses are aligned with the output portions of their optical axes coincident and with light traveling in the opposite directions for

each lens. The switching mirror crosses this common lens axis at 45 degrees, reflecting light in opposite directions to the two vidicons, which are equidistant from the common lens axis. Rotating the switching mirror 180 degrees about the common lens axis exchanges vidicons without causing any defocus.

As with the orthogonal configuration, image displacement with the opposed camera, single mirror configuration is proportional to $\sqrt{2}$ times the thickness of the switching mirror, and it is desirable to make the mirror as thin as possible. Two 90-degree folds are required to boresight the axes of the A and B lenses. This makes the opposed camera configuration naturally compatible with the three-mirror, all-reflecting designs, since these require an internal folding mirror to make the output image accessible without a large central obstruction. An internal folding mirror may be included in the Cassegrain design as well.

The third technique, the opposed camera, double mirror switching technique shown in Fig. D-3, eliminates both defocus and lateral displacement of the image. The opposed cameras are offset from each other, and two separated mirrors are required. These need be coated on one side only, however, so the mirror substrate thickness may be chosen to give the best mechanical properties. To switch vidicons, the two mirrors are rotated about a common axis in pinwheel fashion, as shown by the dashed lines in Fig. D-3.

The fact that the images do not shift means that the boresight axes of the two lenses can be centered in the field of view of the vidicons at all times. This has the advantage of minimizing the field of view over which each lens must be corrected, which can affect both image quality and weight in some of the design types under consideration.

The biggest disadvantage of the opposed camera, double mirror technique is that it requires the two lenses to have very large back foci. Depending on the orientation of the vidicon camera head, these minima can range from 190 to 205 millimeters for the all-reflecting and Cassegrain lenses. For the all-refracting lens, the minimum back focus is about 190 millimeters. By contrast, the minimum back focus tolerable with the other two switching techniques is about 120 millimeters for the all-refracting lens, and roughly 150 millimeters for the other three lens designs. The Cassegrain design could be given a 200-millimeter back focus, but only at the cost of an increase in its central obstruction beyond tolerable limits.

The lateral image displacement encountered with the orthogonal camera and the opposed camera, single mirror techniques depends not only on the thickness of the mirror substrate, but also on the positions of the cameras and the lens axes. By shifting these around, the image motion may be confined entirely to one lens, or may be evenly divided between both lenses. Figs. D-4, D-5, and D-6 show how the field of view shifts for several different cases. In each figure, the field of view seen by each vidicon is projected into object space, to show what part of the scene is viewed, relative to the common boresight axis of the two lenses. A mirror thickness of 3.54 millimeters is assumed in both cases, and the corrected field of view required for each lens is indicated by a circle centered on the boresight axis.

In Fig. D-4, the orthogonal camera configuration is set up so that the image motion is confined entirely to the A lens image. The linear shift of the center of the vidicon format relative to the boresight axis is ±2.5 millimeters for the A lens and zero for the B lens. An alternative choice, which has not been plotted, would have the A and B images each shift ±1.25 millimeters.

Figs. D-5 and D-6 apply to the opposed camera, single mirror configuration. Reference to Fig. D-2 will indicate that the optical axes of the A and B lenses are separated (by 5 millimeters for the 3.54-millimeter thick mirror) where they strike the vidicons. If the center of the vidicon format is placed midway between these axes, both images will shift by ±2.5 millimeters when the mirror is reversed, and the fields of view will shift as shown in Fig. D-5. If the vidicon format is centered on the axis of the A lens, only the B lens image will be displaced, and it will be

D-4

displaced ±5 millimeters relative to the center of the vidicon format. In this case, the fields of view will be shifted as shown in Fig. D-6. It will be noted that the B lens field of view lies entirely to one side or the other of the boresight axis, and has no points in common for the two positions of the switching mirror.

If the amounts of image shift indicated in Figs. D-4, D-5, and D-6 are all tolerable from an operational point of view, there may be optical reasons for preferring one over another. Both performance and weight can be affected. Increasing the field of view over which a lens must be corrected can in some instances increase the complexity of the lens design. The field angles involved here should not cause problems with any of the present designs, however. More significantly, an increase in field angle can cause an increase in the clear aperture diameter of some surfaces in the optical design. This affects both performance, through the size of the central obstruction, if any, and weight, through the size of the optical component involved. In general, both effects should be moderate. In the specific case of the all-reflecting A lens, minimizing the field of view may allow a significant reduction in the weight of its primary mirror. The effect of this on the overall weight of the complete optical system can be determined only by a more detailed analysis.
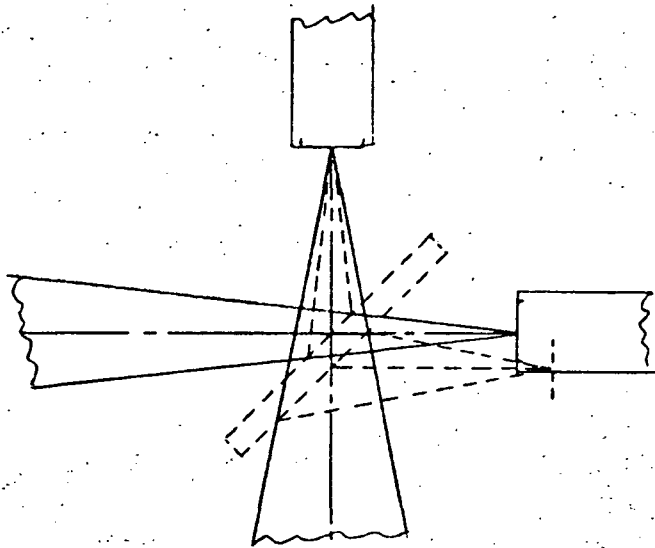
Fig. D-1 — Orthogonal camera switching technique
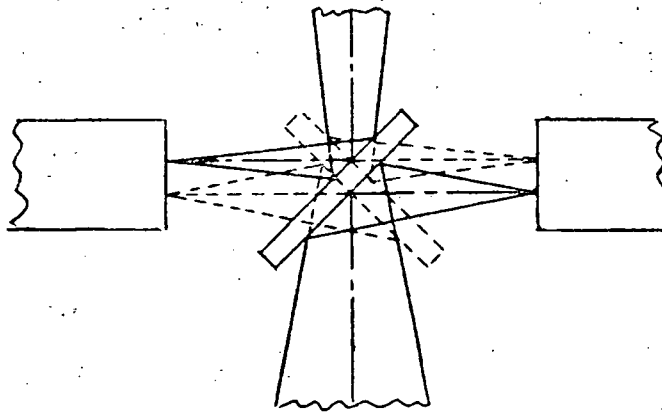
Fig. D-2 — Opposed camera, single mirror switching technique
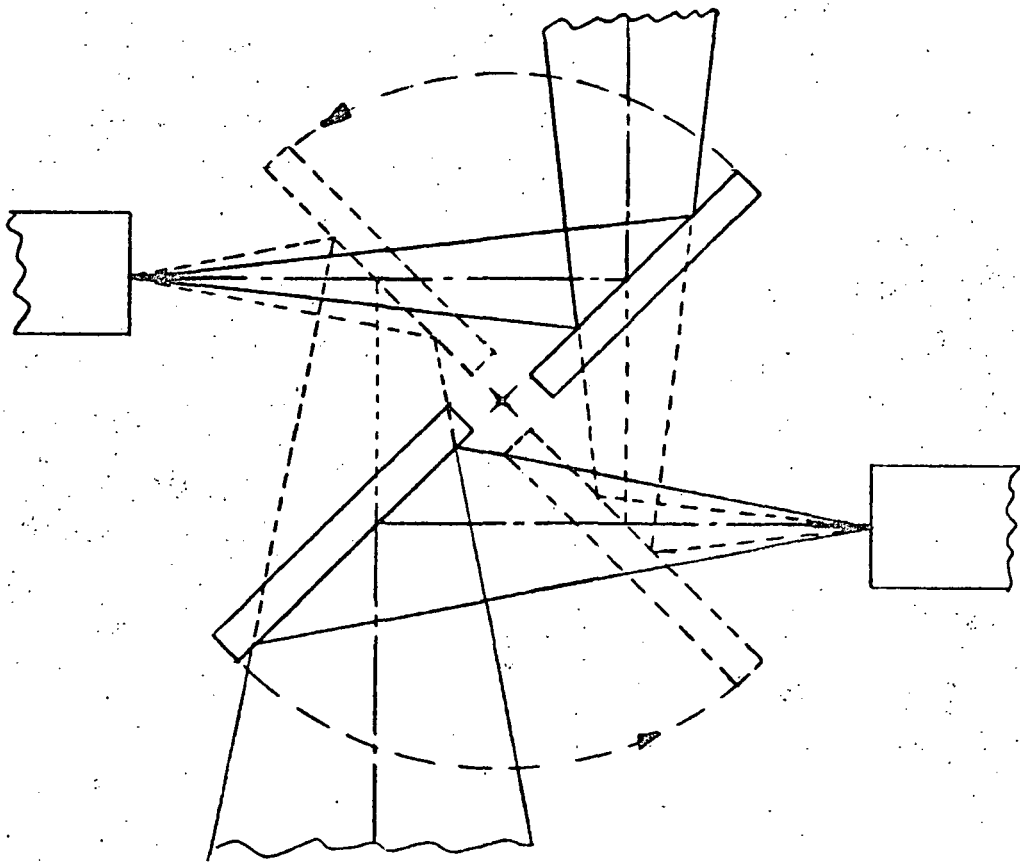
Fig. D-3 — Opposed camera, double mirror switching technique
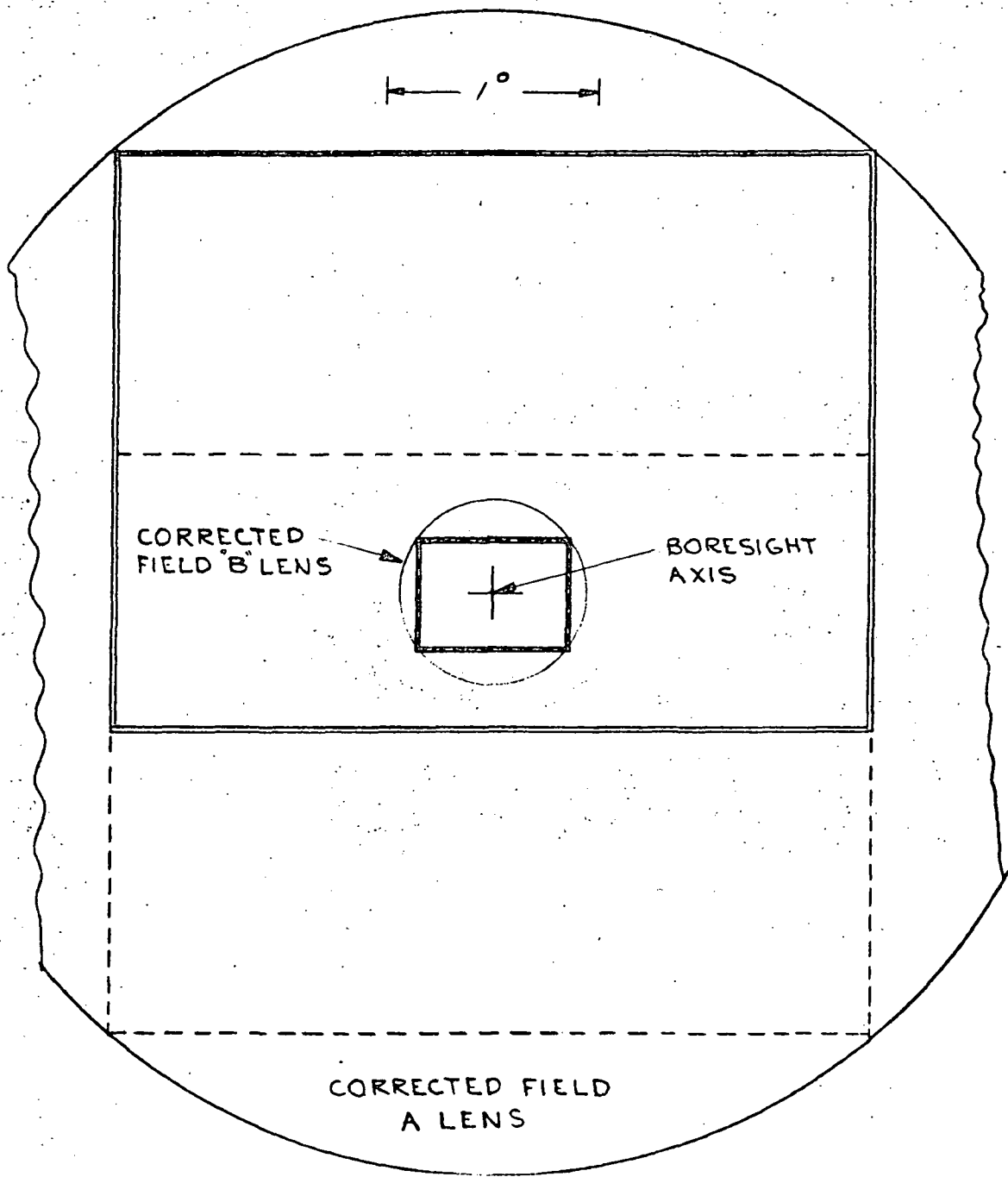
Fig. D-4 — Orthogonal camera switching system fields of view seen by vidicons with switching mirror out (solid lines) or in (dashed lines)
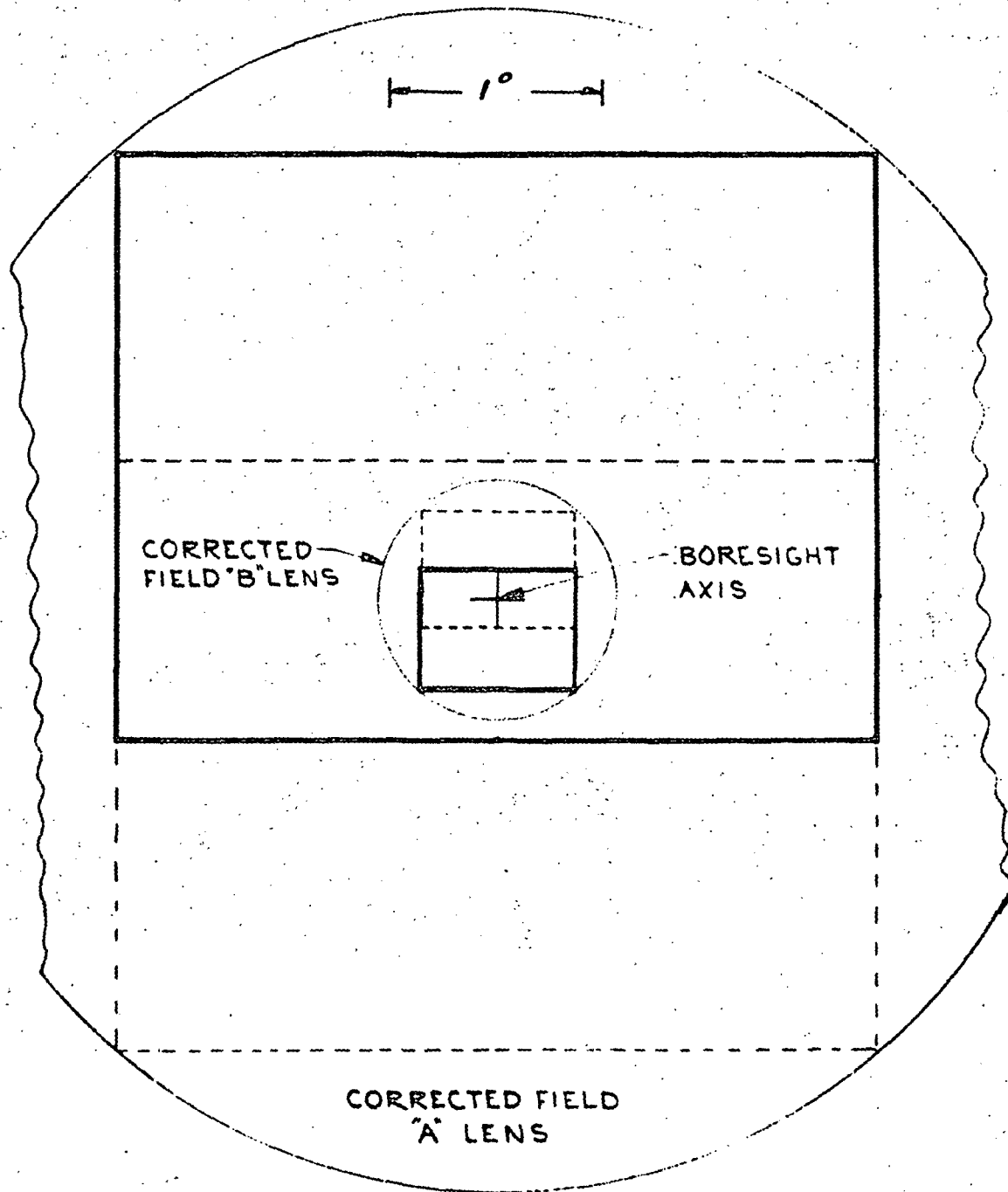
Fig. D-5 — Opposed camera, single mirror switching technique fields of view
seen by vidicons with switching mirror in nominal (solid lines) and alternative
(dashed lines) positions (A and B images shift same linear distance)
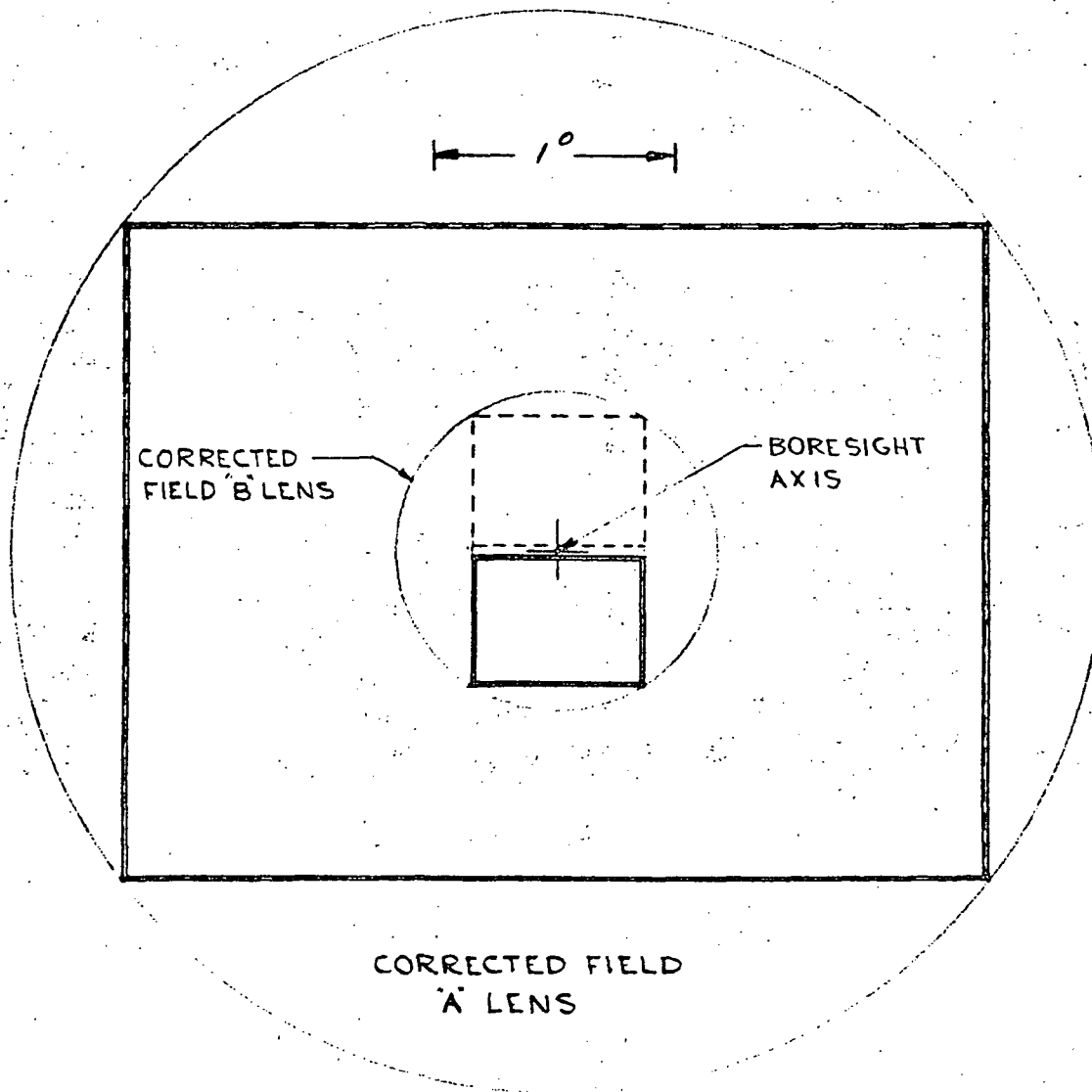
Fig. D-6 — Opposed camera, single mirror switching technique fields of view
seen by vidicons with switching mirrors in nominal (solid lines) and alternative
(dashed lines) positions (motion confined to B lens field of view)

Appendix E

ALL-REFLECTING THREE-MIRROR DESIGNS

Appendix E

ALL-REFLECTING THREE-MIRROR DESIGNS

If an all-reflecting design is to have a flat image corrected over a field of view greater than a few minutes of arc in diameter, it must have at least three mirrors, not counting folding flats. The mirrors are selected so that their powers add up to zero, and their conic constants and aspheric coefficients are selected to correct coma, astigmatism, and spherical aberration. If in addition it is necessary to hold the central obstruction diameter ratio to less than 0.50 percent and provide a long back focus, it is necessary to have an internal image and a relay stage. The internal image provides a constriction at which a folding diagonal can be placed, which minimizes the central obstruction size and folds the image off to one side.

In principle, the positive and negative mirrors can be placed in any order, leading to three general classes, which may be designated NPP, PNP, or PPN, where the order of the letters indicates the order of the positive (P) and negative (N) mirrors. If both internal and external images are real, the internal image will always be between the two positive mirrors. This extends the possible combinations to four: NPiP, PiNP, PNiP, and PiPN, where i indicates the position of the image. In practice, only two combinations offer serious promise of being viable solutions for the A and B lens designs, PiNP and PNiP.

Fig. E-1 shows the layout of a typical PiNP system and a thin lens equivalent of this design. The PiNP design is in essence a prime focus telescope with a finite conjugate inverted Cassegrain relay acting as a corrector group. The two most important characteristics of the design are illustrated by the thin lens equivalent. First, the back focus measured from mirror 3 is substantially greater than one effective focal length (efl), making it possible to obtain a clear back focus (measured from mirror 2) that is a substantial fraction of one focal length. Second, the focal ratio (f/no.) cascade is such that both the system focal ratio (F_3) and the primary mirror focal ratio (F_1) are larger than the intermediate focal ratio (F_2). This makes it possible to design a very fast PiNP configuration without having to manufacture an ultrafast primary.

The cost of the above advantages is that the physical dimensions of the PiNP configuration are large compared to its focal length. It is most suited for use as a fast, short focal length lens with a long back focus, and therefore appears well suited for the A lens. A first-order PiNP design has been completed, and is used in the accompanying layouts. Both system and primary focal ratios are f/2.63, with mirrors 2 and 3 forming a 1:1 relay. For a 5.5-degree field, the central obstruction is about 0.47 on paper, with mirror 2 being the major obstruction. Preliminary lens correction indicates that the design can be well corrected over a 5.5-degree or greater diameter field. The stop for the system is at mirror 3, and an image of this stop is formed by mirrors 1 and 2 well ahead of the center of curvature of the primary. As a result, the size of the primary is much larger than indicated by the axial beam shown in Fig. E-1, if there is to be no off-axis vignetting. Minimizing the size of the field and trimming the primary to fit the rectangular shape of the vidicon image exactly may result in significant savings in weight.

Fig. E-2 shows a typical layout for a PNiP lens and its thin lens equivalent diagram. The PNiP configuration is essentially a Cassegrain telescope with an elliptical mirror relay used as a corrector. In this case, the dimensions of the lens are small with respect to its effective focal length, or can be. The focal ratios cascade in such a manner that the primary mirror focal ratio (F_1) must be substantially faster than the system focal ratio. The clear back focus will be a relatively small fraction of the system focal length as well.

The above properties make the PNiP suitable for the B lens, but highly unsuitable for the A lens. A first-order PNiP configuration has been set up for the B lens, and is used in the accompanying optical layouts. Preliminary lens correction indicates that aspherizing the mirrors provides a well corrected field in excess of the minimum required 1.1-degree diameter. The small central obstruction diameter ratio (~0.30) bodes well for maintaining the desired MTF at 700 nanometers. But the primary mirror focal ratio, which is f/0.9 for system focal ratio of f/4.4, indicates that there may be some serious alignment problems. So far as weight is concerned, the bulk of the weight will be in the primary mirror, which is also the stop for the system. Mirror 3 will shrink only slightly if the field of view is reduced and should have very little effect on overall system weight. Thus if both A and B are all-reflecting designs, reducing the size of the A field by increasing the size of the B field might lead to a moderate system weight reduction.

The other three-mirror configurations should be mentioned here, for completeness, although they are not desirable given the present specifications. Fig. E-3 shows two possible NPiP lenses, one having a real intermediate image and the other having its intermediate image at infinity. The large central obstruction and awkward geometry of the former are immediately evident from examining Fig. E-1a, and need no further exposition. The design shown in Fig. E-1b is more interesting, and was examined during the proposal phase of this study. Mirrors 1 and 2 are basically confocal parabolas, and mirror 3 is a sphere. The system stop is on mirror 1, and mirror 3 is located so that its center of curvature falls on the image of the stop (mirror 1). Super-imposing a Schmidt corrector aspheric on mirror 1 corrects the spherical aberration of mirror 3, and converts the whole assembly into a moderately well corrected wide angle design, in principle. Unfortunately, the central obstruction diameter ratio for this design is always greater than 0.50 and tends toward 0.60 to 0.70. The change in specifications for MTF has eliminated this design from consideration, and no further work has been done on it.

Fig. E-4 shows the PiPN configuration. This has optical properties similar to the PiNP design being considered for the A lens. Its geometry is more awkward, however, and it would not fit within the 20- by 30-inch package constraints at all conveniently. Therefore, no first-order layout or lens design analysis has been performed for this design.

(a) Layout

F/NO CASCADE
$F_3 > F_2 < F_1$

(b) Thin lens equivalent
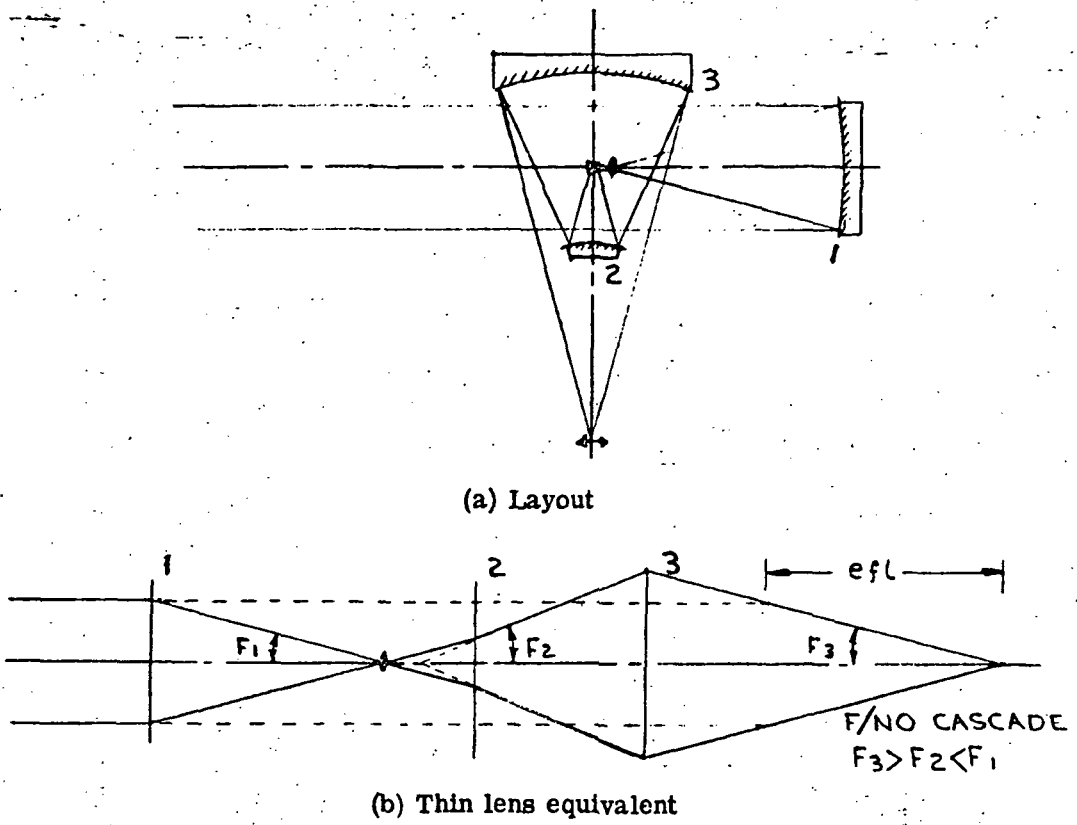
Fig. E-1 — Three-mirror PiNP configuration

(a) Layout

F/NO CASCADE
$F_3 > F_2 > F_1$

(b) Thin lens equivalent
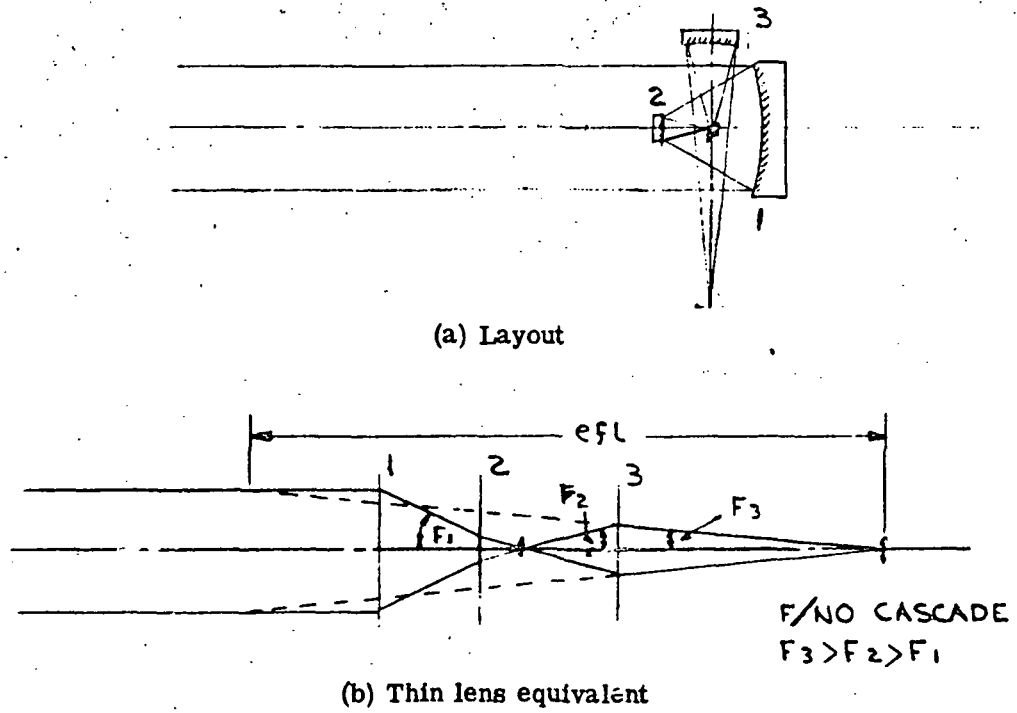
Fig. E-2 — Three-mirror PNiP configuration

E-5

Appendix F

TRANSMITTANCE OF A AND B LENSES

Appendix F

TRANSMITTANCE OF A AND B LENSES

The transmittance of the all-reflecting designs is limited by the central obstruction diameter ratio and the reflectivity of the five mirrors (including the switching mirror) in each. The Cassegrain telescope has one or two less mirrors, depending on whether or not it is folded. The Cassegrain also has two refracting components, whose surface reflectivities must be considered. A filter wheel is common to both designs, and a blank filter substrate must be included to compensate for the optical thickness of the filters. Thus one refracting element with antireflection coating must be added to each design.

The "aperture transmittance," T, of a lens having a central obstruction will be

$$T = 1 - \epsilon^2$$

where ϵ is the central obstruction diameter ratio. For the three cases involved here, the aperture transmittances are as follows:

	ϵ	T, percent
All-reflecting A	0.47	77.91
All-reflecting B	0.30	91
Cassegrain B	0.52	72.96

Two mirror materials are available that reflect well in the spectral range of 350 to 700 nanometers, namely, aluminum and silver. Both require protective overcoatings to prevent degradation, although this problem is not as serious with aluminum as with silver, which forms a sulfide. The reflectivity data used here (see Fig. F-1) are for aluminum coated with SiO_2 and for silver coated with an Itek-designed multilayer coating. Fig. F-1 shows the degree of variation in reflectivity as a function of wavelength for each type. For silver, this variance is due predominantly to absorption in the ultraviolet. The variation in reflectivity for aluminum is due in part to interference effects set up by the SiO_2 coating and in part to an aluminum absorption band near 700 nanometers. The SiO_2 coating was selected to increase the reflectivity in the blue and near-ultraviolet.

Fig. F-1 shows the reflectivity of silver to be clearly superior to that of aluminum at wavelengths above 380 nanometers. At 350 nanometers, the reflectivity of silver is low enough so that a cascade of four mirrors will reduce the lens transmittance to about 40 percent regardless of other factors. The same is true of aluminum at 700 nanometers. It is possible to raise the reflectivity at both ends of the spectral region about 40 percent in a five-mirror system by using some silver mirrors and some aluminum mirrors. Fig. F-2 presents the possibilities. Each curve represents the cascaded reflectivities for all possible five-mirror combinations of silver and aluminum from all silver (5/0) to all aluminum (0/5).

.If the refracting elements in the Cassegrain and the filter blank in all three designs are made of Schott UBK-7 or a similar glass, the bulk transmittance of the glass is sufficiently high to be considered 100 percent, for the glass thicknesses involved. The reflectivity can be reduced over a limited spectral band by coating each surface with an appropriate thickness of magnesium fluoride. Fig. F-3 shows the transmittance of a single surface of UBK-7 coated for maximum transmittance at about 460 nanometers. This is typical of what should be expected.

The data in Figs. F-1, F-2, and F-3 were generated theoretically using Itek-developed computer programs. In practice, even with the best available coating technology, the actual reflectivity and transmittance will be less than this. We estimate that the reflectivity of the two metallic reflectors may be as much as 1.5 percent per surface lower than indicated, and that the transmittance of the refracting surfaces may be 0.3 percent lower than indicated. The possible errors introduced by this effect are indicated in the following results.

The above data have been used to generate transmittance curves for the Cassegrain B lens (Fig. F-4), the all-reflecting B lens (Fig. F-5), and the all-reflecting A lens (Fig. F-6). In each case, curves were generated for all-silver mirror systems and for an optimum mix of silver and aluminum mirrors. Each transmittance curve is plotted as a band, with the upper edge indicating the theoretical value and the lower edge adding the "fabrication" losses noted in the preceding paragraph. In all cases, the design goal is to exceed 40 percent transmittance at all wavelengths.

The Cassegrain designs were considered, one unfolded (three mirrors including the switching mirror) and the other folded (four mirrors). The transmittance of the former can be kept above 40 percent over essentially the entire spectral region by using two silver mirrors and one aluminum mirror. Adding the folding mirror (silver) drops the transmittance below 40 percent at both ends of the spectral range.

Transmittance of the all-reflecting B lens can be kept above 40 percent over the entire spectral range by using two silver and three aluminum mirrors. The transmittance at intermediate wavelengths is substantially higher than for the Cassegrain, due primarily to the smaller central-obstruction diameter ratio.

The transmittance of the all-reflecting A lens cannot be kept above 40 percent over the entire spectral range, no matter what combination of silver and aluminum mirrors is used. This is due again to the larger central obstruction of this design.

Figs. F-4, F-5, and F-6 illustrate clearly the cost of trying to maintain a high transmittance down to 350 nanometers. If the lower wavelength limit is moved up to about 370 nanometers for a transmittance of 40 percent, a very substantial increase in transmittance at the longer wavelengths can be achieved by using only the "protected" silver coating.
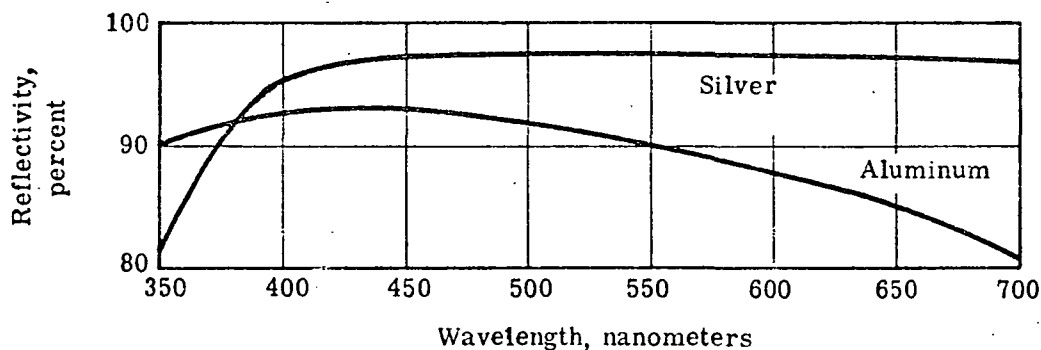

Fig. F-1 — Reflectivity of "protected" silver and aluminum coatings
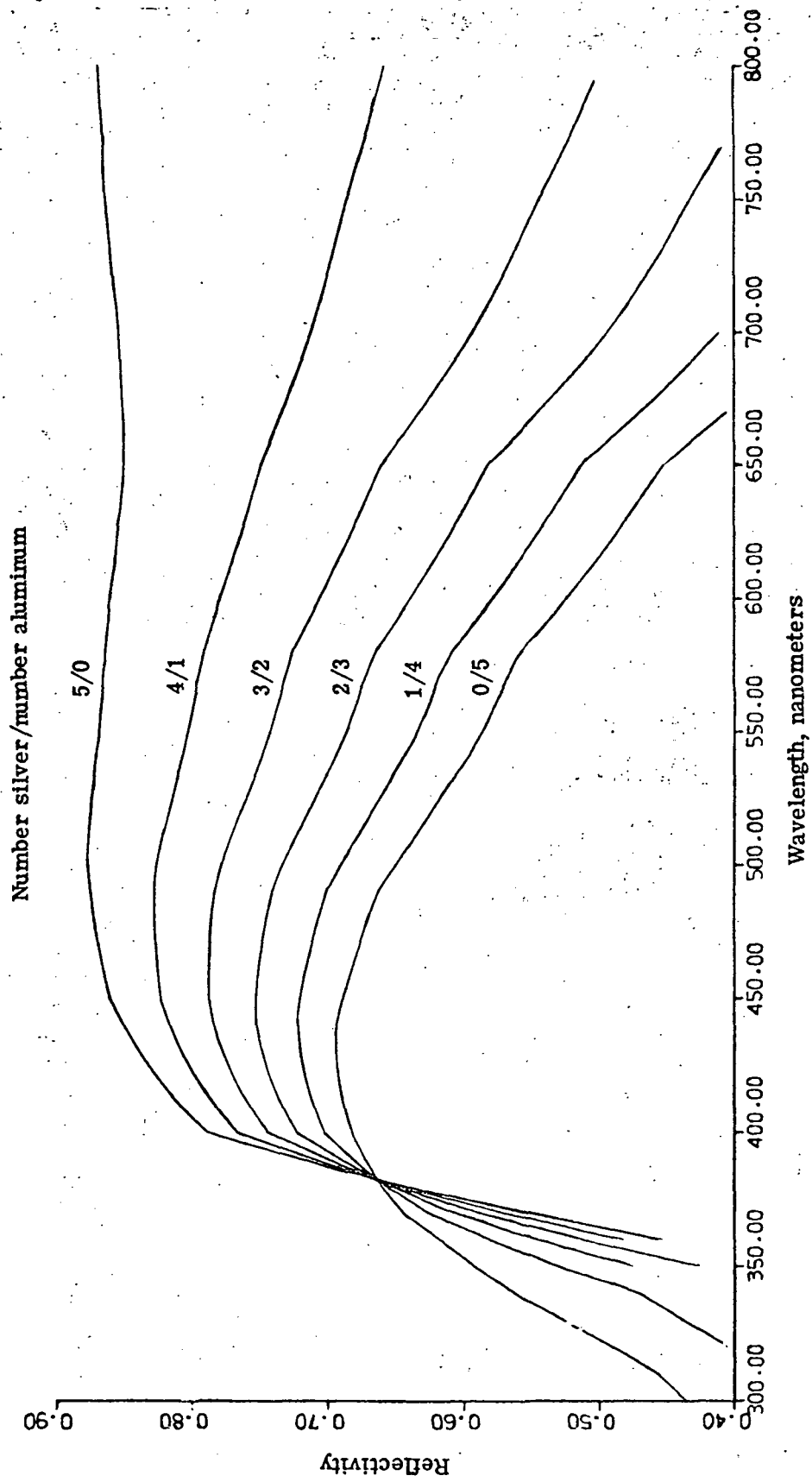
Fig. F-2 — Reflectivity of cascade silver and aluminum mirrors for five-mirror system
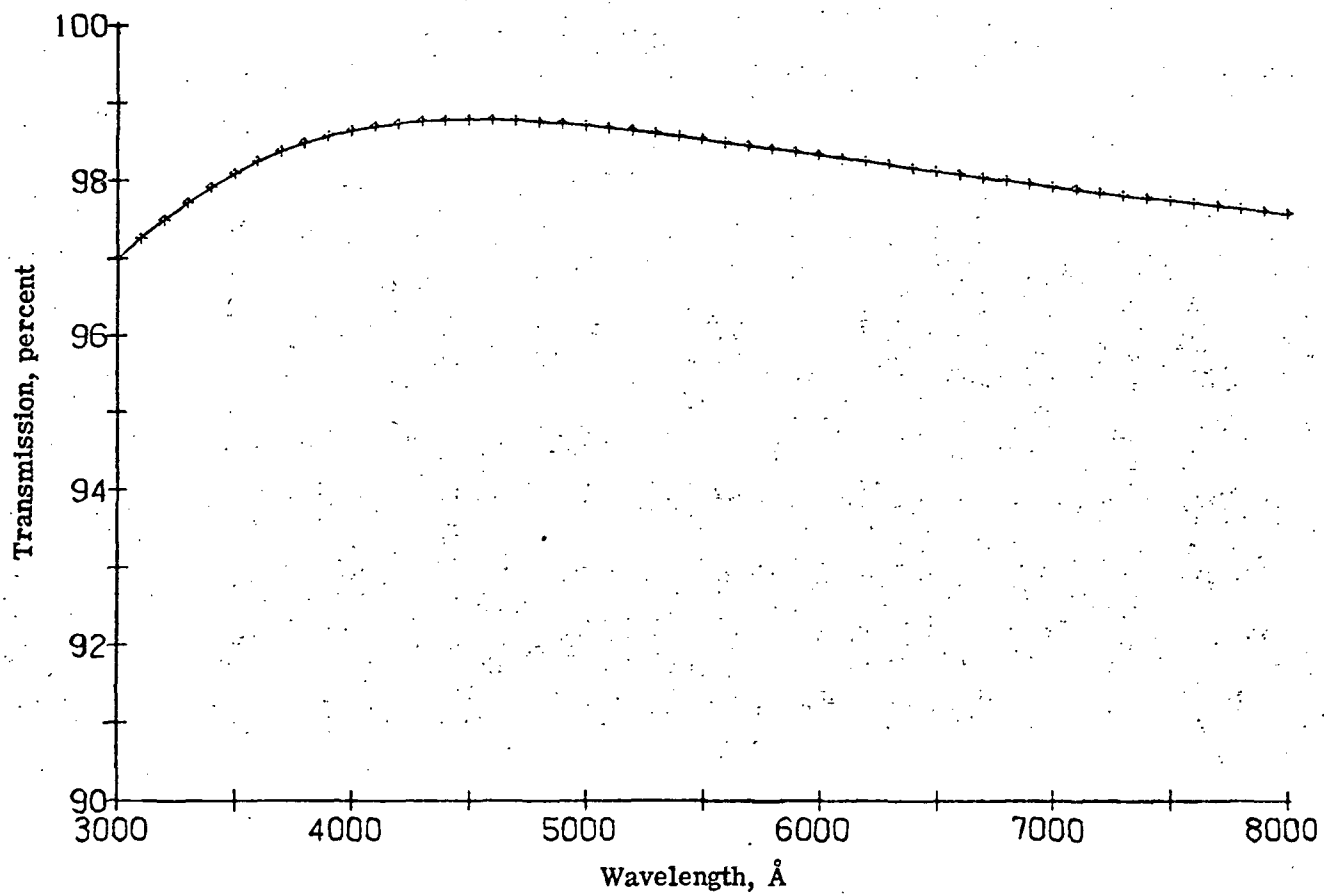
Fig. F-3 — Transmittance through single surface of UBK-7 glass coated with magnesium fluoride (λ = 460 nanometers, light at normal incidence)
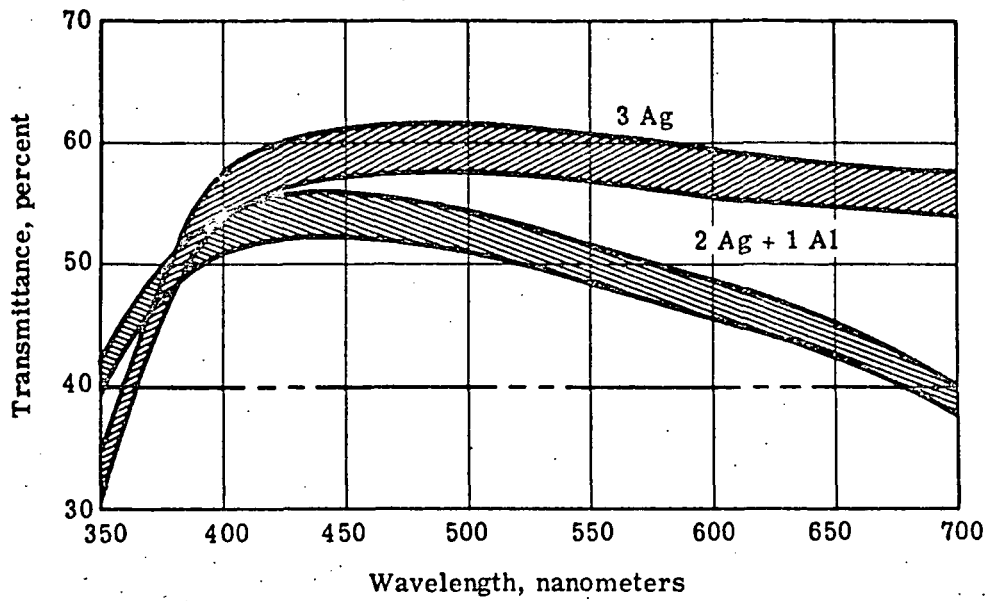
(a) No folding mirror
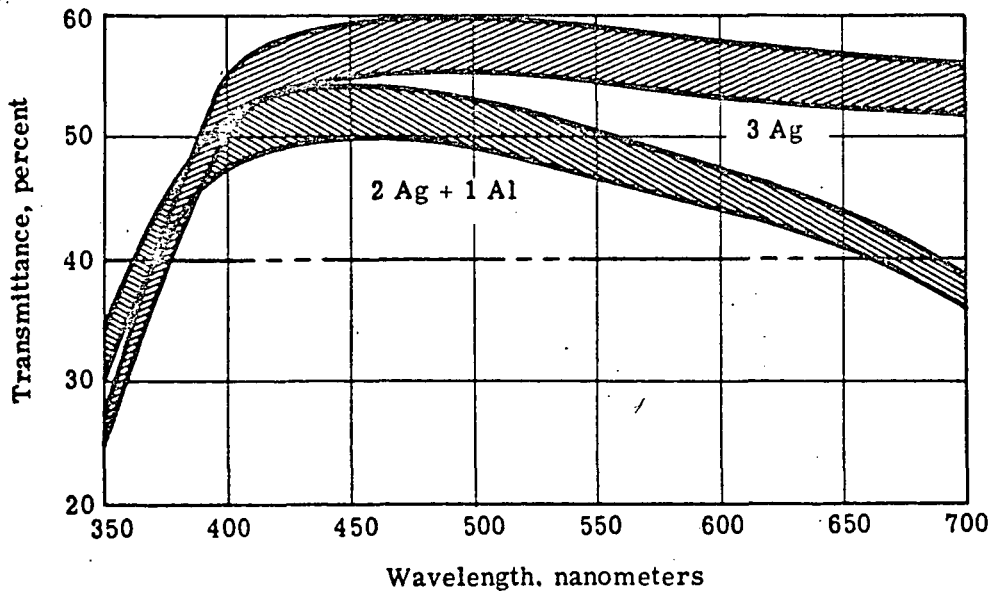
(b) Silver folding mirror

Fig. F-4 — Transmittance of Cassegrain B lens showing effects of coating some mirrors with silver and some with aluminum (0.53 central obstruction, two correctors, and one filter blank)
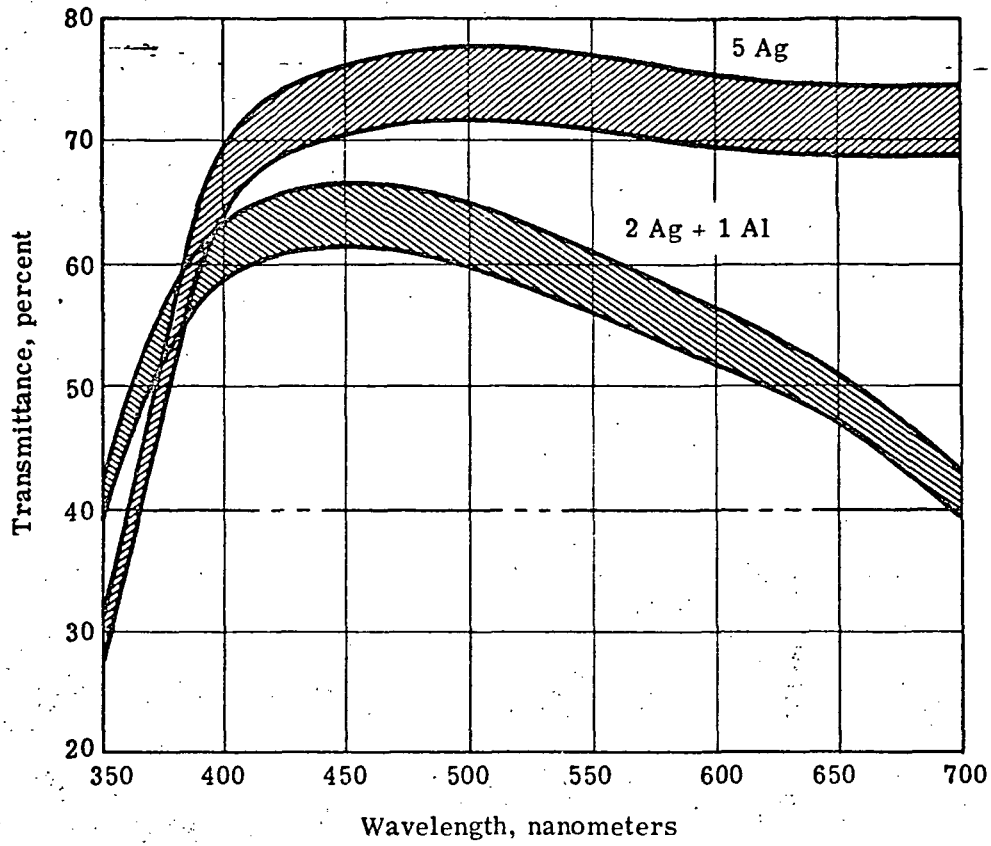
Fig. F-5 — Transmittance of all-reflecting B lens including 0.30 central obstruction and one filter blank
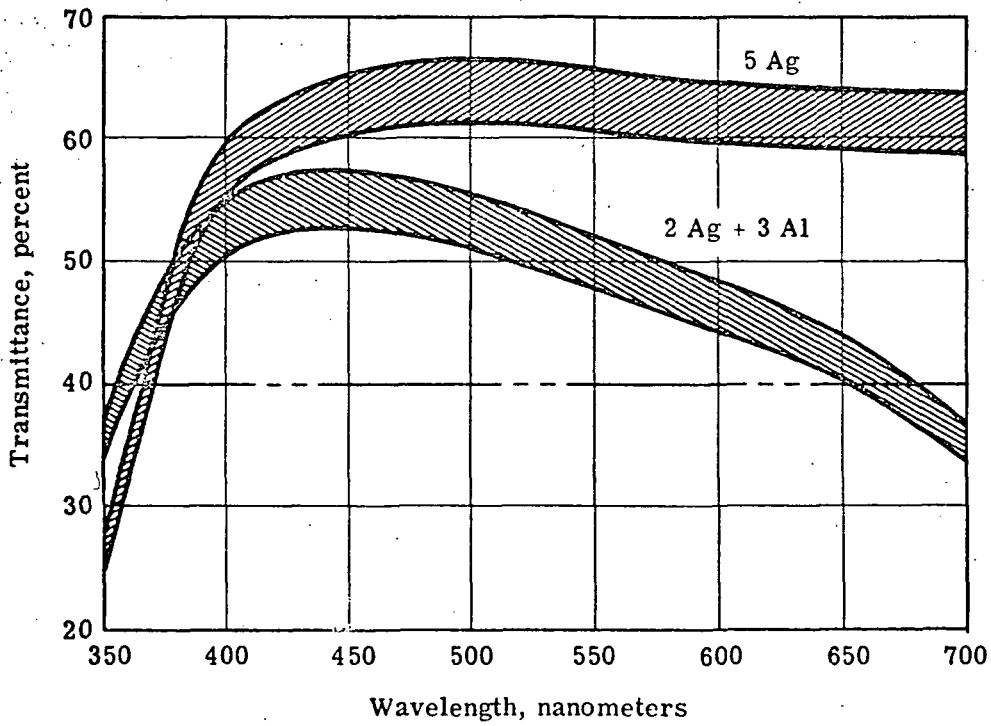
Fig. F-6 — Transmittance of all-reflecting A lens including 0.47 central obstruction and one filter blank

Appendix G

THERMO-OPTICAL CONSIDERATIONS

Appendix G

THERMO-OPTICAL CONSIDERATIONS

THERMO-OPTICAL EVALUATION OF CONFIGURATIONS 3 AND 4

Thermo-optical analyses were performed on baseline configurations 3 and 4 (Section 2-2). The A lens in both configurations is identical and uses all-reflecting optics; the B lens of configuration 3 is all-reflecting and of configuration 4 is a Cassegrain.* Configuration 3 optics are shown in Fig. 2-3, and configuration 4 optics in Fig. 2-4.

The mean operating temperature of the system is assumed to be 7.5 °C, with maximum perturbations of ±27.5 °C (or a total operating range of −20 to +35 °C).

To obtain a first-order estimate of thermal sensitivities, the chassis, all lens element mounts, and the vidicon mounts were all assumed to be of one material, titanium. Lens sensitivities for the all-titanium configuration are given in Table G-1 for temperature soak perturbations. To isolate cell expansion and mirror expansion effects, sensitivities were also determined for mirror expansion effects only. These are given in Table G-2.

For a nonathermalized configuration, the B4 lens appears to be considerably less sensitive to soaks than the B3 lens. This is because the three-mirror configuration of the B3 lens is much more sensitive to spacing and mirror curvature changes as dictated by the lower f/number of the B3 primary mirror. The corrector elements of B4 have zero power, and as a result are relatively insensitive to thermal soaks. The A lens also shows lower sensitivities than the B3 lens because the B3 lens also has a much faster primary mirror than does the A lens.

It is specified that the environment not degrade the system performance to less than 0.50 modulation at 35 line pairs per millimeter. This requirement can be transformed into a performance criterion in terms of defocus, since most of the modulation drop can be attributed to defocus. Fig. G-1 shows through-focus modulation curves for lenses A, B3, and B4. It should be noted that the curves of Fig. G-1 do not represent a final design nor is there an allowance for fabrication and static alignment errors. From Fig. G-1 and using the 0.50 modulation requirement, a total system allowable defocus error can be derived, as shown in Table G-3.

By comparing the values in Table G-1 with those in Table G-3, it is apparent that for both the B lenses and the A lens, an all-titanium, all-low-expansion mirror combination is inadequate over the anticipated temperature range. Hence, athermalization is required.

---

*For ease of reference we shall refer to the B lens of configuration 3 as the B3 lens, and the B lens of configuration 4 as the B4 lens.

TRIAL ATHERMALIZATION OF CONFIGURATIONS 3 AND 4

The athermalization techniques initially considered were:

1. Use of a low expansion* substructure

2. Use of a high expansion glass material for the mirrors. Comparison of Tables G-1 and G-2 shows that the defocus resulting from cell expansion is opposite in sign to that resulting from mirror expansion. Therefore, athermalization can be accomplished by effectively matching cell and mirror materials.

3. Switching to filters of different thicknesses as temperature varies.

In each of these cases it was assumed that relative positions of the vidicon with respect to the lens would change under thermal loading based on the same expansion coefficient as the lens cell. Use of variable expansion shim stock in mounting the vidicon may aid in athermalization. This approach involves the Itek/JPL interface and would receive additional attention during more detailed design phases.

Table G-4 lists some relative advantages and disadvantages of the different athermalization schemes considered here.

Studies have been made considering a low expansion substructure. Thermal sensitivities were determined for the B3 and B4 lenses with this substructure connecting the first two mirror elements, as shown in Fig. G-2. The remaining structure was titanium. These sensitivities are shown in Table G-5. Comparison of these values with those in Table G-3 indicates that the defocus errors due to thermal soak loads will still exceed the total defocus error budget.

The next logical step was to consider the entire structure to include a low expansion substructure. Sensitivities for this configuration are shown in Table G-6. These results show that the defocus errors for lenses A and B4 will be within the total system allowable defocus errors (Table G-3) and demonstrate that the A or the B4 lens with a substructure having a low effective expansion coefficient provides a feasible configuration.

Although there has been a redirection of study effort by JPL toward an all-refracting system for the A lens and the elimination of the redundant vidicon requirement from the A system, this analysis is still valid for the B lens. The final recommended baseline B lens corresponds to the B4 lens. Further discussion of the athermalization effort is included in Section 3.3.1.

Although the final athermalization design effort was directed toward a completely low expansion substructure, the following comments are appropriate to the other proposed methods of athermalization.

A high degree of athermalization for soaks can be achieved through the use of high expansion glasses for the mirrors. However, the system then becomes extremely sensitive to gradients. This technique becomes feasible only if gradients can be controlled to very low levels.

Assuming that it is possible to have three filter thicknesses per wavelength band, the use of interchangeable filters will permit the defocus error to be reduced to 1/6 the total thermally induced focus travel. An undesirable feature of any filter selection technique will be the necessity of some method of environmental sensing. Also, residual focus errors still appear to be significant.

---

*Or effective expansion, e.g., as in the use of two compensating higher expansion materials as weight permits. This could take the form of a self-compensating truss in which the expansion coefficient for members in specific orientations may be different from those in others such that the net expansion parallel to the optical axis is zero.

FEASIBILITY OF AN ALL-REFRACTING SYSTEM FOR THE A LENS FROM THERMO-OPTICAL CONSIDERATIONS

To establish the feasibility of an all-refracting A lens from thermo-optical considerations, three design configurations were selected from the file of conventional lens types. These configurations were then scaled to an 8-inch focal length and an f/number of 3. These lens types were:

1. Apochromatic Petzval*
2. Achromatic Petzval†
3. Achromatic double-Gauss.

Through-focus MTF curves were determined for these three lenses and are shown in Fig. G-3. This figure is independent of cell material, since no temperature perturbations are implied.

Temperature soak performance was also determined for these three lenses and these results are shown in Table G-7 for a temperature soak, ΔT, of $\pm 27.5\,°C$.

The data in Table G-7 (except that for the all-titanium celled apochromat) are also shown plotted in Figs. G-4 and G-5. The apochromat curve and the achromatic double-Gauss curve in Figs. G-3 and G-4 have been shifted so that best focus corresponds to nominal operating temperature. It should be noted that the modulation data make no allowance for fabrication or static alignment errors.

It is apparent from Table G-7 that an unathermalized apochromat (i.e., with a titanium cell and/or the existing glass types and configuration) does not meet the operational requirement of 50 percent modulation over the $\pm 27.5\,°C$ range.

Table G-7 and Fig. G-4 indicate that an athermalized (with, for example, Cycolac spacers) apochromat lens, an achromatic Petzval lens (with either an Invar or titanium cell), or the achromatic double-Gauss lens (with a titanium cell) can most likely be designed to meet the thermal requirements.

From exclusively thermo-optical considerations, the recommended configurations of the limited set considered to prove feasibility is the athermalized apochromat. However, due to mechanical packaging constraints (e.g., long back focal length requirement), the achromatic double-Gauss lens appears to offer the best possibility of meeting all requirements.

One additional possible advantage of the achromatic lens should be noted: the glass configuration of the achromat is essentially athermal. As a result, when combined with a low expansion cell material, the glass and cell can be at different temperatures and the lens will still be effectively athermal. However, the current heavily insulated baseline coupled with the slowly varying loads expected suggests that this is not critical here.

---

* Both PSK-53 and alternative versions.
† For example, as used in the Itek NASA optical bar panoramic camera.

Table G-1 — Lens Sensitivities for All-Titanium Configuration Temperature Soak

Lens Configuration	ΔT, °C	RMS Wavefront Error Without Refocus, wavelengths	Defocus, inches
A	+27.5	1.89	−0.0100
	−27.5	2.03	+0.0107
B3	+27.5	3.79	−0.0504
	−27.5	3.80	+0.0513
B4	+27.5	0.799	−0.0131
	−27.5	0.807	+0.0132

Notes:
1. Nominal temperature = 7.5 °C.

2. $\bar{H}$, fractional normalized field height, weight for rms wavefront error analysis:

$\bar{H}$	Weight
0.0	1.0
0.7	1.0
1.0	1.0

3. $\lambda = 550$ nm.

4. Mirror material = ULE fused silica.

5. Sign convention for defocus:
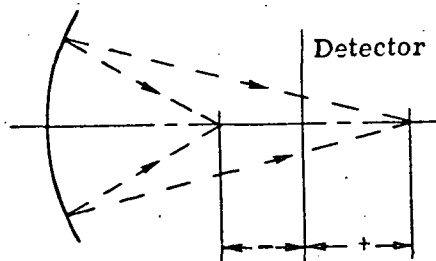
6. System f/numbers: A, f/2.64; B3, f/4.4; B4, f/4.4.

Table G-2 — Lens Sensitivities for Mirrors Only, Temperature Soak

Lens Configuration	Mirror Material	ΔT, °C	RMS Wavefront Error Without Refocus, wavelengths	Defocus, inches
A	BK-7	+27.5	1.65	+0.0087
		−27.5	1.60	−0.0084
	Fused silica	+27.5	0.098	+0.0005
		−27.5	0.077	−0.0004
	ULE	+27.5	0.005	0.0000
		−27.5	0.016	+0.0001
B3	BK-7	+27.5	3.37	+0.0451
		−27.5	3.28	−0.0433
	Fused silica	+27.5	0.200	+0.0027
		−27.5	0.158	−0.0021
	ULE	+27.5	0.010	+0.0001
		−27.5	0.033	+0.0005
B4	BK-7	+27.5	0.677	+0.0111
		−27.5	0.654	−0.0107
	Fused silica	+27.5	0.040	+0.0007
		−27.5	0.031	−0.0005
	ULE	+27.5	0.003	+0.0001
		−27.5	0.007	+0.0001

Notes: 1. See notes for Table G-1.

2. Cell expansion coefficient = 0.
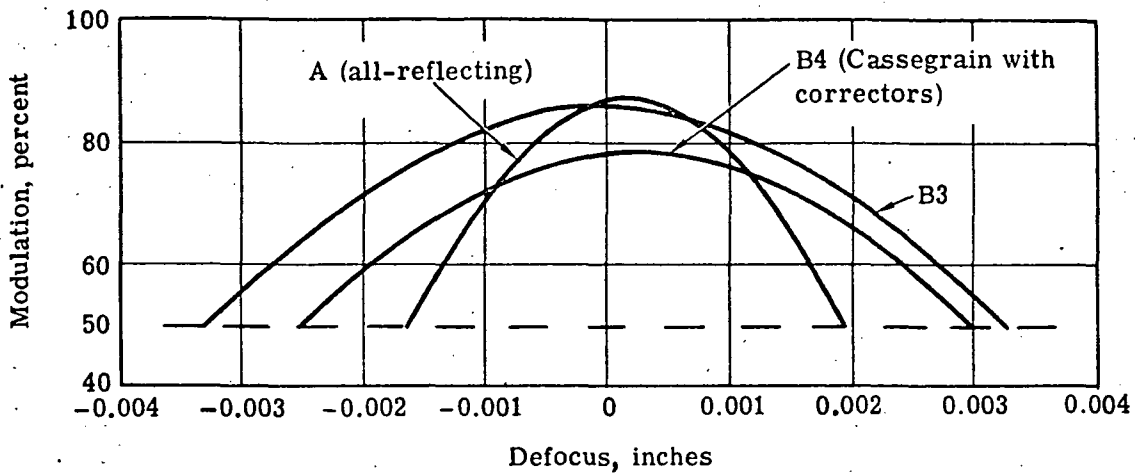
Fig. G-1 — Modulation versus defocus—on axis, 35 line pairs per millimeter λ = 400 to 700 nanometers, undegraded performance (paraxial focus, positive defocus indicates image falls behind detector)

Table G-3 — Total System Allowable Defocus
for Lenses A, B3, and B4

Lens Configuration	Total System Allowable Defocus,* inches
A	±0.0018
B3	±0.0033
B4	±0.0028

*Or equivalent wavefront error, rms $\approx$ defocus/ $8\sqrt{12}$ (f/no.)^2. Allowance for uncorrelated fabrication/static alignment errors as well as other dynamic error sources results in values similar to these for thermal components.

Note: Data based on Fig. G-1 and the operational requirement of 50 percent modulation at 35 line pairs per millimeter.

Table G-4 — Athermalization Alternatives

Alternative	Advantages	Disadvantages
1. Low expansion substructure (e.g., Invar, $\alpha = 1.5 \times 10^{-6}/^{\circ}C$)	1. Relatively insensitive to gradients	1. Possible weight penalty 2. Possibly damage sensitive (Cer-Vit/ULE)
2. High expansion glass for mirrors	1. No weight penalty	1. Very sensitive to gradients 2. Differences in relationship of detectors to optics in A and B may complicate glass choice for simultaneous system athermalization in all switching modes (parfocalization)
3. Change filter thickness	1. Filter wheel already part of design	1. Corrects in discrete steps, correction limited by number of filters 2. Increased weight 3. Requires selection of filter based on environmental sensing
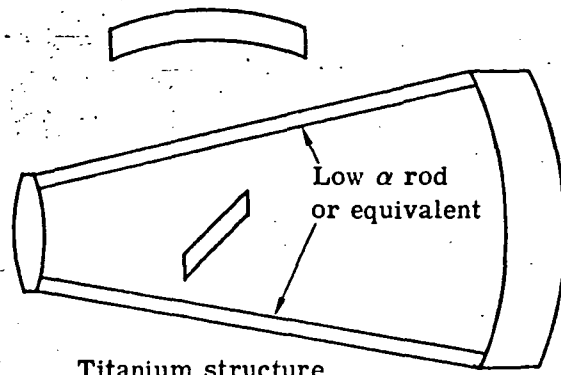
(a) B3 lens
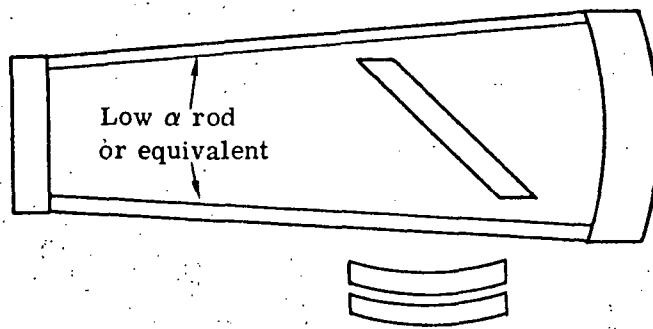
(b) B4 lens

Fig. G-2 — Low expansion substructure

Table G-5 — Lens Sensitivities for Low Expansion
($\alpha = 1.5 \times 10^{-6}$/°C) Substructure as Shown in Fig. G-2

Lens Configuration	ΔT, °C	RMS Wavefront Error Without Refocus, wavelengths	Defocus, inches
B3	+27.5	1.06	−0.0142
	−27.5	1.11	+0.0148
B4	+27.5	0.232	−0.0038
	−27.5	0.240	+0.0039

Note: See notes for Table G-1.

Table G-6 — Lens Sensitivities for a Configuration Using a
Single Low Expansion (1.5×10^{-6}/°C) Cell Material

Lens Configuration	ΔT, °C	RMS Wavefront Error Without Refocus, wavelengths	Defocus, inches
A	+27.5	0.330	−0.0017
	−27.5	0.351	+0.0019
B3	+27.5	0.658	−0.0088
	−27.5	0.701	+0.0094
B4	+27.5	0.142	−0.0023
	−27.5	0.151	+0.0025

Notes:
1. See notes for Table G-1.
2. Entire structure of one material as opposed to the two materials of Fig. G-2.
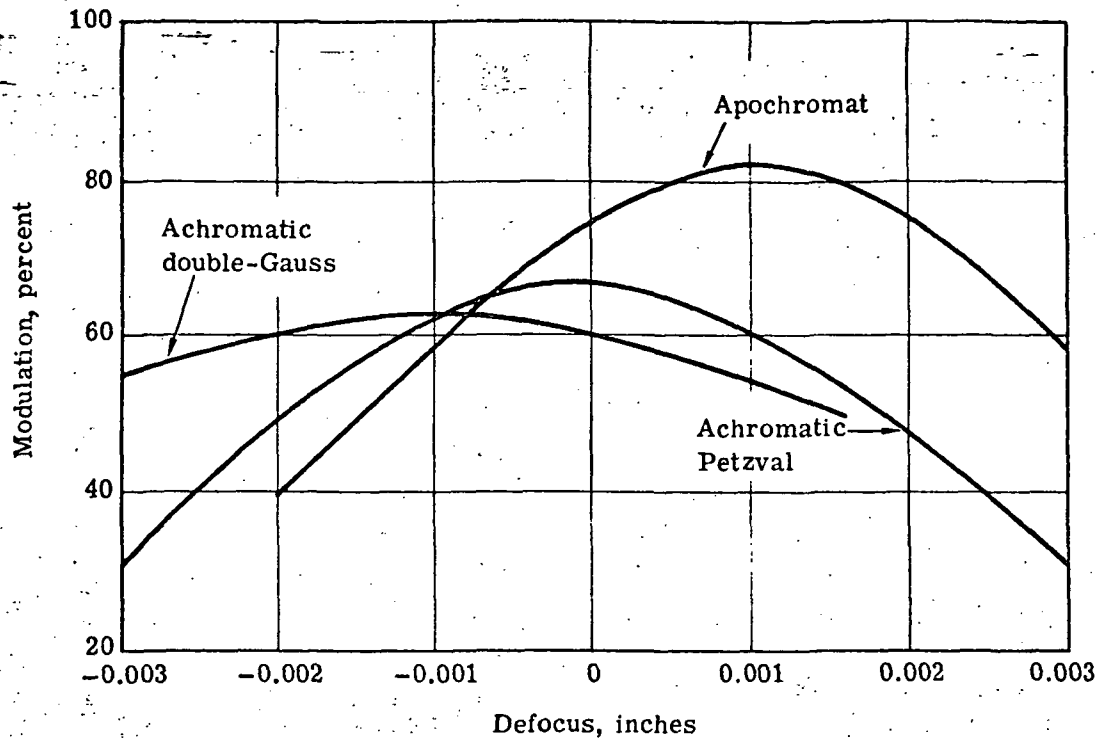
Fig. G-3 — Modulation versus defocus—on axis, 35 line pairs per millimeter, λ = 400 to 700 nanometers (see notes to Fig. G-1)

Table G-7 — All-Refracting Systems for A Lens*
Defocus Due To Temperature Soak

Configuration	ΔT, °C	Defocus From Best Focus, inches	Modulation at 35 lp/mm†
Apochromat, all-titanium cell	±27.5	±0.0105	≪0.5
Apochromat, estimate for athermalized system with cycolac spacers	±27.5	0.0014	0.69
Achromatic Petzval, all-titanium cell	±27.5	∓0.0007	0.64
Achromatic Petzval, Invar cell	±27.5	0.0004	0.65
Achromatic double, Gauss, titanium cell	±27.5	∓0.0014	0.58

*Lenses sealed to 8-inch focal length, f/number = 3.
†No allowance for fabrication or static errors.
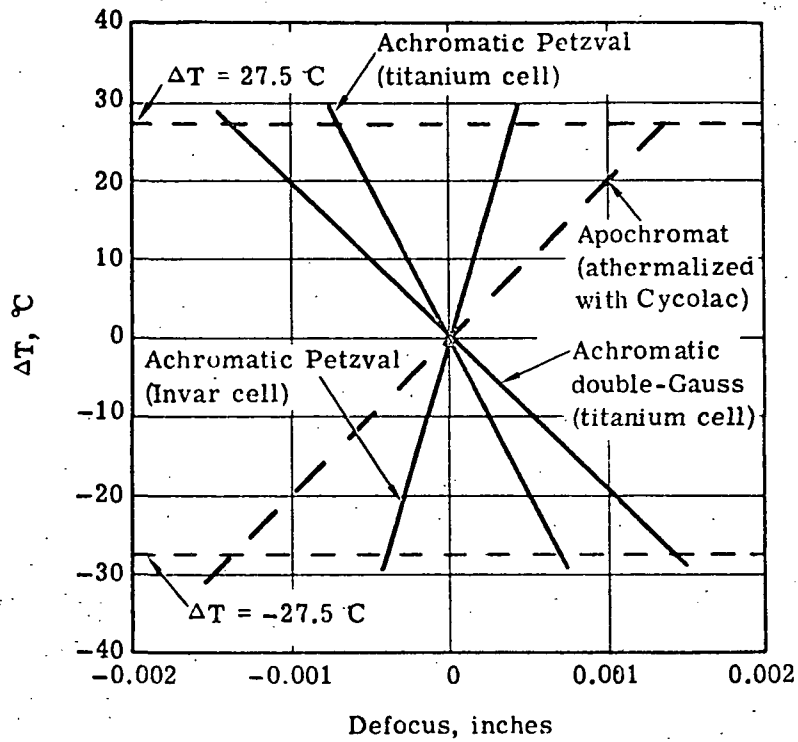
Fig. G-4 — Defocus versus soak temperature—on axis, 35 line pairs per millimeter, λ = 400 to 700 nanometers
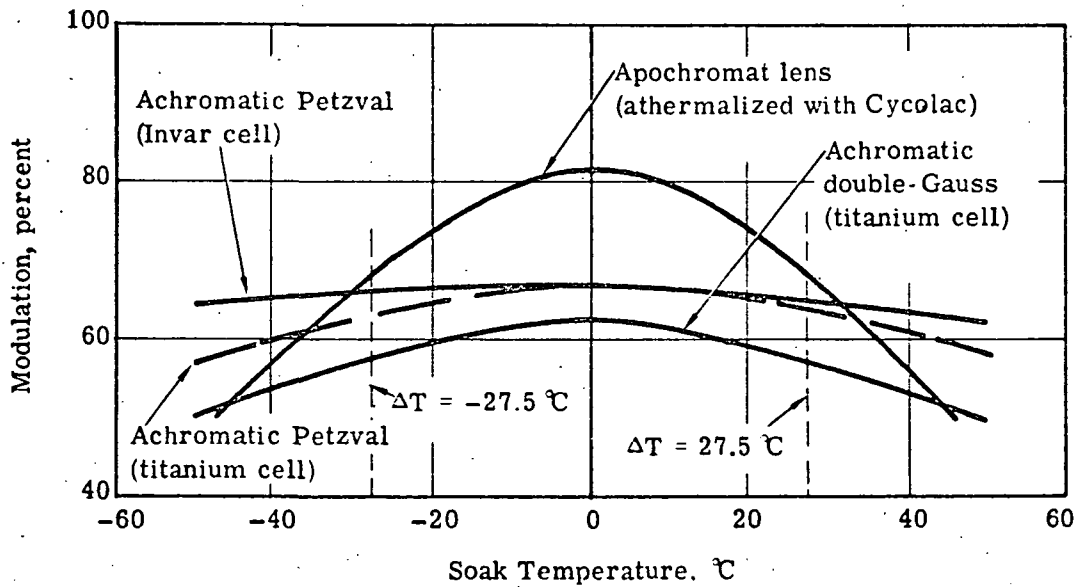
Fig. G-5 — Modulation versus soak temperature—on axis, 35 line pairs per millimeter, λ = 400 to 700 nanometers, no allowance for fabrication or static error